The influence of hydrostatic pressure on the macro- and micro-structures of aluminium-4% copper alloys

THE INFLUENCE OF HYDROSTATIC PRESSURE ON THE MACRO- AND MICRO- STRUCTURES OF ALUMINIUM-4% COPPER ALLOYS.

by

LEE, Ho-In

A Thesis submitted in partial fulfilment of the requirements for the award of the degree of Master of Science of the Loughborough University of Technology in December 1976.

Supervisor: Dr. A.A. Das,
Department of Engineering Production.

ACKNOWLEDGEMENTS

I would like to thank Professor R.J. Sury and Dr. K.T. Chang (KIST in Korea) who gave me an opportunity to study here, and Dr. A.A. Das for his helpful encouragement and invaluable suggestions during the course of this work. I am also indebted to Dr. G.F. Modlen for his helpful guidance in setting up the strain gauges on the load cell, and all the technical staff of the Department for their help, particularly Mr. B.J. Goodman, Mr. W.R. Abrey, Mr. J. Manning, Mr. R. Pearson and Mr. A. Haigh.

ABSTRACT

The work reported in this thesis was carried out in two sections:-

(i) An examination of the effect of hydrostatic pressure on the macro- and micro- structures derived during solidification of Al-Cu alloys

(ii) Some observations on crystal growth in an ammonium chloride/water analogue system, with a view to explore possible similarities with the mode of solidification in Al-Cu alloys.

Two different alloys were used: one a commercial alloy (LM11) which contained Ti as a grain refining agent, and the other a Al-4% Cu alloy which was made up from 99.99% pure aluminium and 99.9% pure copper without additions of any grain refining agents.

The pure Al-4% Cu alloy solidified in the die showed a mixed columnar and equiaxed structure, but when pressure was applied, up to 110MN/m^2, during solidification the structure produced was equiaxed. At very high pouring temperatures, a columnar structure was produced under pressure in the pure alloy.

The commercial Al-Cu alloy showed equiaxed grain structures even when poured at high temperatures and solidified without the application of pressure; possibly due to the presence of the grain-refining agents, although the equiaxed structure was much finer under pressure.

The fineness and distribution of the equiaxed zone in the small ingots (ϕ 50m/m) solidified under pressure greatly depended on the actual temperature gradient ($\frac{\partial T}{\partial x}$) and the liquidus temperature gradient.

It might be referred to have resulted from the increase of heat extraction through the mold, and the restriction of diffusion, as well as the degree of constitutional supercooling ahead of the solid-liquid interface.

The rapid heat extraction is a result of conductive heat flow since the air gap between the casting and the die is eliminated by the application of pressure. Diffusion is dependent on time as well as temperature, so that a more rapid solidification rate restricts diffusion away from the solid-liquid interface resulting in a higher degree of constitutional supersooling.

There was a tendency for severe normal segregation of a copper rich pool in the central region of the ingots cast under pressure. This was also influenced by the rate of heat extraction through the mold. When the final maximum die temperature during or after solidification under pressure was kept below 280^{o}C, the severe normal segregation of copper to the centre of the ingot could be eliminated.

When the Al-Cu alloys were cast at even lower pouring temperatures with lower initial die temperatures, the resulting structures consisted of extremely fine equiaxed grains with complete absence of the normal segregation of copper in the central region observed in castings poured at higher temperatures.

This fine equiaxed structure may be thought to have resulted from the effect of two factors:- (i) the lower pouring temperature and the lower die temperature may have caused simultaneous nucleation throughout the casting section (similar to the idea of "big bang" nucleation), and

(ii) a solid skeleton formed in the ingot casting after pouring is then fragmented by the application of pressure which would create new centres for growth of grains from the remaining liquid.

The application of a two-step pressure during solidification was much more effective for dendrite fragmentation. It was thought to be due to the collapse of solid skeletons in liquid and perturbations of solid-liquid interfaces already formed during the first step. This hypothesis is supported by the actual observations made during the crystallisation of the ammonium chloride/water analogue system. A further point to note is that alloys poured at low temperatures are likely to have been severely undercooled by the application of pressure as a result of the change in the equilibrium freezing temperatures of the alloys (Clausius-Clapeyron relationship) which would also tend to produce a large number of fine equiaxed grains in the ingot structure.

It was observed that the micro structures of ingots solidified under pressure showed fine dendritic substructures within the equiaxed grains. This would also result from the rapid cooling rate influencing the number of growth centres and possibly the rapid growth rate affecting the dendrite morphology. Since growth rate was observed to increase under pressure in the analogue system of ammonium chloride/water, it is reasonable to assume that a similar effect is produced in the Al-Cu alloys under pressure.

CONTENTS

I. INTRODUCTION

1. History.
2. Objectives of this study.
3. Scopes of this study.

1. INTRODUCTION

Squeeze casting, variously called liquid metal forging, or extrusion casting, is a manufacturing method which combines forging and casting in a single operation: that is, molten metal is metered into a metal die cavity, where it is held for a predetermined period of time, then forged to final shape while still molten. The well known advantages of the squeeze casting process are that high production rates and reduced metal losses (since no gates and risers are necessary) result in economic production; control of grain size and porosity can be achieved maximising mechanical properties; and complex components, frequently of thin section, can be accurately cast with a fine surface finish and close dimensional control of the parts, generally requiring only minor secondary operations.[1]-[9] As a result of the advantages in this process, for many years components have been widely produced by squeeze casting process in lead, zinc, magnesium, aluminium and copper alloys, the melting points of which range up to about 1000°C, and recently many attempts have been made to extend the advantages to ferrous and other alloys which melt at far higher temperatures.

1. History

It is difficult to establish the origin of the squeeze casting process. Historically, casting and forging processes have been involved separately, so that in the past it was quite unusual to find casting and forging operations combined together within a particular manufacturing plant. However, the rapid development of the machine building industry, with its associated increase in machine tool workloads, has made it essential to improve

preliminary processes so that the work conforms as closely as possible in configuration, accuracy and surface finish to the finished components, thus reducing metal losses in machining. It is conceivable that the hybridization of casting and forging processes might result in these requirements for certain manufacturing applications.

Die casting is one of the most important processes contributing to reductions in metal losses in machining and to high production rates, but the application of die casting is restricted in a number of ways:[2] the process cannot be used for a large group of important, thick-walled (over 6m/m), and heavy components; this is because, during its shrinkage in the short filling period (1/5 − 1/10 sec), the casting cannot be fed through an ingate, which tends to solidify before the casting itself. Thus, it has been necessary to study new techniques for obtaining cast components of accurate contour and good surface finish as well as a high degree of density, possible by applying external pressure during solidification or using a modifying agent in molten metal so that many fine nuclei could be formed quickly and uniformly, operating over the whole area of the cast metal upto the point of its complete solidifcation. Many new processes have, thus, been created; for example, the Harrison Process,[10] the Autoforge Process,[11] the Acurad Process[12][13] and the Pore-Free Die-Casting Process.[14] Both the Harrison and Autoforge Processes involve a unique method of producing a preform which is subsequently forged. The Acurad is a modification of the diecasting process which utilises an inner plunger for applying a relatively

low final pressure through a wide gate to feed shrinkage in the solidifying casting. The Pore-Free Diecasting is a special method in which diecasting is accomplished by filling die cavities with an active gas, which easily combines chemically with molten metal to produce a solid compound. In other words, the above processes except the Pore-Free diecasting process are still inferior to ordinary diecasting with regard to productivity, while ordinary diecasting has the disadvantage of being unable to maintain high quality. As a result, squeeze casting, giving high quality as well as high productivity, has been studied vigorously.

In the development of squeeze casting as a viable production method for ferrous and nonferrous components, much progress has been made in the Soviet Union since the late 1930's,[2] but the current state of this method's art in the United States has been underdeveloped up-to-date.[6] In the Soviet Union, the process has been applied in quantity production in more than 150 plants, and at many of these plants, more than 200 different types of pressure diecast components have been made from various nonferrous alloys, cast iron and steel.[2] The GKN Group Technological Centre of Great Britain has set about the development of ferrous and other alloys which melt at high temperature with IIT Research Institute as a joint venture in the early 1970's,[3] and the United States' interest in this process has accelerated since the late 1960's and some 400 companies have shown an interest in supporting research into commercial uses of squeeze casting.[3] At the same time, interest in this process was prevalent in Germany and Japan, and some development work has

been conducted in a number of countries. Squeeze casting is still very young in the history of founding and the process itself has been very poorly developed in spite of growing up in a technological world - both in the fields of research and development.

2. Objectives of this study

The casting defects, which include porosity, segregation and shrinkage cavities, cannot be entirely eliminated, even using various heat treatments and metal forming processes.[15] The original casting structure persists and has a marked influence on final properties. Fortunately, the original casting structure which can occur in normal casting processes can be somewhat improved by the addition of pressure in the normal casting process.[16][17] The essential features of the squeeze casting process are that porosity and shrinkage cavities can be eliminated, and that fine equiaxed structures can be obtained.

Some work has been reported on the phenomena of feeding molten metal to shrinkage cavities,[18][19] whereas, the origin of the fine equiaxed grains has not yet sufficiently investigated to show how or when the equiaxed grains begin to form. Generally, it is known that final ingot structures markedly depend on the degree of convection movement in the melt during solidification.[20] However, it is not known whether the application of pressure during solidification promotes convection and whether the convection is the sole mechanism originating the equiaxed zone in the castings solidified under pressure. This work was conducted in

an attempt to ascertain at which stage during solidification under pressure equiaxed grains originate and then help to provide a further understanding of castings solidified under pressure.

3. Scopes of this study

The work was divided into two categories as follows:

(i) Some observation on freezing phenomena by using ammonium chloride solutions as an analogue of a metal system.

(ii) Influence of pressure on macro- and micro-structures of Al-Cu alloys.

Through some observation on freezing phenomena by using the particular apparatus the growth of crystals from the melt was observed and then the influence of pressure on the grain structures were examined in aluminium casting alloys.

(i) Some observation on freezing phenomena by using ammonium chloride solutions as an analogue of a metal system

This part was carried out to investigate the influence of pressure on crystal multiplication by using ammonium chloride solutions. It has been well known that ammonium chloride/water system could be used as an analogue for observing metallic solidification phenomena. It is due to the ammonium chloride freezing in a non-faceted manner and acting as a metal while the water is rejected as impurities or alloying elements.[21] In this work, an ammonium chloride solution having 37% wt. composition was used, and crystallisation phenomena were observed in this solution frozen at atmosphere and under pressure, depending on the pouring temperatures.

A series of photographs of 5 seconds interval were taken for about 4 minutes.

(ii) Influence of hydrostatic pressure on macro- and micro-structures of Al-Cu casting alloys

In this work, typical aluminium base alloys, which solidify over an extended range, i.e., Al-4% Cu alloy and commercial Al-Cu alloy (LM 11), were investigated by solidifying in a cylindrical mold (ϕ50m/m) under hydrostatic pressures. The basic factors, which contribute to improving quality of castings solidified under pressure, were discussed: i.e., die temperature, pressure level and the holding time of the metal in the mold. Pressures were checked by using two pairs of biaxial strain gauges of the foil type. Mold and metal temperatures were checked by using Alumel-Chromel thermocouples connected to a three-pen recorder. The solidification behaviours were considered by observing macroscopic and microscopic structures.

II. GENERAL ASPECTS OF METAL CONSOLIDATION UNDER PRESSURE

1. Mechanics of metal consolidation.
2. Solidification rate and heat conditions.

II. GENERAL ASPECTS OF METAL CONSOLIDATION UNDER PRESSURE

Squeeze casting can be grouped into two types as follows: (i) the process of casting solidified under pressure and (ii) the extrusion casting process. In the first process, molten metal is poured into a permanent mold in the free state and subjected to pressure to consolidate the metal. The pressure forces the molten metal against the mold walls, creating hydrostatic compression without much movement of metal; the only movement being the internal displacements during solidification shrinkage. In the second, i.e., extrusion casting process, a two-stage operation is carried out; the hydrodynamic pressure forms the casting contours when the die cavity is being filled with molten metal and immediately transformed into a constant peak pressure. The actual consolidation begins at the constant peak point. The constant pressure, acting vertically with the full force of the press through the punch on the metal, compacts it, first by crystallisation under pressure and then by plastic deformation, depending on the magnitude of the pressure applied.

The consolidation of metal, either in the process of casting solidified under pressure or in the extrusion casting process, would take place by the same mechanism, except for the movement of molten metal. In order to obtain a clear idea of the mechanism of metal under pressure, therefore, it is convenient to study the phenomena of cylindrical shapes rather than by complex shaped components.

1. Mechanics of metal consolidation[22][23]

The structure of the metal during the primary crystallisation (i.e., the solidification of the melt) markedly affects all the properties

of the casting. Under conditions of conventional casting it is difficult to avoid shrinkage cavities and to control zonal structure due to the difference in solidification rates near the walls and in the centre of the casting. The application of pressure during the primary crystallisation, however, improves the structure and properties of the metal in several ways; (i) by increasing the number of the crystallisation nuclei, (ii) reducing microporosity and shrinkage, (iii) altering the mutual solubilities of the components of the alloys and (iv) suppressing gas nucleation. These reasons can be explained through the mechanics of metal consolidation.

When examining the mechanism of metal consolidation, it is essential to clarify the concept of consolidation. As far as casting requirements are concerned, consolidation is nothing more than the elimination of basic defects; blow holes, porosities and shrinkage cavities. Since all the casting defects mentioned are formed during solidification, it is above all essential to apply pressure during this period. When solidification under pressure is almost complete and the metal is in a solid - liquid or highly plastic state, the period of metal consolidation in the wide sense (i.e., by plastic deformation) can begin.[22]

In this circumstance, the shrinkage cavities become filled, the metal continues to be forced under continuous pressure into areas where intercrystalline microporosity remains and it will be difficult for gases to evolve from solution. The metal consolidation by applying pressure is effected in the temperature range between the temperature at which linear shrinkage starts and the solidus

temperature: when shrinkage cavities form, the surrounding metal contains much of the liquid phase, so that a timely application of the appropriate pressure can extrude metal into these cavities without difficulty. Practically, the pressure must be applied at the start of crystallisation (because evolution of gases is checked a very short time after pressure is applied to the metal) and kept up until a solid - liquid or plastic state has been reached in order that the shrinkage cavities can be eliminated and the metal consolidated. However, elimination of shrinkage cavities and porosity is a much more complex problem, depending on the conditions under which the alloy solidifies and crystallises. The supply of molten metal from within to shrinkage cavities can be explained by the following basic propositions. Shrinkage begins before final solidification of an alloy. Compression of a casting, which determines linear shrinkage, becomes possible only after a rigid crystalline frame has formed. The temperature at which a solid frame forms on a casting is either within the crystallisation range or coincides with the solidus temperature. The curve showing temperature at which linear shrinkage starts, divides the temperature-concentration region between liquidus and solidus into two fundamentally different parts: the upper part, within which the primary crystals are separated from each other by molten metal and in which alloys, being in a liquid-solid state, have the basic properties of a liquid mass, including that of taking the shape of the vessel enclosing them; and a low part, within which the primary crystals form a frame which contains the liquid phase. In this latter part, between the temperature curve for the start of linear shrinkage and the solidus, alloys which are in the solid-liquid state have the basic

properties of a solid body, including that of retaining the shape given to that body.

On the other hand, shrinkage porosity can be explained as follows: unfilled pores remain in the central zone between the dendrites, and within the dendrites between the individual axes; and these alloys show shrinkage porosity instead of shrinkage cavities on transition from the molten to the solid state. Under normal conditions, it is difficult to prevent porosity because the dense mass of dendrites resists the flow of molten metal and the gases evolving from solution also tend to prevent porous areas from filling with metal; Even with enlarged shrinkage head, porosity cannot be eliminated altogether. Under pressure, however, it is not hard to eliminate shrinkage porosity due to accelerating collapse of porosity, while solubility of gases can be increased by increasing pressure (Sievert's law). For example, gas porosity and blow holes are not usually encountered in billets manufactured by crystallisation under pressure, since gases can be held in solution even at low specific pressures ($\% \underline{H}^2 \propto P_{H_2}$).

Some theories on formation of segregation can be discussed in the mechanism of metal consolidation as well. Segregation occurs in normal casting when the casting processes remain incomplete. Both normal and inverse segregation are due to movements of the melt along the channels in the crystalline skeleton due to differences in pressure within the ingot. The pressure differences are produced either by shrinkage and crystallisation or by intensive evolution of gases. The tendency to growing segregation is connected with the temperature range of the solid-liquid state between the liquidus

and the temperature at which linear shrinkage commences. Some studies of ingots under piston pressure have shown that application of pressure during solidification of alloys can be effective in preventing a certain type of segregation. For example, the application of pressure was greatly effective in preventing gravity segregation of sealing rings for automobile cylinders (60% Pb + 2.5%Ni + 37.5%Cu).[24] Pressure increases the movement of solute metal remaining between the axes of the dendrite or between the crystals which separate out at the start of solidification. This can help to reduce dendritic segregation; whereas, extreme normal segregation can be observed under pressure rather than at atmosphere in Al-4.5%Cu casting alloy.[25]

Porosity, shrinkage and segregation mentioned in the above are closely connected with solidification rate. A high solidification rate helps to ensure that most of the metal displacements are completed while the metal is still in the solid-liquid state, before it has had time to solidify completely. The metal displacements by applying pressure during solidification is one of the factors which contribute to an increase in solidification rate and to equalisation of the internal structure. Thus, the Clausius-Clapeyron equation can be considered,

$$\frac{dT}{dP} = \frac{T_M \cdot \Delta V}{\Delta H}$$

where, $\frac{dT}{dp}$ is the amount of change of freezing temperature by the application of pressure, T_M normal freezing temperature, ΔV the change in volume on freezing and ΔH the latent heat of fusion or enthalpy. For example, if the specific pressures are increased by 1500kg/cm^2, 5000kg/cm^2 and 18000kg/cm^2, the corresponding increases

in the liquidus temperature are about 11°C, 71°C and 110°C for aluminium. These experimental values are in good agreements with the values calculated theoretically from Clausius-Claypeyron's equation, and this provides the theoretical basis for the experimental conclusions on the increase in solidification rate when pressure is increased. It forces fresh metal into the cavities between the dendrite branches, overcoming the capillary force which prevent such feeding under normal casting conditions. These help to equalise the structure in all zones and to improve mechanical properties. The pressure transmitted by the punch directly to the metal also has a mechanical effect on structure equalisation. The displacement, contact and mutual pressure of metal crystallites during solidification is another factor insuring a finely divided structure and increased solidification rates.

Solute distribution ahead of an advancing solid-liquid interface can be controlled considerably by hydrostatic compression of the molten metal in the mold. It does not mean, however, that pressure is proportional to diffusion, which is considered to be atomic migration. In fact, it is expected that atomic migration would be slowed down by high pressure:[26] that is, diffusion coefficient for concentration units increases with temperature and decreases with pressure.[27] Generally gaseous diffusion coefficients are in the neighbourhood of $0.1 cm^2/sec$ and liquid diffusion coefficients are nearly always close to $10^{-5} cm^2/sec$.[26] Whereas, diffusion coefficients in solids vary over many orders of magnitude. They are usually very temperature dependent according to the relation $D = Do \exp(-Q/kT)$. Furthermore, the diffusion coefficients

in a given solid are dependent on the structural perfection of the solid,[28]-[31] thermal history,[30] ionising radiation,[32] strain,[33-37] orientation,[38] trace of impurities,[39][40] nearby concentration gradients of other impurities,[41] and hydrostatic pressure.[42] In the squeeze casting process, solidification rate is much quicker than in the normal casting process. Therefore, the castings solidified under pressure have not enough time for diffusion in the liquid state. Diffusion coefficients in the squeeze casting may be mainly considered in the solid state after applying pressure. Generally diffusion coefficients are not greatly influenced by pressure, compared with the influences of temperature in solid state. Diffusion coefficients in solid decrease with increasing pressure, but it is not exponentially dependent upon the increasing pressure. On the contrary, diffusion coefficient increase with increasing temperature and it is exponentially dependent upon the temperature (Appendix A).

Consequently, consolidation under high specific pressures begin when molten or semi-molten metal is forced into the shrinkage cavities and the final consolidation takes place as a result of plastic deformation when it is in the plastic state. This not only eliminates shrinkage defects but also reduces intercrystalline microporosity to some extent, which invariably leads to improved mechanical properties.

2. Solidification rate and heat conditions in casting

The solidification rate K when casting under given conditions of cooling, i.e., at a given mold surface temperature and with a given

material, is found by Lightfoot solidification formulae:

$$x = K\sqrt{t}$$

where K is a constant value

Since the ingot temperature changes during cooling, the mean value of K is adopted:

$$K = \frac{x}{\sqrt{t}}$$

where x is the mean wall thickness it is the solidification time in minutes

It is shown in Fig. II-1 that an 80m/m diameter ingot, cast from Al-11.5% Si alloy, crystallises under atmospheric pressure in about 2.1 minutes, while the solidification time for a similar ingot under 2000kg/cm^2 pressure is reduced to approximately 0.6 minutes: there is a reduction of three times under pressure. This means there is a difference in the solidification rate before and after application of pressure. When metal is held in the mold before applying pressure, it remains molten at the centre and in a semi-molten state near the mold walls. The solidification rate increases substantially from the moment the punch meets the metal, due to the application of pressure and the forcing of metal against the mold walls. In other words, the increase in solidification rate is due to heat exchange between the mold and the casting: when the ingot crystallises under pressure, the metal mold is quickly heated to higher temperature per unit of time, compared with solidification at atmospheric pressure.

Since solidification under pressure produces particularly suitable conditions for rapid metal cooling, this subsidiary factor, as well as the pressure itself,helps to produce alloys with fine grained

structures and improved mechanical properties, and high cooling rates are effective in the casting of alloys containing brittle phases, which solidify as finer crystals under these cooling conditions: for example, the mechanical properties of Al-10%Si alloy by using solidification under piston pressure increases 1.3–1.5 times in tensile strength, 3–4 times in elongation and 2–2.5 times in impact strength.(96)

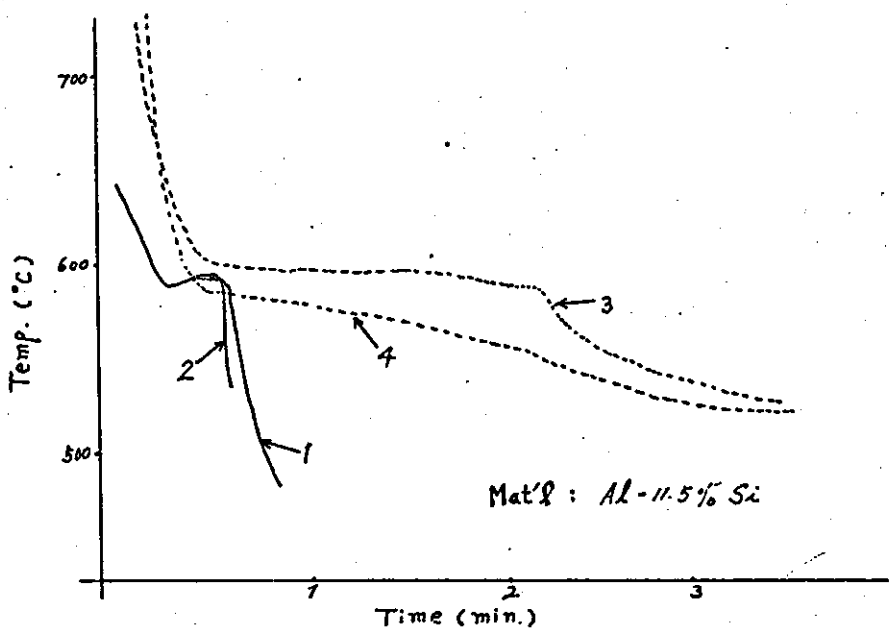

Fig. II-1 Cooling curves for an 80m/m diameter solidification of :-

1. casting centre in 2000kg/cm^2
2. casting periphery in 2000kg/cm^2
3. casting centre in atmosphere
4. casting periphery in atmosphere

In many cases, heat conditions are of decisive importance in casting high quality products by solidification under pressure, just as they are in die-casting. For example, segregation can be somewhat eliminated by selecting the appropriate heat

conditions in casting. Segregation occurs due to the way in which the alloys solidify. When the temperature of the alloys falls below the liquidus, heavily branched dendrites begin to develop rapidly from the basic solid solution, which has a higher temperature than that at which the alloy finally solidifies. Considerable amounts of the readily fusible phase remain in the molten state between the dendrite branches at this time. Since the ingot solidifies in successive stages from the periphery to the centre, conditions arise in which the low melting point phases are displaced into the ingot centre. This leads to an increase in the amount of low melting phase components in the ingot centre: the phenomena of normal segregation. The maximum possible uniformity of solidification can be obtained by pouring the metal into a hot mold coated with a lubricant of low thermal conductivity to reduce heat transfer as well as by applying pressure.

The main purpose of applying pressure is to eliminate the basic casting defects: gas porosity, blow holes, shrinkage cavities and lack of density in the structure. Very low specific pressure is all that is required to eliminate blow holes and gas porosity, but some higher specific pressure is necessary to eliminate shrinkage porosity and cavities. The proper specific pressure to obtain sound structure is greatly dependent upon the system and composition of alloy.

III. A REVIEW OF CRYSTAL GROWTH FROM MELT

1. Interface growth and solute distribution

   1.1 Some considerations of interface growth

   1.2 Solute distribution at steady state

   1.3 Solute distribution at non-steady state

2. Constitutional supercooling and dendritic growth

   2.1 Constitutional supercooling

   2.2 Dendritic growth

   2.3 Dendritic morphology

3. The formation of equiaxed structure

   3.1 Variables affecting the formation of equiaxed grains

   3.2 Equiaxed formation by grain multiplication

   3.3 Equiaxed formation by creating new nuclei.

III. A REVIEW OF DENDRITIC GROWTH FROM MELT

When a metal or alloy is poured into a mold and allowed to solidify, the grain structures may be described in various ways, depending mainly on the rate of heat extraction, the amount of metal and its composition and the potency of the nucleants that are present. The classical picture of the grain structure of a casting or metal has been described schematically in three parts: the outer chill zone, the intermediate columnar zone and the central equiaxed zone.

The presence and extent of these zones in casting structures are now known to depend both on nucleation and on crystal multiplication.[43]

1. Interface growth and solute distribution

On considering the grain structures of castings it is necessary to examine the nature of the interface between the growing solid and the liquid.

1.1 Some considerations of interface growth

Once nucleation has occurred, crystal growth begins and the structure developed can be related to the growth conditions of the solid-liquid interface, in particular to the undercooling. The shape of the solid-liquid interface depends on the temperature distribution during solidification and some undercooling must exist to advance the interface. It is possible to have growth with either a positive or a negative temperature gradient in the liquid, as shown in Fig. III-1.

If the temperature is maintained in the metal as shown by curve (1) of Fig III-1(a), the interface will remain stationary, and if the

situation shown by curve (2) exists, the interface can advance due to some undercooling.

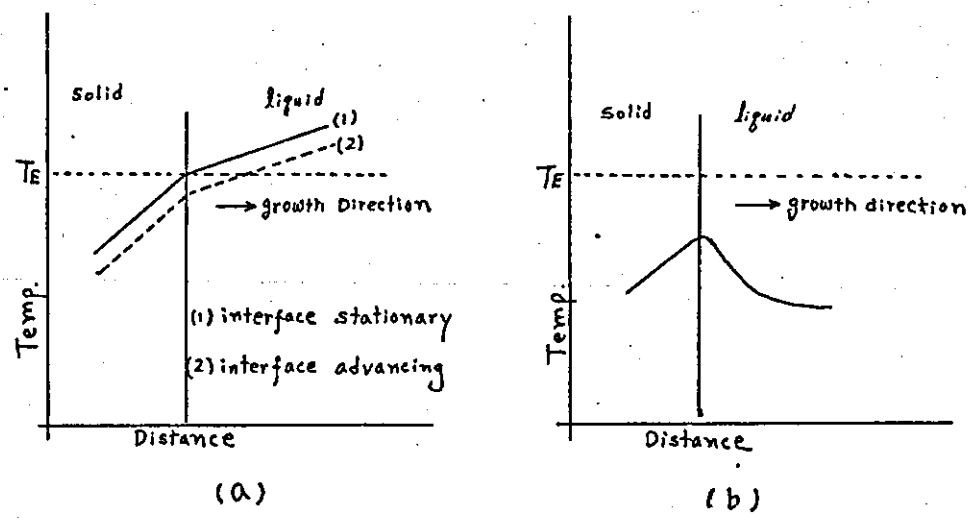

Fig. III-1 Temperature distribution in crystal growth

(a) planar growth with a positive temperature gradient in the liquid.

(b) dendrites growth with a negative temperature gradient in the liquid

When the temperature gradient in the liquid is positive in a pure metal, the interface shows no growth form but is plane and structureless. The resulting solid is not perfect, however, since a macromosaic structure (striations) is usually observed in single crystals. When the temperature gradient is negative as shown in Fig. III-1(b) the liquid ahead of the interface is thermally undercooled, i.e., it is below the thermodynamic freezing temperature, and the structures are dendrites. However, generally dendritic solidification in a pure metal does not occur or is restricted to only a minor fraction of the thickness of the casting because the rate of heat abstraction is slower than the speed of dendritic growth.[44]

In alloys, on the other hand, the undercooling will be produced indirectly by changes in temperature and composition: that is, constitutional supercooling. This type of undercooling is primarily the result of the difference in composition between the solid and liquid phases during solidification. This difference in composition not only produces undercooling when the temperature conditions are suitable but also it is responsible for the segregation that exists in the final solid alloy.

In the absence of constitutional supercooling, the behaviour growth is essentially the same as that of pure metals with the exception of solute redistribution which is associated with the initial and final transients in the solidification process. The existence of a zone of constitutional supercooling ahead of the interface will make an initially planar interface unstable and prone to perturbation in shape. The transition from stability to instability can be shown when the slope of the actual temperature is made equal to the slope of the liquidus temperature curve at the interface. This will be discussed in the following section of constitutional supercooling.

Interface growth by undercooling has been limited to either steady state or transients which monotonically approach steady state: e.g., the supercooling theory has dealt with the question of which state, solid or liquid, is thermodynamically stable in front of an initially plane front interface. The nature of interface growth, however, is not always so simple as to provide these conditions. Fluctuating and periodic growth phenomena are not only frequently observed but are often very difficult to avoid. As a result, a quite different approach to the problem of interface breakdown has been recently

considered, concerned with whether a state is dynamically achievable: a dynamical approach as to whether the perturbation in plane front growth will grow or shrink depends on the interaction of the perturbed solute and thermal fields, on liquid-solid surface energy, and on interface kinetics. This treatment has some advantages, particularly since it predicts some of the parameters, e.g., cell size, which were not treated in the original analysis of constitutional supercooling.[45] Mulins and Sekerka[46]-[49] have studied this point of view. Although many explanations have been devised for these phenomena, it appears that many questions remain unanswered due to the handicap of basic experimental difficulty and mathematical complexity. Thus, the recent direct observations of interface behaviour in inorganic or organic analogues of metals[50][51] and in thin films in the electron microscope,[52] have given valuable confirmation of the different theoretical mechanisms.

1.2 Solute distribution at steady state (low growth rates)

The distribution of solute in the solid, when solidification is complete, is different from that in the liquid, although the total amount of solute is unchanged. This leads to solute segregation on both a microscale and a macroscale. There are two extreme cases in solute redistribution. First, the solute increase may disperse in the liquid by diffusion only. Alternatively, conditions of mixing by convection may exist in the liquid which rapidly spread the excess solute throughout the bulk of the liquid. The following equations, which deal with the quantitative aspects of solute redistribution in normal solidification, employ the assumptions of equilibrium at the liquid-solid interface and no significant undercooling before nucleation or from effect of curvature of the liquid-solid interface.

(i) Solute distribution by diffusion only

Tiller[53] and others mathematically analysed the solute segregation produced in the solid and liquid during solidification.

Using the assumptions:-

(a) convection in the liquid is negligible

(b) Diffusion in the solid is negligible

(c) Initial composition (Co) is constant in the solid

(d) Interface is planar and its temperature is in solidus line

(e) The value of the equilibrium partition ratio (ko) is constant

Under these conditions the solid being deposited must have a composition Co and the form of the solute distribution will be as shown in Fig. III-2.

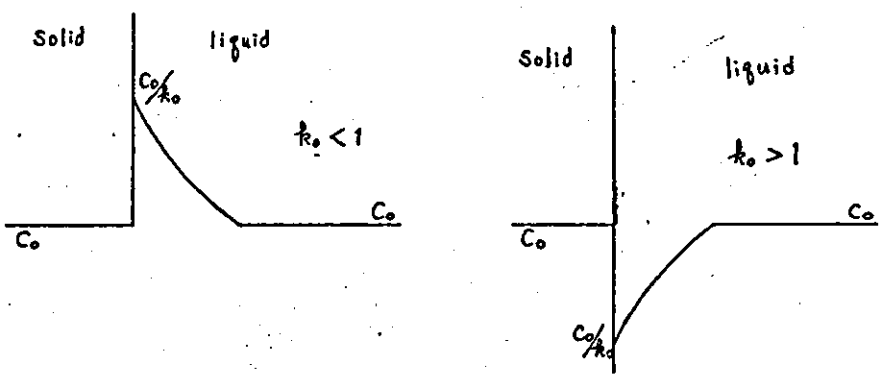

Fig. III-2 The solute profile ahead of the interface during steady-state solidification with solute re-distribution by diffusion only

The amount of solute being rejected at the interface by solidification, should be equal to the amount that diffuses away

from it, and Fick's 2nd law can be considered in this case;

$-\frac{\partial C}{\partial t} = -D\left(\frac{\partial^2 C}{\partial x^2}\right)$ and thus the solute velocity (R) to move in the liquid is $\frac{\partial x}{\partial t}$.

The steady state differential equation describing the solute flow in the liquid is, therefore,

$$D\left(\frac{\partial^2 C}{\partial x^2}\right) + R\left(\frac{\partial C}{\partial x}\right) = 0 \qquad \text{(III-1)}$$

This has a general solution

$$C = A + B \exp\left(-\frac{Rx}{D}\right)$$

Applying the boundary conditions

$$C_L = C_0 \quad \text{at} \quad x \longrightarrow \infty$$

$$C_L = C_0/k_0 \quad \text{at} \quad x \longrightarrow 0$$

Substitution in the equation of general solution gives the result

$$C_L = C_0\left[1 + \frac{1-k_0}{k_0}\exp\left(-\frac{R}{D}x\right)\right] \qquad \text{(III-2)}$$

(ii) Solute distribution by complete mixing in the liquid

This condition leads to maximum segregation during normal freezing.

Using the assumptions:-

(a) No diffusion in the solid

(b) Complete mixing in the liquid

(c) ko is constant

The form of the final solute distribution in the solid has been analysed by Pfann.[54] The solute profile is given by

$$C_S = C_0(1-g)^{k_0-1}\cdot k_0 \qquad \text{(III-3)}$$

where g is the fraction solid.

Since no diffusion in the solid is assumed, the average liquid composition after a fraction g has solidified must be

$$C_L = C_0(1-g)^{k_0-1} \qquad \text{(III-4)}$$

(iii) Solute distribution by partial mixing in the liquid

The case of partial mixing in the liquid can be solved approximately by assuming that the liquid is completely mixed except for a stagnant layer immediately in front of the interface; that is, there is a sufficient convection to ensure uniformity beyond the stagnant layer δ at the interface which is gradually broken down by the stirring effects (Fig. III-3).

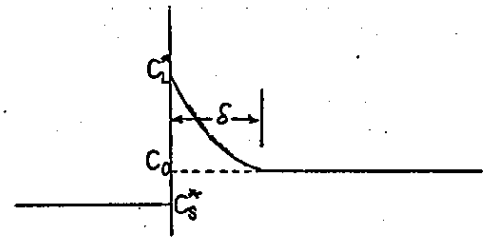

Fig. III-3 The effect of the partial mixing on the nature of the solute layer at the interface.

The solute distribution in the solid is then given by the equation of complete mixing except that the ko is replaced by k_E (effective partition ratio)

$$C_S = k_E C_0 (1-g)^{k_E - 1} \qquad (III-5)$$

Burton[55] and others derived an expression for k_E as a function of R. D. ko and δ. They assumed that the equation of the solute distribution in the liquid by diffusion could only be applied in the stagnant layer up to a value of $x = \delta$, and the equation of the solute distribution by partial

mixing is given by

$$k_E = \frac{k_0}{k_0 + (1-k_0)\exp(-\frac{R}{D}\delta)} \qquad \text{(III-6)}$$

by using the boundary conditions

$C_L = C_s^*$ at $x \longrightarrow \infty$

$C_L = C_L^*$ at $x \longrightarrow o$

$C_L = C_o$ at $x \longrightarrow \delta$

where, C_s^* and C_L^* are interface composition in solid and liquid.

Experimental determination of solute distributions under different conditions of mixing have been carried out using various techniques, i.e., by microanalysis of a rapidly quenched specimen under conditions of no mixing in the liquid,[56] by using radiography for the directly continuous observation of the interface[57] and by directionally solidifying Sn alloys containing radioactive tracers.[58]

1.3 Solute distribution at non-steady state

While the diffusion process of solute distribution is effective at low growth rates and for high values of diffusion coefficient, it is not appreciable at high growth rates or for low values of diffusion coefficient. Generally the total amount of solute incorporated into the stagnant layer increases as the growth rates decrease and the diffusion coefficient increases, as shown in Fig. III-4.

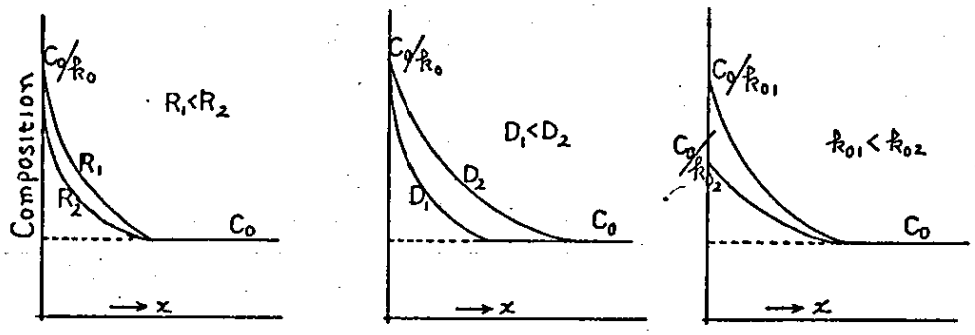

(a) growth rate (b) diffusivity (c) partition ratio

Fig. III-4 Changes in the solute concentration ahead of a growing interface for changes in the growth parameters.

Fig. III-4 illustrates, schematically, the way the solute concentration profile changes in front of the interface with changes in the variables R, D and ko (<1), respectively. It is seen that a short, steep pile-up is produced at high growth rates and for low solute diffusion coefficients. Of particular importance are the extreme solute accumulations that can occur near the interface for systems in which ko is very small. For solute concentrations higher than about 0.5% the solute pile-up effects are very marked and the physical nature of the interface alters to a non-planar configuration. Under these conditions, the foregoing equations which are mentioned in the solute distribution at steady state are no longer valid, although they can be used to give some approximate indication of the solute distribution near the interface.

Considering the changes of the localised solute distribution in the solid by changing the growth rates, the effects are shown in Fig. III-5.

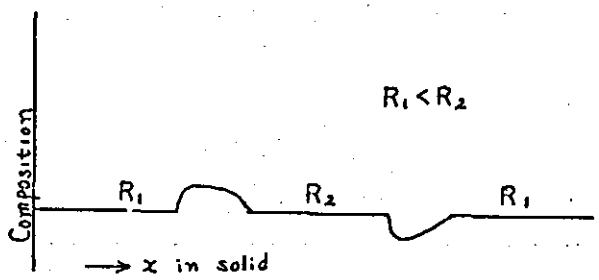

Fig. III-5 The effect of changes in the growth rate on the localised solute distribution in the solid.

Thus, if a fluctuation in the growth rate occurs during solidification of an alloy with $k_o < 1$, the amount of solute in the interface pile-up will need to increase when the growth rate slows down, or to decrease when the growth rate speeds up. These changes will lead to a localised deviation from the steady state while the solute pile-up changes. The need for an increase in the amount of solute in the pile-up with a decreased growth rate means a local decrease in the amount of solute deposited in the solid as the growth rate changes. Thus a region depleted in solute will appear in the solid. The reverse is true if the growth rate is increased.

Calculation of solute redistribution at non-steady state needs to be done using the time-dependent form, and the non-steady state differential equation describing the solute flow in the liquid is therefore, obtained by modifying the above equation (III-1),

$$D\frac{\partial^2 C}{\partial x^2} + R\frac{\partial C}{\partial x} = \frac{\partial C}{\partial t} \qquad \text{(III-7)}$$

Smith[59] and others have obtained an exact solution for this case using the above differential equation and with the steady state solute distribution at initial interface velocity as initial boundary conditions. The results were that the characteristic length ($\frac{D}{k_o R}$) of the perturbations that form is much greater than D/R for small ko and increases with decreasing ko as in the initial transient. Also, as would be expected intuitively, the maximum solute content in the banded region increases with increasing velocity change. Mollard and Flemings[60] have studied the solute distribution of two-phase composite alloy/at non-steady state. Their experimental results confirmed the foregoing and showed that concomitant with the increase in velocity is also an abrupt decrease in lamellar spacing. Briefly they concluded as follows:-

(i) Changes in either growth rate or thickness of convective boundary layer δ will result in local variations of composition.

(ii) Changes in growth rate will change both lamellar spacing and composition, while changes in δ will change only composition.

2. Constitutional supercooling and dendritic growth

Most dendritic structures in alloys are the result of undercooling produced by constitutional means, and can be controlled by heat and/or mass transports. If the undercooling is increased by a critical amount over that required for cell formation, all the cells begin to branch and form an array of dendrites; a change to the dendritic structure can be obtained by introducing more thermal and constitutional supercooling.

2.1 Constitutional supercooling

If a possible temperature gradient is maintained in the liquid during growth (Fig. III-1(a)), the interface may be planar and the segregation patterns described in the solute distribution at steady-state may occur. However, if solidification occurs at so fast a rate that the atoms cannot diffuse sufficiently to produce compositional equilibrium, a concentration gradient is set-up in the liquid adjacent to the advancing solid-liquid interface. This build-up is produced by the local enrichment of the liquid with impurities or a second alloy element, as shown in Fig. III-6, depending on the type of equilibrium diagram.

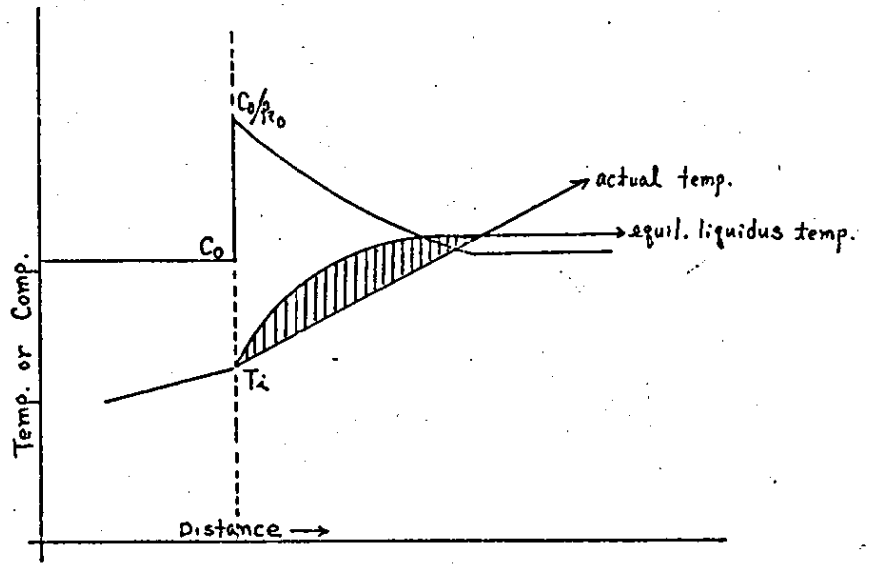

Fig. III-6 Constitutional supercooling ahead of an interface

Thus, Chalmers and coworkers[53][61] pointed out that the solute accumulation, which exists ahead of the interface when no mixing or no convection occur in the liquid, could lead to constitutional

supercooling. Considering the case of no mixing in the liquid, the solute distribution ahead of the interface is given by

$$C_L = C_o \left[1 + \frac{1-ko}{ko} \exp \left(- \frac{R}{D} x\right) \right]$$

The build-up of solute in the liquid at the interface reduces the liquidus temperature of this portion in the melt and each composition in the liquid ahead of the interface has a particular liquidus temperature as shown in Fig. III-6. The equilibrium liquidus temperature (T_L) is given by

$$T_L = T_m - mC_L \qquad \text{(III-8)}$$

where T_m is the melting point of the pure metal and m is the slope of the liquidus line in the phase diagram. For a solute distribution, the equilibrium liquidus temperature corresponding to different points ahead of the interface will then be,

$$T_L = T_m - mCo \left[1 + \frac{1-ko}{ko} \exp \left(- \frac{R}{D} x\right)\right] \qquad \text{(III-9)}$$

For the steady-state solidification of an alloy of initial composition (Co), the interface temperature (T_i) is

$$T_i = T_m - \frac{mCo}{ko} \qquad \text{(III-10)}$$

Thus, the liquidus temperature can be rewritten as

$$T_L = T_i + \frac{mCo\ (1-ko)}{ko} \left[1 - \exp \left(- \frac{R}{D} x\right)\right] \qquad \text{(III-11)}$$

The actual temperature in the liquid, on the other hand, is given by

$$T = T_i + Gx \qquad \text{(III-12)}$$

where G is the temperature gradient in the liquid ahead of the interface.

When the actual temperature is superimposed upon the curve for equilibrium liquidus temperature, as in Fig. III-6, part of the liquid is below its normal liquidus temperature. This undercooling, termed constitutional supercooling, is a direct result of the concentration gradient that exists in the liquid. The zone of constitutional supercooling can be eliminated if the slope of the actual temperature is made equal to or greater than the slope of the liquidus temperature curve at the interface. Thus for no constitutional supercooling the following relationship is required,

$$G > \left(\frac{dT_L}{dx}\right)_{X=o} \qquad \text{(III-13)}$$

By differentiating the equation of equilibrium liquidus temperatures, the following condition is easily shown,

$$\frac{G}{R} > \frac{mCo(1-ko)}{D\ \ ko} \qquad \text{(III-14)}$$

The terms in the above equation are grouped with growth parameters on the left-hand side, and material and system parameters on the right-hand side. The nature of this equation allows one to define conditions under which constitutional supercooling occurs. These are:

(i) low temperature in the liquid

(ii) fast growth rates

(iii) steep liquidus lines

(iv) high alloy contents

(v) low diffusion coefficients in the liquid

(vi) very low ko for ko < 1 or very high ko for ko > 1

The exactness and theoretical validity of the constitutional supercooling criterion have been criticised on the basis that it was deduced by the application of equilibrium arguments to a dynamic system;[49] the above constitutional supercooling criterion is applicable only for unstirred system. For stirred melt, Hurle[62] and Bardsley[63] have shown that, by appropriately changing the boundary conditions in the equation of solute distrbution by diffusion only, the results can be described by the condition,

$$\left(\frac{dT}{dx}\right)_o \geq mCo \cdot \left(\frac{1-ko}{ko}\right)\frac{Rk_E}{D} \qquad \text{(III-15)}$$

On the other hand, Mullins and Sekerka[61] have theoretically studied the growth or decay of perturbations in shape of the surface. Their techniques were to calculate the time dependence of the amplitude of a perturbation which was introduced into the shape of the planar interface; if the amplititude increases, the interface is unstable and so on. They derived the criterion that instability occurs when

$$m\left(\frac{\partial C}{\partial x}\right)_0 - \left(\frac{2}{K_S + K_L}\right)(K_S G_S + K_L G_L) > b \qquad \text{(III-16)}$$

compared with the constitutional supercooling criterion of

$$m\left(\frac{\partial C}{\partial x}\right)_0 - G_L > 0 \quad \text{for instability}$$

where b arises from the surface tension (capillarity) between solid and liquid, which tends to keep the interface planar.

Experimentally b has been found to be negligible for many systems[62] but at high growth velocity it cannot be neglected due to the

surface energy. The plot of G/R versus Co for Mullins-Sekerka criterion by considering the surface energy is shown in Fig. III-7.

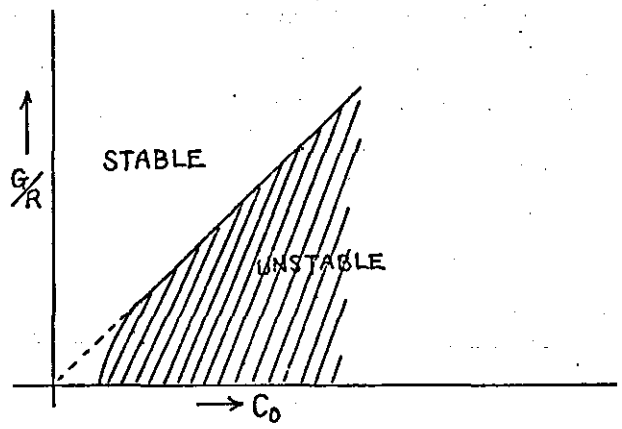

Fig. III-7 The plot of G/R versus Co for stability/instability

They also predicted that there is a critical velocity, dependent on the interfacial tension, above which instability is impossible and the region of absolute stability would exist when

$$\frac{k_o T_m \gamma R^2}{m \left(\frac{\partial c}{\partial x}\right)_o D^2 L} \geq 1 \qquad \text{(III-17)}$$

This will occur at high growth velocities when the surface energy effect will completely dominate the solute effect.[65] Sharp and Hellawell[64] measured the cell spacing in Al-Cu alloys which had been undirectionally grown at accelerating growth rates and quenched immediately after breakdown. They compared their results with the wave length of fastest growing perturbation predicted by the Mullins and Sekerka analysis. A satisfactory agreement could be obtained only if the surface energy was assumed to have a very high value. They suggested that a more reasonable value for the surface energy could be used to give a good correlation with the experimental results if a correlation factor was included in the analysis to take account of the interface shape transition during breakdown.

2.2 Dendritic growth

The constitutional supercooling criteria which were mentioned closely predict conditions required to initiate breakdown of a plane front in metals solidifying without facet formation.

As the growth velocity is increased, the changing shape of the growth structure will be proceeded by the sketch shown in Fig. III-8.[66]

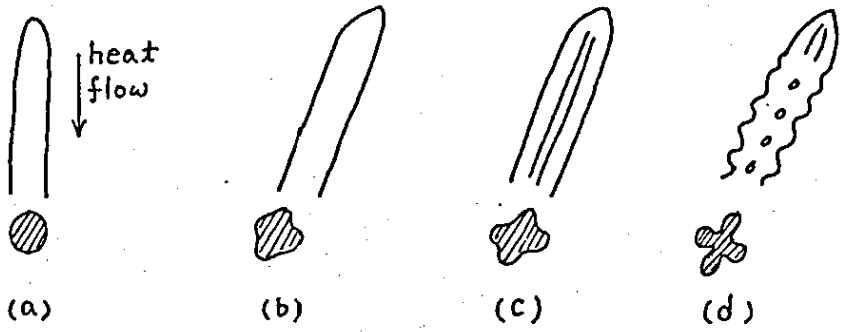

Fig. III-8 Sketch of the changing shape of the growth structure as the growth velocity is increased.

(a) regular cell growing at low velocity

(b) regular cell growing in <100> dendrite direction

(c) flanged-cell or cellular dendrite

(d) dendrite exhibiting the start of periodic lateral branch

At low degrees of constitutional supercooling a cellular interface develops from the planar interface after first becoming pock-marked and then showing elongated cells. As the degree of supercooling increases the cell caps become extended and eventually branch to form cellular dendrites. Practically, the constitutional supercooling required to breakdown a plane front in metals solidifying without facet formation, is so small that it is within

experimental error.[67] It is, therefore, difficult to observe the cellular and/or cellular dendrites structures without controlling the growth velocity. In normal solidification, this kind of supercooling required for growth can usually be ignored, because it is small compared with the temperature gradient that must be present to remove the latent heat of fusion that is liberated when liquid transforms to solid. It follows that the overall rate at which crystals grow is governed by the rate at which heat is extracted from the region where growth takes place: the rate at which solid is formed in a cooling melt is determined by the rate at which the latent heat is removed. Free dendritic growth usually takes place in this case where the latent heat is conducted from the growing crystal into the liquid. The conditions for cell formation, cellular dendritic and free dendritic growth in alloys are shown in Fig. III-9.

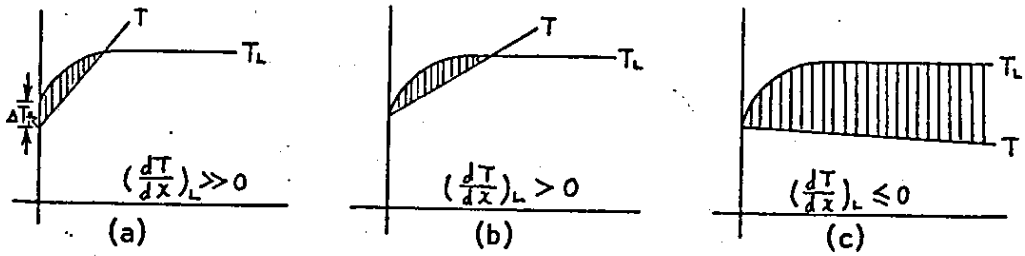

Fig. III-9 The effect of the extent of supercooled layer on the formation of structures in alloys.

(a) condition for cell formation

(b) condition for cellular dendritic growth

(c) condition for free dendritic growth

Free dendritic growth takes place in the case with negative temperature gradient in the liquid as shown in Fig. III-9(c). This implies that the whole of the liquid would be supercooled by an

amount that could be very large, tens or hundreds of degrees[68] while the temperature of the cellular dendritic interface is within a few degrees of the equilibrium liquidus temperature. This difference increases with increasing rate of heat extraction. When the liquid is poured into a mould, the heat is extracted through the mold wall, and a heat balance on a unit area of the solid-liquid interface indicates,

$$K_s\left(\frac{\partial T}{\partial x}\right)_s - K_L\left(\frac{\partial T}{\partial x}\right)_L = -Q_f V_i \qquad \text{(III-18)}$$

assuming that the temperature of the interface remains constant. Where Ks, K_L are the thermal conductivities in the solid and the liquid, V_i is the velocity of the interface and Q_f is the heat required for fusion ($-Q_f$ is the heat liberated on freezing).

Considering the effect of solute in an alloy on dendritic growth, in an isothermal system the solid can grow only as fast as the solute rejected diffuses away from the interface. This is because heat has a diffusion coefficient roughly 10^4 times greater than the solute and so getting rid of the heat is no longer rate controlling. Generally, an equation for the velocity of the advancing interface in an alloy is given by,

$$V = -\frac{D_L}{C_L - C_S}(\nabla C)_\eta \qquad \text{(III-19)}$$

Thus, D_L replaces the thermal conductivity (K_L), and the solute ($C_L - C_S$) that must be removed per unit volume converted from liquid to solid, replaces the heat (Q_f) that must be removed per unit volume converted from liquid to solid. There is one major difference between pure metals and alloys. In pure metal, the rate of

growth is controlled by the rate at which heat is conducted out into the surrounding liquid, while, in the alloy, the growth rate is mainly controlled by the rate of the solute which is diffused away from the interface. In the case of the alloy, diffusion of the solute, which is inherently a much slower process than the conduction of heat, is limiting, and so the dendrites grow much more slowly than in pure metal. It is, therefore, much easier to observe the dendrite structure in alloys than in pure metals. The solute distribution between the dendrites in alloys, occurs in the same way as for cellular dendrites, because the process would be essentially no different, except for a negative temperature gradient in the liquid. It can be, therefore, explained by the constitutional supercooling criteria discussed in the previous section.

2.3 Dendrite morphology

Dendritic solidification is characterised by a morphology resulting from the growth of long, thin spikes in specific crystallographic directions, with regular branches in other equivalent directions.[69] The branching habit extends to secondary, tertiary and sometimes higher orders. In face-centred and body-centred cubic structures, dendritic growth is observed to take place in the cube directions, of which there are three that are mutually perpendicular. The main qualitative experimental observations are: (a) that dendritic growth takes place when the melt is supercooled, (b) that the directions of growth are always strictly crystallographic, (c) branching occurs at roughly regular spacing, and that only a small proportion of the liquid is solidified in this way.

For quantitative observations, the following four aspects can account for dendritic growth; they are: (a) total amount of solid formed as a function of initial supercooling of the liquid, (b) direction of growth in relation to the structure, (c) spacing and relative lengths of the branches, and (d) speed of growth as a function of the temperature of the liquid.

(i) Direction of dendritic growth

It was pointed out by Weinberg and Chalmers[70] that the arms of dendrites always grow in crystallographically determined directions : e.g., <100> dendritic growth for F.C.C. and B.C.C., <110> for B.C.T., and $<10\bar{1}0>$ for H.C.P. However, the general explanation for the crystallographic features of dendritic growth must be related to anisotropy of the relationship between growth rate and kinetic driving force.

(ii) Speed of growth

The problem of predicting the speed of growth as a function of undercooling has not yet been solved satisfactorily. Jackson[71] has stated the problem in the following terms. The total supercooling of the ambient liquid may be regarded as being divided into three parts: (a) the temperature difference (ΔT_c) between the interface and the liquid remote from the interface, (b) the difference (ΔT_R) in temperature between the interface and its equilibrium temperature, and (c) the difference (ΔT_r) between the equilibrium temperature of the tip and that for a planar interface. If there is a steady state rate of advance it will occur when all three parts of the supercooling have constant values. However, it is unlikely that steady

state conditions can be achieved in dendritic growth, because the size of the dendrite tip and the temperature distribution around it may fluctuate in a periodic manner. Mullins and Sekerka[46] suggested that the tip should grow until it becomes large enough to be unstable, and then breakdown into a number of separate tips, each of smaller radius, as shown in Fig. III-10.

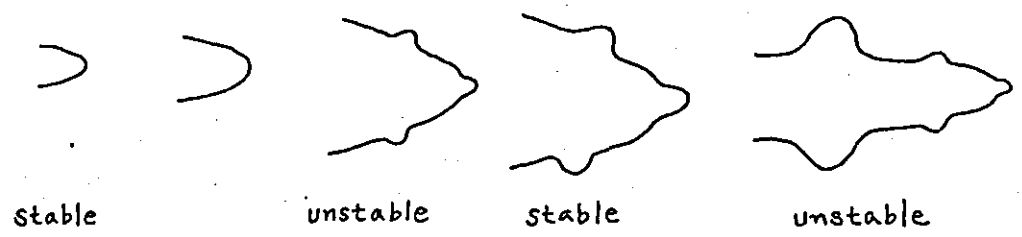

Fig. III-10 Branching of dendrites

The finer the dendrite tip becomes the faster it grows but for any given degree of undercooling there exists a critical radius (r^*). If the tip radius (r) gets much larger than $2r^*$ the tip breaks up into two growing tips, while if the tip radius gets much below $2r^*$ the velocity drops towards zero: Those bumps which develop most rapidly are those with a radius of roughly $2r^*$.

On the other hand, if it is assumed that the tip radius approaches a critical radius, surface tension plays a dominant role.[72] This means that if $r \rightarrow r^*$, the velocity of the dendritic growth depends mainly upon the surface tension, rather than upon the supercoolings which have been discussed by means of satisfying diffusion conditions during solidification. In this case, unfortunately any theory based on steady state growth can be at best an approximation.

(iii) Spacing of dendrite arms

Dendrite morphology in usual casting processes remains largely unchanged over wide ranges of cooling rate. It simply becomes finer as heat is extracted at greater rate. One exception to this rule is that at very high cooling rates, when primary arm spacing becomes very small, secondary and tertiary arms may be absent. The mechanism of spacing adjustment is similar to that by which cells adjust their spacing. The driving force is the constitutional supercooling in the region between the two primary dendrite arms. Primary dendrite arm spacing depends on the product of thermal gradient and growth rate GR, as does cellular spacing, and results which have been reported correlate well with this parameter.[97][98]

Secondary dendrite arm spacings also depend directly on cooling rate, for both columnar and equiaxed grains. Results are plotted either versus average cooling rate during solidification time t_f. The resulting plots are closely similar since

$$t_f = \frac{\Delta T_s}{GR} \qquad \text{(III-20)}$$

where ΔT_s is the non-equilibrium temperature range of solidification. Relationships found between dendrite arm spacing and thermal variables have the form,

$$d = a t_f^n = b(GR)^{-n} \qquad \text{(III-21)}$$

where the exponent n is in the range of 1/3 to 1/2 for secondary spacings and generally very close to 1/2 for primary spacings. Whereas the final secondary dendrite arm spacing is

usually much coarser than the one that forms initially. When this coarsening proceeds to a significant extent, some mechanism other than simple constitutional supercooling determining the final spacing must be looked for. Theroretical study has been made of the morphology of coarsening by Fleming et al.[73] Constitutional supercooling, which was sufficient near the dendrite tip to form the arms, is reduced to such a low value back from the tips that the effect of the radius of curvature on melting point becomes relatively more important. The result is remelting of some of the arms. The coarsening process influence dendrite structures in other ways than simply by altering final dendrite arm spacing. One effect is to decrease microsegregation.

Finally, it is necessary to refer to the stages of dendrite growth during solidification: at first the liquid can solidify dendritically, but later it can solidify only by the extraction of heat from the solidifying material and the heat would be removed by conduction through the solid which had already formed. It was shown by Weinberg and Chalmers[70] that the "filling-in" stage is much slower than the dendritic growth.

3. The Formation of equiaxed structure

The structure of a casting is of great importance since many material properties, especially mechanical properties, depend on grain shape and size. Investigations into the mechanism of formation of the equiaxed zone have been carried out by many workers.[74]-[78]

Nevertheless, there is no conclusive evidence in support of any

of the mechanism proposed for equiaxed grain formation. The significant mechanisms are grain multiplication by the melting-off of the arms of growing columnar dendrites, and dendrite fragmentation by the tearing-off of the arms due to the shear stresses exerted by the flowing liquid. It has been considered that the principal mechanism for producing the nuclei for equiaxed formation is dendrite remelting, although dendrite mechanical deformation and fracture can occur to some degree, in normal solidification. On solidifying under pressure, however, the dendrite fragmentation by the shear stresses will be an important factor for forming equiaxed grains.

3.1 Variables affecting the formation of equiaxed grains

The formation of an equiaxed zone depends on (i) the presence of nuclei in the liquid ahead of the liquid-solid interface and (ii) conditions in the liquid being such that the nuclei will grow. Much work has been carried out to determine the origin of nuclei in the equiaxed zone, but there is no conclusive or unique mechanism for this formation. It is generally accepted that the formation of this zone occurs by the growth of crystal nuclei in the melt ahead of the columnar interface and by the creation of crystal nuclei in the melt. These kinds of nuclei may be formed by the influences of the variables which are superheat, alloy element, solute concentration, convection and so on.

(i) Superheat

Fig. III-11, 12 show Chalmers experimental results in Al-Cu and Cu alloys cast in a standard graphite mold (ϕ2" x 3" height).

The grain size of the equiaxed zone was found to decrease as the pouring temperature was lowered as shown in Fig.III-11. Below a certain pouring temperature the casting consisted entirely of equiaxed crystals and as the pouring temperature increased the columnar zone increased as shown in Fig. III-12. The results can be used not only as the basis for an explanation of the sequence of processes that occur during solidification in a mold, but also as useful data to predict the grain structures of a casting. Practically it is difficult to predict the formation of the equiaxed zone. This is because so many different aspects of the process can vary: because the various physical parameters, such as temperature gradient, heat capacity and diffusion time, depend in quite different ways on the dimensions of the mold.

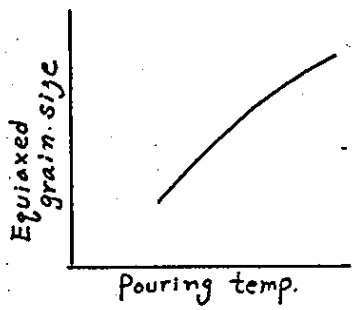

Fig. III-11
Variation of equiaxed grain size with pouring temperature (79).

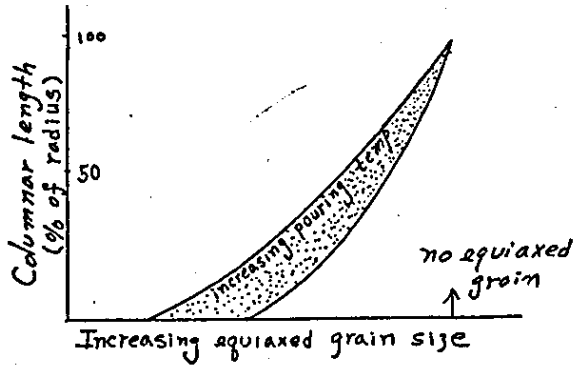

Fig. III-12
Variation of columnar length with pouring temperature and equiaxed grain size (79)

(ii) Solute concentration

The effect of solute concentration on the columnar to equiaxed transition is complex. It is generally assumed that increasing the solute concentration promotes equiaxed zone formation and

and retards columnar growth (from Chalmers experimental results).

(iii) Alloy elements

Tarshis, Walker and Rutter[75] studied the effect of different solute elements on the grain structure of Al and Ni castings. The grain size of the castings were measured and plotted against the parameter $P = \frac{m(1-k_0)}{k_0} C_\infty$. Their results showed a marked change in the grain structure as a function of this parameter, as shown in Fig. III-13 for Al alloys including various elements each 1 atomic percent.

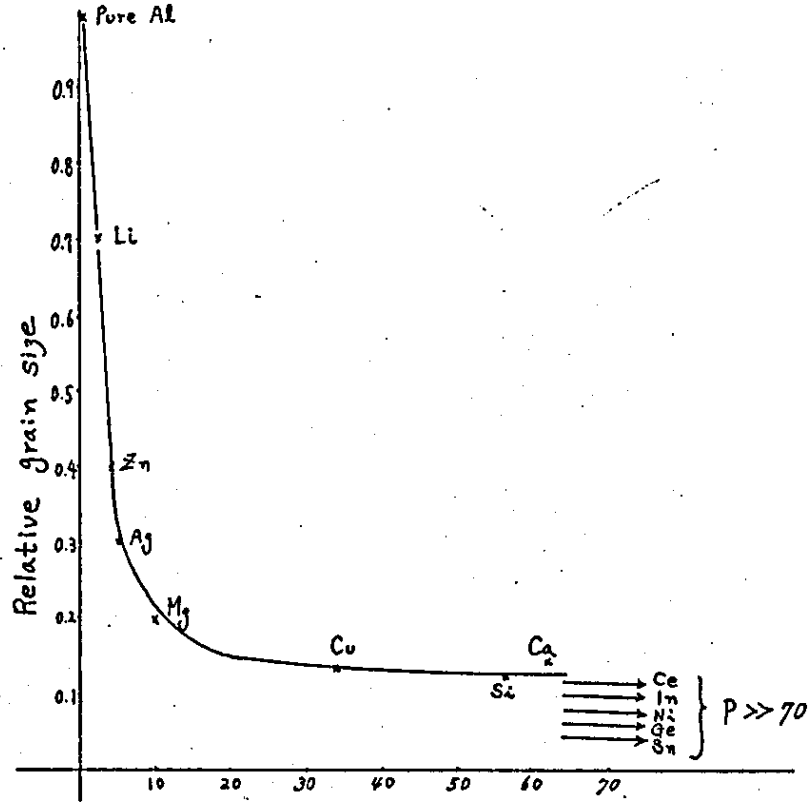

FIG. III-13 Variation in grain size of Al binary alloys for different alloying elements (1 at %)

No explanation was given for the use of $P = \frac{m(1-k_o)}{k_o} C_\infty$, but it is the parameter of an alloy that determines the conditions for breakdown of a planar interface and the possible development of constitutional supercooling.

(iv) Convection

The columnar to equiaxed transition is markedly effected by the temperature profile in the liquid which is determined by thermal conduction and convection. The amount of convection in a casting represented by the maximum velocity (Vm) of fluid flow past an advancing liquid-solid interface, has been shown by Cole and Bolling[80] to be approximately given by

$$V_m \approx K \ H^3 \ G_L$$

where K is a constant, H is the height of liquid and G_L is the imposed temperature gradient in the liquid. The amount of convection decreases with the increasing temperature gradient (G_L): a higher temperature gradient in the liquid prevents the columnar to equiaxed transition. Uhlmann[81] et al cast Al-2% Cu alloys into graphite molds (ϕ5cm x12.5cm H) at different superheats, some in the presence of a magnetic field. This has been shown to reduce convective motion in a liquid metal. They observed that above a certain superheat and with a sufficiently strong magnetic field the equiaxed zone could be eliminated. Below this superheat, the casting was equiaxed even in the presence of the magnetic field. Cole and Bolling[82] passed an electric current through a undirectional casting across which was a magnetic field.

This arrangement gave increased fluid flow down the liquid-solid interface. They observed a layer equiaxed zone and a more rapid temperature drop in the liquid in the presence of the field and the current.

3.2 Grain multiplication

Mechanisms previousiy suggested for the establishment of final dendrite arm spacing in alloys had generally assumed that all arms that form are stable throughout solidification. However, it has now been apparent that the dendrite formed at the start of solidification is highly unstable. Jackson[74] et al suggested that the equiaxed zone could be formed from crystals which arose from the partial remelting of dendrites and could occur under isothermal conditions as a result of surface energy. Some observations on alloys and organic materials, which solidified in similar ways to metals, showed that dendrite arms could melt off as a result of growth rate fluctuations during solidification. The growth rate fluctuations were assumed to occur in casting as a result of convection. Flemings[73] et al suggested that one way in which the remelting can occur would be by the coarsening of dendrite structure during solidification as well as during isothermal holding, and that driving force for the coarsening is a reduction of liquid-solid surface area. They also proposed that the growth rate fluctuations by convection would accelerate the melting-off of dendrites, as shown experimentally by Jackson et al.

Before examining the columnar to equiaxed transition by this mechanism and not by creating new nucleii, it is essential to set up a terminological difference between grain multiplication and dendrite fragmentation in this subject. This is because the transition when solidifying under pressure may be different from those in normal solidification.

Grain multiplication will be defined as the case when new crystals occur by the melting-off of the growing crystals due to temperature fluctuations in the moving liquid, and dendrite fragmentation will be the case when new crystals mainly grow from fragments torn off the existing dendrites by the shear stresses exerted by the flowing liquid. Generally, the original source of occurrence of the new crystals, in both cases, can be traced back to the motion of liquid by superheat and by thermal and solute convection as mentioned in the previous section. However, as a means of creating the new crystals, dendrite fragmentation will be different from remelting: that is, dendrite fragmentation mainly occurs by the shear stresses in the liquid-solid interfaces. In normal castings, the production of new crystals for equiaxed formation is mainly through dendrite remelting although mechanical deformation and fracture of growing dendrite can occur to some degree.[45] Dendrite fragmentation, which occurs under isothermal conditions as a result of surface energy effects, produced relatively few new crystals over a relatively long time, compared with grain multiplication projected by Jackson's experimental work.[74] Tiller and O'Hara[83] also suggested that

dendrite fragmentation would be difficult, even though a stress on the dendrite as a result of convection could produce new crystals since the yield-point of a metal was negligibly small at its melting point. In solidifying under pressure, however, dendrite fragmentation will be able to play an important part (rather than grain multiplication) in some cases. This is possible because of the increasing shear stresses and extremely rapid solidification so that dendrite remelting cannot take place. This is opposite to normal castings in some respects.

Grain multiplication usually occurs by superheat, volume concentration, thermal and constitutional convections in the wide sense, but they can also be explained by the thermal recalescence occurring due to the latent heat of solidification. This heat induces an upward fluid motion and may carry upward very tiny grains with the ascending flow. This phenomena has been observed by using the analog material of ammonium chloride water solution.[84] Additional verification for the convective flow induced by latent heat liberation has been shown by temperature measurements in ingots of Zn-3% by Cole and Bolling.[85] There was an increase in temperature of about 1°C only when the equiaxed zone forms, while when growth was entirely columnar, the cooling curve showed only the usual plateau at the freezing temperature. Southin[86] found that by applying heat to the top surface of the casting, the surface dendrites and the equiaxed zone could be eliminated. Of course, the columnar to

equiaxed transition could take place by the motions of bubble, dissolved gases, oxides, impurities and so on, in the molten metal. The variation of the equiaxed zone with superheat, convection, volume concentration, recalescence and the motions of heterogenous substances, could also be accounted for by transport manipulations: by the applications of magnetic field, electromagnetic field, vibration, Coriolis field (rotating the convecting fluid), ultrasonic waves, pressure and so on.

The liquid metal movements can be increased or decreased by controlling the transport manipulations mentioned above. When the liquid and solid motions are increased during solidification, heat transfer increases, and thus its change directly influences solute boundary layer thickness (δ) and shear stresses may be developed.[85] For example, when liquid flow motions do not contact the interface, δ extends farther into the liquid, and all solute flow is by conductive processes only. Whereas when they contact the interface, δ becomes narrower and solute flow is by convective as well as by conductive processes. In addition, if the interface is dendritic, shear stresses cannot be supported and dendritic bits may be detached. The application of a stationary magnetic field is one of the methods to reduce heat transfer due to reduced natural convection. A magnetic field decreases heat transfer rate by a viscous-drag effect: that is, the fluid is constrained by Lorentz forces to move in a plane normal to the directions of field and flow. At large magnetic field,

therefore, the liquid metal transfers heat by conduction only. As the field strength is decreased below a critical value, convective flow begins to transport heat from the inner to the outer wall, and the temperature difference across the layer decreases. With further reductions in the field, convection increases and the temperature difference decreases further. The influences of magnetic field strengths on convection and temperature fluctuation is shown in Fig. III.14.

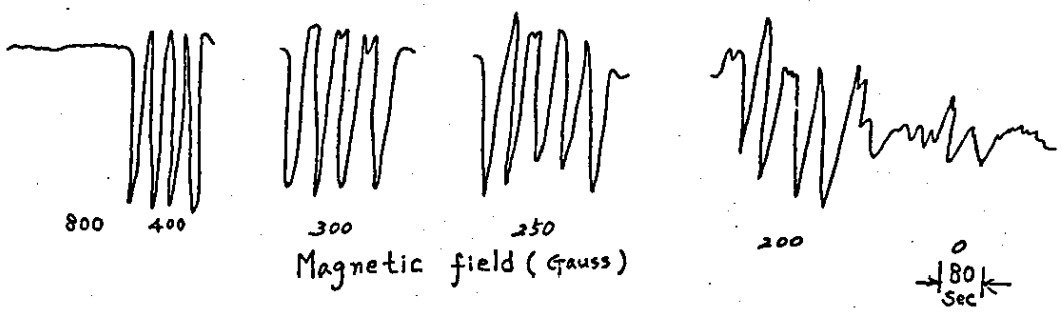

Fig. III-14 Influences of magnetic field strengths on convection and temperature fluctuations (85)

Thus, at large applied magnetic field (800 gausses), there is no convection and no temperature fluctuations; at a lower field strength (400 gausses), overstable oscillations are seen; as the field strength is decreased, the oscillations become less perfect and eventually decay into the irregular temperature fluctuations characteristic of natural convection. The reduction of fluid motion in the presence of a magnetic field was also observed by using radioactive tracers as a measure of convection.[99]

On the other hand, Crossley[87] et al found that the fine

equiaxed structure (800~1000 grains per cm^2) in aluminium (SAE 1100) was obtained when fluid flow of molten was interrupted during solidification, by magnetic stirring: by currents of 200 amp and 8000 amp-turns magnetic field applied during solidifcation. Cole and Bolling[82] also observed a larger equiaxed zone and a more rapid temperature drop in the liquid in the presence of the magnetic field and the current. This method has been applied commercially to continuous casting. Crossley[87] et al examined the influence of mechanical rotation applied to aluminium (SAE 1100) by using the imposed rotational speed 250 rpm. When the periodic accelerated rotational motion was applied, fine grain structure resulted in the material, while when uniform rotational motion was achieved the structure reverted to predominantly columnar with small areas of equiaxed grains close to the mold wall. They proposed that viscous shear in the liquid has a significant effect on equiaxed formation. Introduction of ultrasonic waves were also shown to increase heat transfer rate in a molten metal and to alter the solute distribution. There can be other ways of changing heat flow rates and the rates of mass transport in addition to the methods already mentioned.

Above all, the essential feature about equiaxed formation is that local temperature gradients must be maintained at a sufficiently low level so that a new crystal will not remelt but can survive and grown, no matter how it is produced.

3.3 Equiaxed formation by creating new nuclei

Fine grain equiaxed structures are isotropic and their properties are markedly superior, and so these structures are required in casting for all but a few very specialised applications, e.g., magnet alloys, single crystal turbine blades. These structures can be achieved by encouraging conditions favourable to the formation of nuclei, suppressing columnar growth. Generally two main approaches have been adopted, namely, (a) the control of nucleation by control of the casting conditions, and (b) the use of physical methods by stirring, vibration and so on, to induce dynamic grain refinement. The (b) method was discussed in the grain multiplication section, and for the (a) method constitutional supercooling and big bang theories have been proposed by Chalmers.

(i) Nucleation by constitutional supercooling

At first, Rutter and Chalmers[61] developed the constitutional supercooling theory to explain cellular structures, and Winegard and Chalmers[88] more vitally applied it to explain the formation of the equiaxed zone in ingots. As shown in the constitutional supercooling criterion, when the value of RC_∞/GD_L increased, the constitutionally supercooled zone increase and the structure alters from cellular to dendritic. The temperature gradient (G_L) in the liquid is initially high due to the superheat. As this gradient decreased during cooling, the zone of constitutional supercooling is extended and the amount of supercooling is increased. Thus, Winegard and Chalmers proposed that sufficient constitutional supercooling would develop to promote heterogenous nucleations at

some stage during solidification. They extended the concept of constitutional supercooling to explain the columnar to equiaxed transition.

This theory can explain the effect on the grain structures which depend on superheat and concentration of a casting during solidification, since it can affect the amount of constitutional supercooling present at a particular time. Many studies have been made to determine the influence of R, G_L and C_∞ on the columnar to equiaxed transition through the unidirectional growth experiments. Plasket and Winegard[89] grew Al-Mg alloys unidirectionally in graphite crucibles ($\phi 3^{cm}$) and observed the columnar to equiaxed transition at known values of growth rate (R) and temperature gradient (G). Their results, plotted as $G/R^{\frac{1}{2}}$ against solute content C_∞, showed a curve with a linear region at low solute content. Cole and Bolling[65] showed as well that the relationship between G/R and C_∞ at the transition was the linear region at low composition in Pb-Sb alloys. Chalmers and Billoni[76] reported a similar curve to that of Plaskett and Winegard for $G/R^{\frac{1}{2}}$ against C_∞ at the transition in Al-Cu alloys. However, there appears to be no significance in $G/R^{\frac{1}{2}}$ and a similar form of curve can be obtained using G/R instead. These investigations indicated that the columnar to equiaxed transition could be affected by G/R and C_∞ .

Further evidence supporting the constitutional supercooling theory of equiaxed zone formation is the satisfactory explanation it gives for the behaviour of inoculants. It is

generally accepted that these produce a large number of heterogenous nuclei which are able to nucleate the metal at very small supercoolings, and it has been found that a solute element which is rejected ahead of the growing interface must be present as well to produce grain refinement.

On the other hand, Uhlmannet al[81] observed that the temperature in the centre of a casting dropped very rapidly to give a zero temperature gradient in the liquid for most of the solidification, with or without a magnetic field. Under conditions of reduced convection, even though the temperature gradient in the liquid was zero, the castings were completely columnar. This means that the equiaxed zone may not be formed by a constitutional supercooling nucleation mechanism. Therefore, the constitutional supercooling nucleation mechanism may not be a sufficient condition for growth of equiaxed crystals; i.e., there may be conditions where it does not apply to the formation of equiaxed zones.

(ii) Steady state theory

Chalmers[90] proposed the big bang or steady state theory of formation of the equiaxed zone, to explain the inconsistencies. This theory assumed that nucleation occurred only during the initial chilling. The equiaxed zone then consisted of crystals which survived and grew in the liquid until they formed a network that inhibited further growth of the columnar zone.

The evidence in support of this theory is as follows:

(a) The correlation between columnar length equiaxed grain

size and pouring temperature is accounted for; a high pouring temperature gives a thinner zone in which nucleation can take place, hence fewer free chill crystals, combined with a higher probability of the free crystals being remelted before the temperature of the liquid falls to a level at which they can grow. There are, therefore, relatively few free crystals; they survive and grow for a relatively long time before impinging on each other and forming a continuous network. Conversely, a low pouring temperature produces many nuclei of which a high proportion survive, giving a continuous network early in the process, with the result that the columnar zone is short and the equiaxed grain is small.

(b) The equiaxed zone is not formed purely as a result of temperature changes in the liquid.

(c) The presence in the columnar zone of small equiaxed crystals is predicted by this theory.

Jackson et al[74] observed big bang nucleation in simulated metal castings of ammonium chloride solution. When the ammonium chloride was poured at a low superheat, i.e., near its saturation temperature, copious nucleation was observed on pouring. The nuclei survided to form a completely equiaxed structure. At higher superheats the big bang nuclei did not survive, however, an equiaxed zone was still formed at a later stage in the solidification. However, the experiments of Walker[75] made it clear that some other mechanism could also be occurring. Another mechanism of significance is

that in which crystal multiplication occurs by the melting off and/or the tearing off of the arms of growing columnar dendrites.

Another way of stimulating nucleation in undercooled liquids has aroused much interest in past years, i.e., the introduction of vibration to an undercooled liquid. Walker[75] and Hunt and Jackson[50] have shown that a pulse of sufficient intensity causes nucleation to begin in undercooled liquid nickel and in water. The most generally accepted explanation is that the pressure resulting from the collapse of a void formed by cavitation is very high. Hunt et al[91] demonstrated that extremely large pressures ($\sim 10^5$ $atm.$) are generated by the collapse of a cavity and the change in pressure lowers the freezing temperature of the liquid, and thereby results in nucleation. Many attempts have been made to apply these ideas to the grain refinement of commercial castings and ingots. However, it is now understood that when vibration is introduced during solidification, the ensuing convection can also cause grain refinement by a grain multiplication mechanism, not due to enhanced heterogeneous nucleation.

IV EXPERIMENTAL SET-UP

1. Instruments used
2. Design and Making of Dies
3. Installations for measuring temperature and pressure
   - 3.1 Thermocouples for mold and metal temperatures
   - 3.2 Load cell and strain gauges

IV. EXPERIMENTAL SET-UP

When castings are solidified under pressure, the basic factors which make important contributions in improving the casting quality are die temperature, pouring temperature, pressure level, and the holding time of the metal in the mold before and during pressure application. In these experiments, the apparatus were set up to measure these basic factors. An apparatus was also constructed for some observations on the freezing phenomena by using ammonium chloride/water system as an analogue material.

1. Instrument used

The particular apparatus for analogue studies was simply made to observe the crystallization and multiplication phenomena under pressure, as shown in Fig. IV-1 and Photo 1.

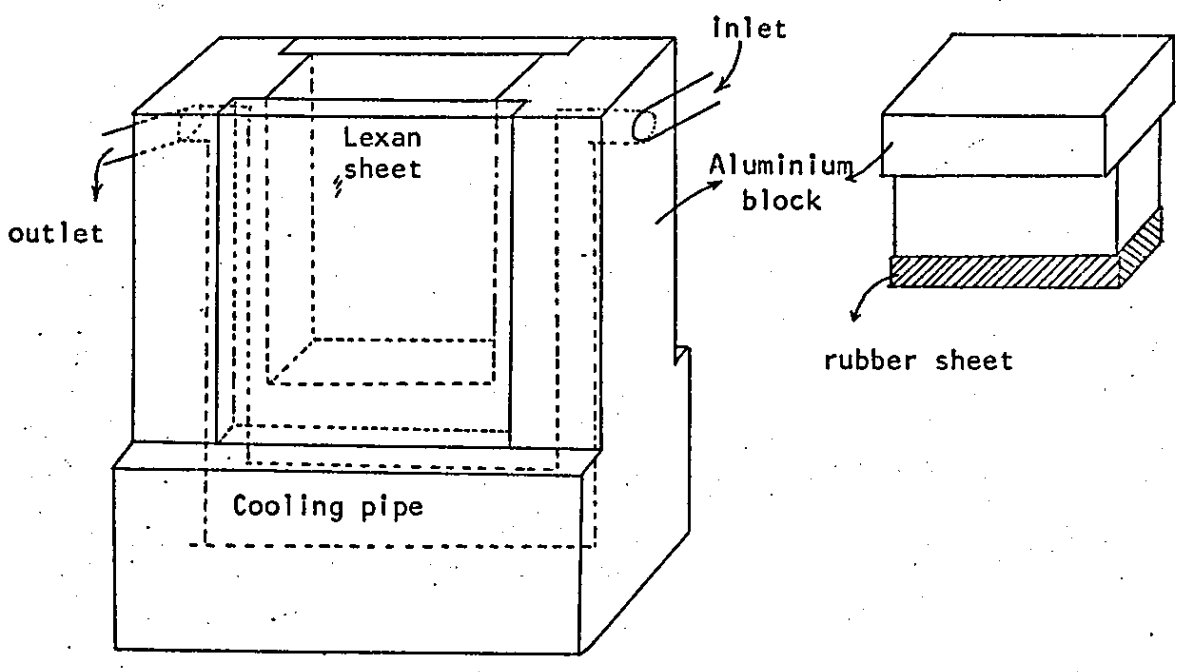

Fig. IV-1 The particular apparatus for observing the freezing phenomena under pressure

The main apparatus were established to study the influence of the basic factors on the macro- and micro- metallographies of Al-Cu alloys solidified in a cylindrical die under hydrostatic pressure. The instruments used for these experiments were set up as shown in Fig. IV-2 and in Photo 3.

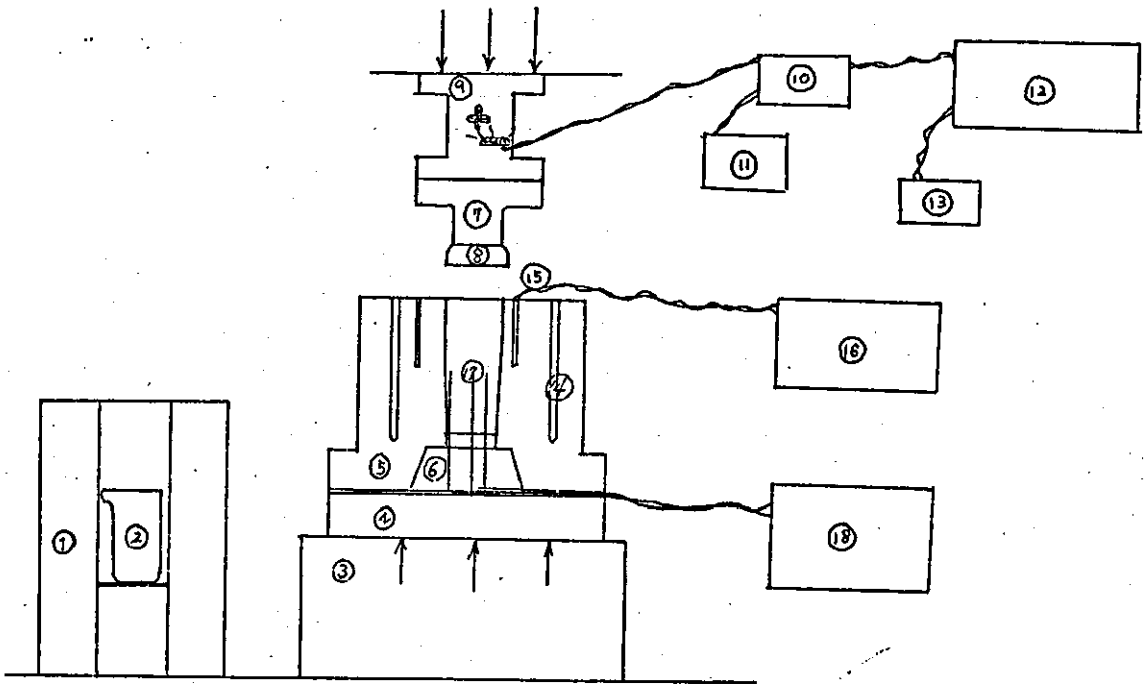

Fig. IV-2 The instruments of the main apparatus: 1. furnace, 2. crucible, 3. press, 4. bottom plate, 5. container, 6. bottom die, 7. punch, 8. punch tip, 9. load cell, 10. amplifier, 11. power supplier, 12. X-Y recorder, 13. timer, 14. heater, 15. thermocouple, 16. pen recorder, 17. thermocouple, 18. pen recorder.

The specifications of the instruments are as follows:

1. furnace: 3 KW, 240 V, pot type furnace (100 ϕ x 250 m/m) heating element Ni-Cr wire.
2. crucible: clay graphite pot, inside dia 73 m/m, outside

dia 85 m/m , depth 160 m/m

3. press: Turner Plastic (max. 50 ton), stroke 450 m/m, press speed ≈ 0.05 m/sec.
4. base plate: D2 Tool steel
5. container: 〃
6. bottom die: 〃
7. punch: 〃
8. punch tip: 〃
9. load cell: 〃
10. amplifier: 0 ~ 1 mA(D.C.) into 0 ~ 500Ω and 0 ~ 1 volt into high impedance. (Type 605A Strainstall Ltd)
11. power supplier: 12V, 60 m/a max. (Type 605)
12. X-Y recorder: Moseley 7035 AM, Hewlett Packard
13. timer: Moseley 17108 AM, Hewlett Packard
14. heater: pipe heating element
15. thermocouples: mineral insulated alumel-chromel thermocouples, cable diameter of hot junction 2$^{\phi}$m/m x 230 m/m BICC Pyrotenax Ltd
16. pen recorder: three pens recorder (Model B-34) with three pen drive units, three measuring circuit units and three amplifiers. (Rikadenki Kogyo Co.,Ltd)
17. thermocouples: alumel-chromel wires (0.0148 inch diameter , T.1. and T.2. alloys made in British Driver-Harris Co.,Ltd)
18. pen recorder: three pens recorder (Model L1040) with three pen drive units, three measuring circuit units and three amplifiers. (Linseis Co.)

2. Design and Making of Mold

The dies designed to carry out these experiments consisted of container, base plate, bottom dies, punch and its tips (Appendix B). Fig. IV-3 shows the schematic drawing of cylindrical dies. The inner die cavity was about 50 m/m in diameter by 110 m/m height.

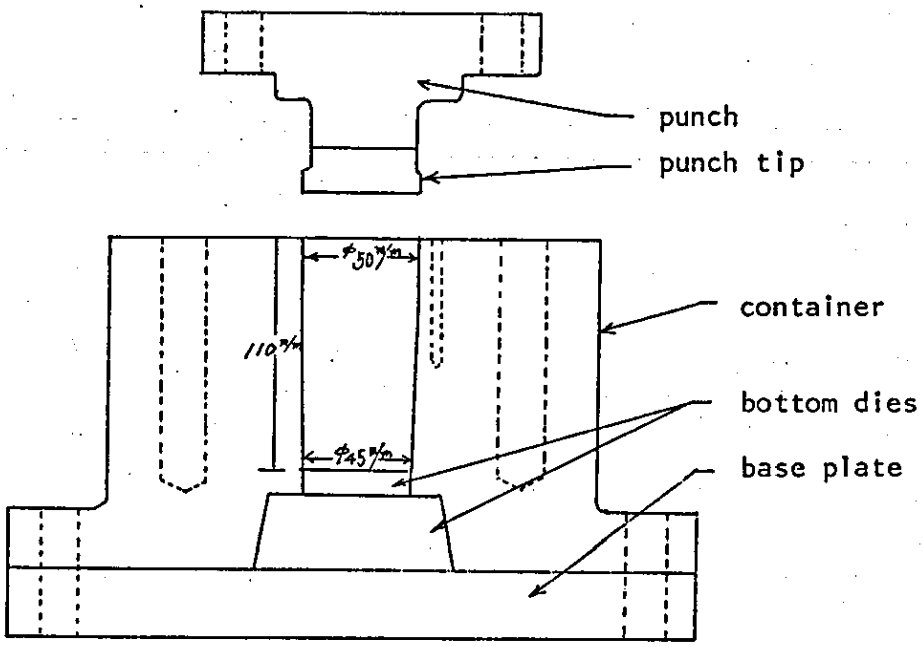

Fig. IV-3 The schematical drawing of cylindrical dies.

The container was 180 m/m in diameter by 150 m/m height and the wall thickness was 65 m/m. Practically it is desirable to use dies with the least permissible wall thickness. The greater the mass of mold per unit of casting surface, the greater the amount of heat which may be accumulated in the mold. The four holes (14.2 ϕ x 110 m/m) were located in the die to accommodate cartridge heaters for die heating. The four holes (3.2 ϕ x 70 m/m) for thermocouples were made at a distance of 10 m/m, 20 m/m, 30 m/m and 40 m/m apart from the internal surface of the inner die, and they were located in the middle between the heating holes for measuring the die temperatures accurately and uniformly as far as

possible, according to the distance from the inner surface. The mold was tapered about 1 degree to facilitate ejection of the ingots, but the upper part of the mold (at a height of about 30 m/m) was straight to serve as a guide for the punch. The tolerance between the punch tip and the upper part of the mold was made within 0.15 m/m. Three thermocouple holes were made in the bottom die to check the metal temperatures: one was in the centre, others were at a distance of 10 m/m and 20 m/m from the centre of the bottom die.

The die materials were D2 Tool steel used for cold working dies. The dies were heat treated in a controlled atmosphere furnace (300 x 300 x 1000 m/m) and cast iron chips were used to prevent surface oxidation of the dies. The heat treatments of the dies were carried out as shown in Fig IV-4. The container was held for 4 hours in 700°C for preheating and for 1 hour in 1020°C for austenitizing. The other dies were held for 2 hours in 700°C and for 30 minutes in 1020°C. The tempering temperatures were kept in 570 ~ 580°C for more than 2 hours: for the container 4 hours and for the others 2 hours.

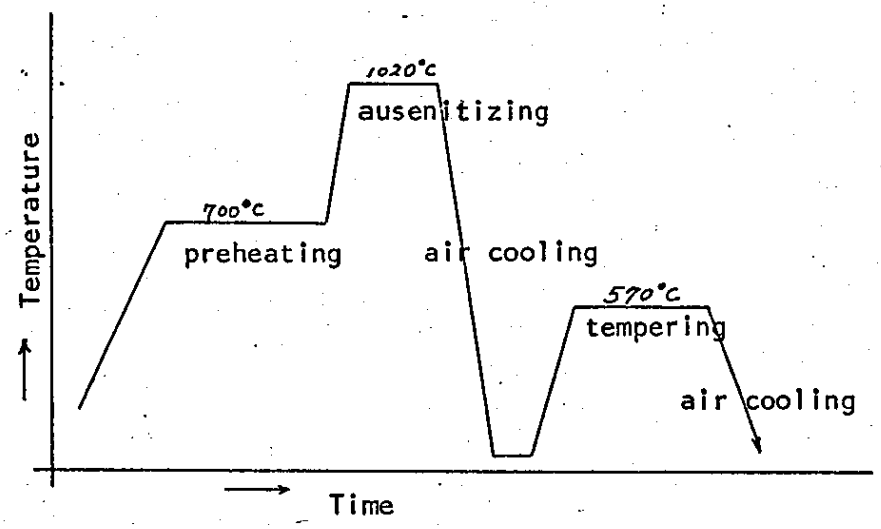

Fig. IV-4 The operation process for die heat treatment

The hardness of the dies after heat treating are shown in Table IV-1. The hardnesses were controlled within about Rc 45 by controlling the tempering operations. However, the hardness control of the container was not easy due to the handling difficulty in the air cooling and tempering operations. As shown in Table IV-1, the hardness distribution of the container was not formed uniformly. Double tempering operation was not used here, and there was some time delay in the air cooling process, especially in the container.

Table IV-1 The hardness distributions of the dies

	Hardness (Rc)		average (Rc)
	after air cooling	after tempering	
punch	not measured	44, 44, 47, 45, 46	45
punch tip 1	not measured	44, 50, 48, 49	48
punch tip 2	not measured	45, 46, 45, 47	46
bottom small die	not measured	47, 50, 52, 51	50
ring die	54, 53, 50, 55	45, 43, 48, 50	46
bottom die	50, 48, 51, 50	46, 46, 45, 44	45
base plate	42, 52, 44, 46	40, 38, 39, 40	39
container	not measured	not uniform (< 35)	not uniform

3. Installations for measuring temperature and pressure

A cylindrical type load cell with two pairs of biaxial strain gauges was made for measuring pressure level, and Alumel-Chromel thermocouples were used for measuring die and metal temperatures.

3.1 Thermocouples for die and metal temperatures

The thermocouples used for measuring the die temperature were Alumel-Chromel thermocouples with mineral insulated tube, supplied by BICC Pyrotenax Ltd. The thermocouples for measuring the metal temperatures were made with Alumel and Chromel wires of 0.376 m/m diameter supplied by British Driver-Harris Co Ltd. The wires were insulated from each other and from the melt by using twin bore alumina insulator (diameter 3 m/m and hole diameter 0.8 m/m). Thermocouple junction was then made at the end of the alumina insulator with the other wire using an oxygen-gas flame. Both wires and the alumina insulator were inserted into stainless tube (3.2 m/m inner diameter, 3.7 m/m outer diameter and 40 m/m long) which was fixed at the bottom of the mold cavity. Cold junctions were not used for measuring metal temperatures or die temperatures. The accuracy of temperature determination was $\pm 2 \sim 3^{\circ}C$. A Cambridge portable potentiometer was used for calibrating the thermocouples with known thermocouples several times. The thermocouples which were made agreed well with the known thermocouples.

3.2 Load cell and strain gauges

The general use of resistance type gauging methods may require the use of four separate circuits: power supplying, gauging, amplifying and recording circuits. In these experiments, all of them were used. A simple D.C. power supplier (12 V) was used for the supply circuit. An amplifier was used for the amplifying circuit which has the function of increasing the magnitude of the signal from the gauging circuit without distorting or warping the signal. A Moseley X-Y recorder was used for the recording circuit. The

gauging circuit with load cell was made in order to fit the experimental apparatus. D2 tool steel was used for load cell material and heat treated for stress relief of load cell at 570~580°C, for 1 hour (furnace cooled). Cylindrical type load cell was selected and the design was based on maximum load 40,000 Kg with cross area 2,000 m/m^2. The load cell was 67.38 m/m in outside diameter, 29.35 m/m in inside diameter and 80 m/m in height, as shown in Fig. IV-5.

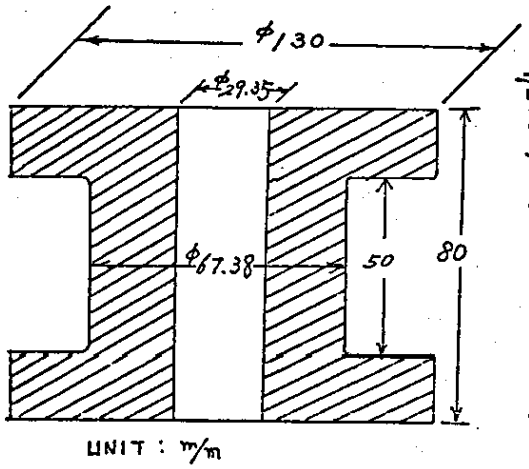

Fig. IV-5 Schematic drawing of load cell.

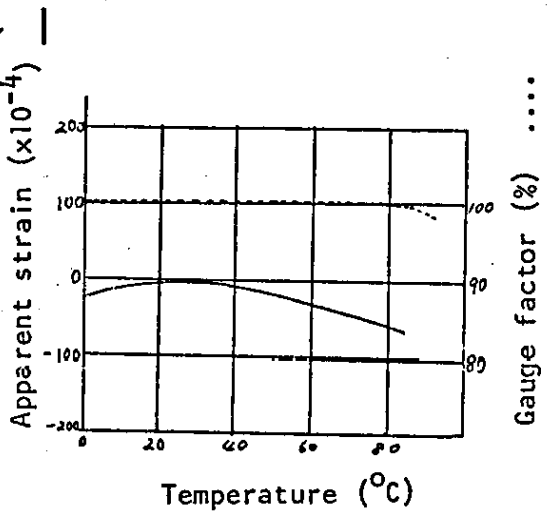

Fig. IV-6 The change of gauge factor and strain according to the temperature.

The gauge circuit selected was a full bridge type circuit, which is a well known method for establishing the values of resistance and change in resistances, as shown in Fig. IV-7. (See overleaf).

Two pairs biaxial strain gauges of foil type were used and the terminals were tin-plated. The specifications of the strain gauges were gauge length 6 m/m, gauge factor 2.14, gauge resistance 120 + 0.5 Ω (type FCA-6-11, Tokyo Sokki Kenkyujo Co.,Ltd), and the

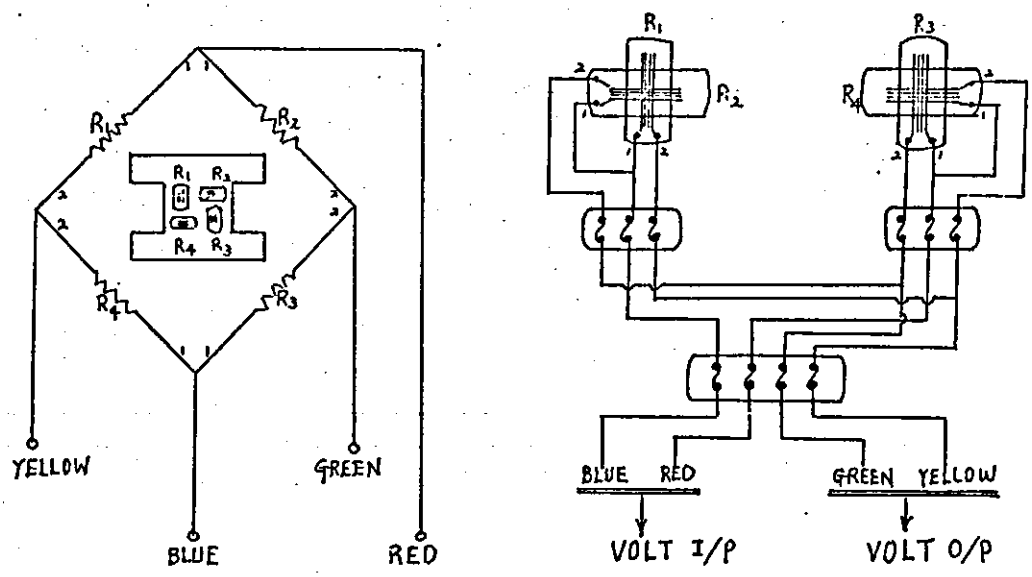

Fig. IV-7 Strain gauge circuit on the load cell

terminals were heat resistant for 10 to 20 seconds at 230°C, and insulation was 10^2 to 10^4 MΩ . Generally the techniques of putting the strain gauges on the load cell is important in making accurate gauge circuits. In order to obtain the best possible results from the strain gauge installation, it is necessary that care and attention is given to the preparation of the gauge, the surface of the load cell and the bonding techniques. For the surface of the load cell, an area larger than the installation was cleared of all rust, and smoothed with a fine grade emery paper (No. 600). Then the area was degreased with the solvent of Propan 2LO (ISO-Propyl alcohol) and aceton, and neutralised with NEUTRALISER A and NEUTRALISER 5 (manufactured by Micro-Measurement U.S.A). The gauges were applied as soon as they were removed from the packets. All products of the abrasion were removed and the back of gauges

were wiped with a tissue. For the bonding, BR 610 (manufactured by Micro-Measurement U.S.A.) was used, and in each case the layer of the cement between the gauge and the load cell surface was as thin and uniform as possible. For the installation protection, M. COAT "A" + M.COAT "D" + M.COAT "C" (manufactured by Micro-Measurement U.S.A) were used. Lead-out wires were raised and looped in order to keep them free from strains taking place in the test object. Printed circuit terminals were used and an excessive amount of solder on the terminals was avoided. The gauge circuit is shown in Photo 2.

The strain indicated by amplifier is for the active gauges (R1 and R3) and the others (R2 and R4) for the dummy gauges. Indicated strain (E_i) corresponds to change in resistance (ΔR_i) and $\Delta R/R1 = Ks \cdot \Delta L/L$ where Ks is gauge factor. Actual strain in longitudinal direction is given by

$$E_{act} = \frac{E_i}{\nu - \nu E_i + 1} \approx \frac{E_i}{1 + \nu}$$

where E_i is strain indicated by meter and ν is poisson's ratio (≈ 0.3). Thus, the unknown loads can be found by the equation of $L/AE = E_{act}$, where L is load, A is cross area and E is young's modulus. However, load cell should be calibrated using one of the presses to apply known loads so that output can be checked. Fig. IV-8 shows the calibrated graph by the known loads and digital multimeter or X-Y recorder. Mechanical and instrumental errors were within 2%.

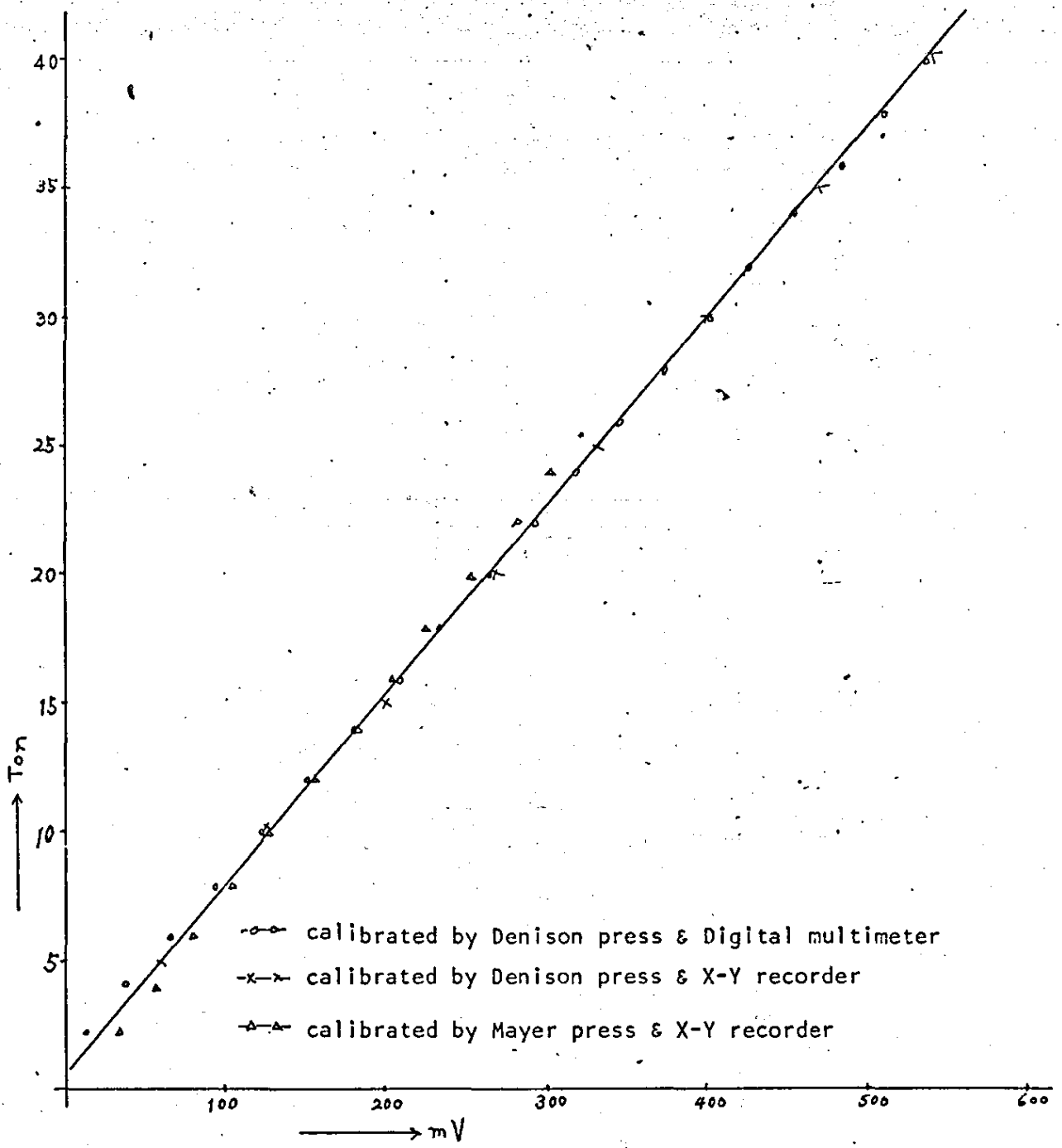

Figure IV-8 Calibration graph of load cell

V SOME OBSERVATIONS OF CRYSTALLISATION PHENOMENA UNDER PRESSURE BY USING AMMONIUM CHLORIDE SOLUTIONS

1. Procedure (I)
2. Results (I)
   - 2.1 Effects of pouring temperatures on crystallisation
   - 2.2 Effects of pressure on crystallisation
3. Some considerations
4. Summary

V. SOME OBSERVATIONS OF CRYSTALLISATION PHENOMENA UNDER PRESSURE BY USING AMMONIUM CHLORIDE SOLUTIONS

Jackson et al[74] first showed that the ammonium chloride/water solution system could be used as an analogue of a metal system, and since then it has been used with success in a number of investigations to model study of metallic solidification phenomena. However, no references were found in the literature which described the freezing phenomena of ammonium chloride/water system under pressure. In the present work the freezing of an ammonium chloride/water system was investigated to observe the influences of pressure on the system.

1. Procedure (I)

A rectangular aluminium mold with Lexan sheet windows on two opposite walls was used to observe the freezing. The details of construction are shown in Fig. IV-1 and Photo 1. Liquid nitrogen was used for cooling the mold. The cooling systems was made in the aluminium block, as shown in Fig. IV-1. The coolant inlet of the mold was connected with a plastic pipe and a glass funnel. They were insulated with glass wool and aluminium foil. When liquid nitrogen was poured into the inlet funnel, external temperature of the surrounding region of the mold could be maintained at about $0 \sim 5^{\circ}C$. The punch for applying pressure was also cooled by liquid nitrogen. A rubber sheet was attached to the bottom of the punch to prevent leakage of ammonium chloride solution when pressure was applied. This reduced leakage but did not eliminate it completely. Cleaning the apparatus thoroughly before each experiment, helped to reduce leakage. The pressure applied was about 30 N/cm^2 (3 Kg/cm^2). The ammonium chloride used was of ordinary commercial purity supplied by Fison Ltd. A saturated solution of ammonium chloride was prepared at a

temperature of 65°C. 37 wt% ammonium chloride was found to give saturation at this temperature. The freezing phenomena were recorded photographically by using a Nikon camera with f 3.5 lens, and the progress of crystallisation was recorded by taking a series of photographs at 5 second intervals for a total period of about 4 minutes.

2. Results (I)

2.1 Effects of pouring temperatures on crystallisation phenomena

Saturated ammonium chloride solutions (65°C) were heated to two different temperature levels, i.e., 70°C and 80°C before pouring into the mold. When solutions were poured at temperatures above 80°C, e.g., 90°C, there was no clear cut distinction in the mode of freezing when compared to solution poured at 80°C. However, when solutions were poured nearer the saturation temperature, e.g., 70°C, the freezing mode differed considerably from those poured above 80°C. A critical change of freezing behaviour was observed to exist between pouring temperatures of 70°C and 80°C. These experiments were repeated several times under the same conditions and the reproducibility was very good.

Photo 4 shows the progress of freezing with time, when poured with a 70°C superheat. A dense muddy solution was instantly formed on pouring at 70°C, containing many ammonium chloride crystals. The small particles of solid formed in the liquid then sank downwards when they had grown to large sizes. These sinking crystals produced some movement in the liquid. This liquid movement had a sweeping effect on the crystals growing from the mold wall which was continuously being washed into the liquid. The sweeping effect in the early stages of crystallisation accelerated a formation of

equiaxed grains. Within one minute after pouring, most of the crystals existing in the liquid came down and movement of the liquid was also greatly reduced, as shown in Photo 4(b). These crystals settled to form an equiaxed region occupying approximately half the lower part of the mold. Crystals then continued to grow from the wall at a much lower rate producing a solid region in the upper part of the mold, as shown in Photo 4(c). Some of the crystals at the solid-liquid interface in the upper part of the mold were swept into the bulk liquid . Some of the crystals swept into the bulk liquid appeared to be dissolved, but as freezing continued crystals began to grow in the remaining liquid. Some crystals formed on the top surface of the solution came down through the liquid, from the early stages to the later stages of crystallisation, but they were much bigger in size during the later stages. A free equiaxed crystal attached to the crystallised zone on the wall, then appeared to grow in common with the crystals on the wall, as shown in Photo 4(d) and (e). Photo (d) and (e) also show that a large equiaxed crystal in the liquid disappeared completely. It was thought that a complete remelting of free equiaxed crystal in the liquid could occur as well as partial remelting at the solid-liquid interfaces. Voids appeared and then disappeared in the early stages of crystallisation, as shown in Photo 4(a) $\sim$ (c). The voids were observed in the crystal zone formed in the early stages, but not during the later stages.

Photo 5 shows successive stages of freezing of the solution saturated at 65°C and poured at 80°C. At 80°C, a clear liquid was produced in the early stages of crystallisation, unlike the muddy appearance when poured at 70°C. Some crystals appeared in the liquid

during pouring, but they disappeared immediately. Convection patterns were set up with the liquid moving down the lateral walls past the growing solid from the walls, and up the centre of the mold. Up to 30 seconds after pouring, crystal growth was restricted to the mold walls only, and the liquid movement remained gentle, as shown in Photo 5(a). After one minute, liquid motion became more vigorous and many crystal particles appeared in the liquid, as shown in Photo 5(b). The crystals particles were carried upward by convection currents when they were small, but sank when they grew larger. They fell on the dendrites growing up from the bottom of the mold and gradually filled the central region. New crystals also dropped down through the liquid from the top surface, from the early to the later stages of crystallisation. Photos (c) and (d) show that a free equiaxed crystal coming down in the liquid attached itself to the columnar region of the side wall and then the attached crystal was absorbed in the growth pattern of the columnar region. The columnar region was formed from the early stages up to about two minutes, and equiaxed region produced in the central region from about two minutes after the solution was poured into the mold. The formation of equiaxed grains at the later stages was thought to be due to slow cooling and dendrite redissolving.

Simultaneous nucleation was observed when solution was poured at low pouring temperature slightly above the saturated temperature, but big-bang type nucleation could not be observed. Nucleation due to constitutional supercooling could not be distinguished from ones occuring by other mechanisms, because local temperatures in the liquid could not be measured. However, the main reasons for the

formation of equiaxed grains were thought to be due to convection effects and simultaneous nucleation in the early stages, and due to slow cooling rate at the later stages of crystallisation.

2.2 Effects of pressure on crystallisation phenomena

Experiments were then carried out to study the effects of pressure on crystallisation. Ammonium chloride solutions were prepared at a saturated temperature of $75^{o}C$, and were poured from temperatures of $80^{o}C$ and $90^{o}C$. The pressure applied was approximately 30 N/cm^2 (2 Kg/cm^2).

Photo 6 shows successive freezing stages under pressure in the solution poured at $80^{o}C$. A dense muddy solution appeared before pressure was applied, creating many new crystals and forming turbulent liquid movement. When pressure was applied, the crystals created raised violent swirls in the liquid for a moment, and they sank downwards much quicker than without pressure. A sweeping effect was also observed due to convection currents near the crystals advancing from the walls, as shown in Photo 6(b). The crystal particles created by simultaneous nucleation followed by growth quickly sank to the bottom of the mold, and settled to form an equiaxed zone occupying approximately half the lower part of the mold. Crystals then continued to grow from the walls. Photo 6(c) shows that the crystal region growing from the walls was recessed near the upper part of the mold, when pressure was applied. During the application of pressure, the recess was formed by the crystals folding over and compacting together. When the solid region recessed, formation of new crystals by fracturing of dendrites were also observed ahead of the advancing solid-liquid interfaces. At

the later stages the equiaxed crystals formed were consolidated and some separation of water occurred. Fewer new crystals appeared during this period, as shown in Photo 6(d). The freezing rate under pressure was much higher than that at atmosphere. As the punch was taken off, water rich liquid was sucked from crystals toward the punch, and as a result of the negative pressure developing, cracks appeared in the crystals. This effect was not observed when the punch was withdrawn gradually and carefully.

Photo 7 shows successive freezing stages under pressure in the solution poured at 90°C. At pouring temperature of 90°C, crystal growth started from the walls and non-turbulent movement appeared throughout the liquid. When pressure was applied, the convection patterns changed immediately and liquid moved in a disordered way. Crystal growth from the walls became increased and new crystal particles appeared a lot in the liquid. When pressure was continuously applied, a columnar zone growing from the walls was recessed toward the central region, as shown in Photo 7(c). The broken columnar zone was folded and compacted together. It was similar to the crystal fracture occuring under pressure at lower pouring temperature (80°C). However, it appeared that it was more difficult to form a recess when a higher pouring temperature was used. New crystals also emerged from advancing interfaces due to dendrite fracture and redissolution. Fragmentation of columnar crystals seemed to accelerate the formation of new crystals. Some new crystals were also observed to sink into the liquid from the top surface of the mold. At the later stages, the columnar and equiaxed zones were consolidated, separating crystals from the liquid.

To observe effects of punch temperature on recess formation, two types of punches were used: one of them was chilled by liquid nitrogen and the other was not chilled by putting rubber sheet on the surface of the punch. Fig V-1 shows the changes of recess formation according to the punch types used. When the chill punch was used, a recess of columnar or equiaxed zone seemed to make a deep advance toward the central region, and when a rubber sheet was used on the surface of the punch, it seemed to make a shallow advance.

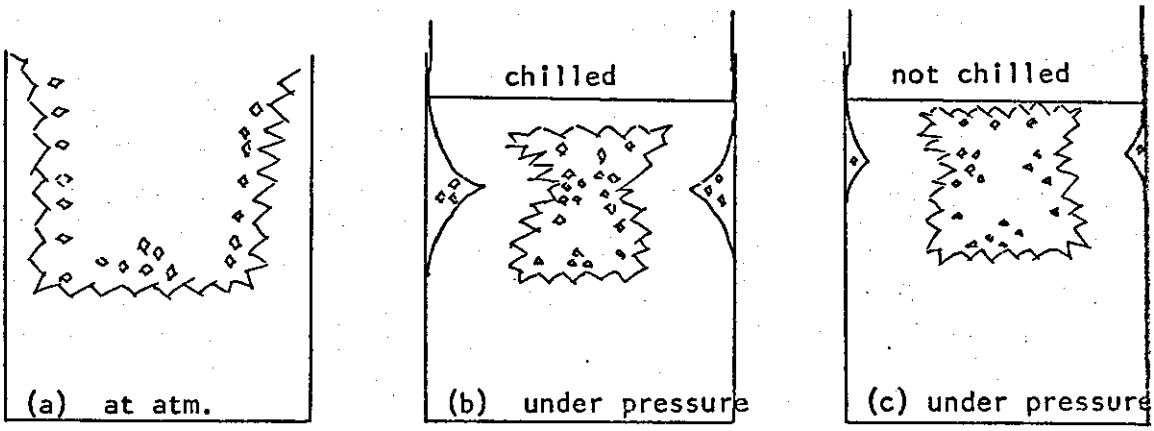

Fig. V-1 Influences of punch temperature on recess formation of dendrite

This effect was thought to occur because fragile grain boundaries collapse toward the central region: thermal conductive forces formed in both directions of the top and the wall will make growth rate disordered, and result in unstable grain boundaries. Unstable boundaries are more likely to occur when the punch is chilled. A recess of columnar or equiaxed zone occured much more easily when the punch was not properly aligned during the application of pressure.

3. Some considerations

Fig. V-2 shows solubility curve of ammonium chloride in water according to temperatures. A eutectic occurs at -15.36°C at a composition of 19.7 wt% NH_4Cl. The f.c.c. ammonium chloride phase grows dendritically in the solutions above the eutectic composition, and the dendrite directions are <100>.[74] When 37 wt% ammonium chloride solution is poured from the temperatures above the saturation temperature, ammonium chloride crystals are precipitated as a primary solid solution, the water being rejected as an impurity. Ammonium chloride solution shows very similar solidification structures to those observed in metal castings. By using ammonium chloride/water solution system, many of the observations which have been made on the equiaxed zone in metal castings therefore, can be accounted to some extent.

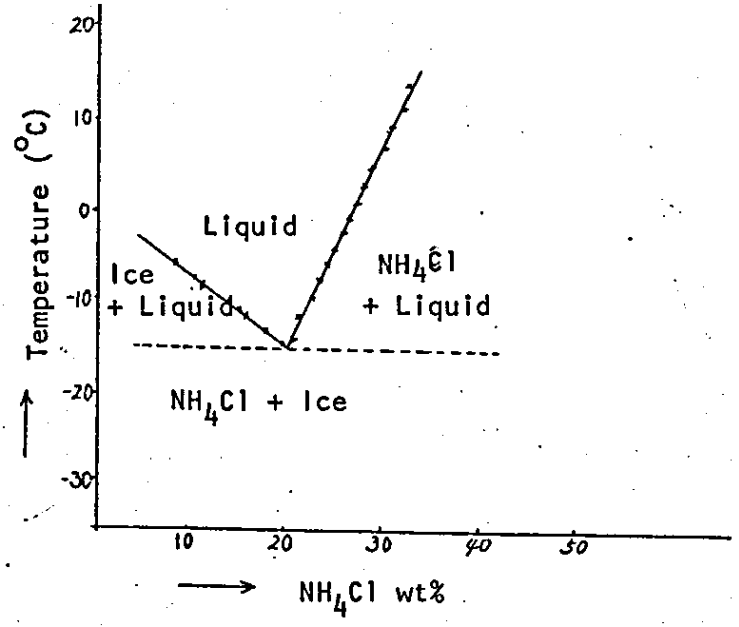

Fig. V-2 The solubility curve of ammonium chloride in water according to temperature [100]

In ammonium chloride solutions the equiaxed crystals were found to be produced mainly by simultaneous nucleation and by convection currents at

at the early stages of crystallisation. It was formed mainly owing to simultaneous nucleation at lower pouring temperature, whereas at higher pouring temperature mainly convection effects. The application of pressure stimulated these effects. Jackson et al[74] also observed copious nucleation in an ammonium chloride solution saturated at 70°C and poured at 80°C into a mold at <-100°C. A similar effect was observed under pressure, although the mold temperature was much higher, i.e., in the region of 0°C.

Dendrite fracture effects under pressure accelerated the formation of equiaxed grains. The behaviours of fracturing dendrites will promote convection currents in the liquid. Thus, some rapid undercooling which leads to more profuse nucleation will be allowed, occuring simultaneously with dendrite fragmentation. Whereas, growth rate of columnar crystals from the walls was also increased during the application of pressure. When the mechanism of equiaxed grain formation, e.g., depression of undercooling, dendrite fragmentation, etc., are not influenced during the application of pressure, columnar grain growth would be accelerated rather than forming fine equiaxed grains. Columnar structures were practically stimulated in Al-Cu casting alloys poured at very high temperature under pressure. When pressure is applied in metal castings, it will be important to control the process parameters, considering the relationships between the factors of equiaxed formation and the increasing columnar growth rate.

In the middle stages of crystallisation, a recess formation also continued to progress and promote convection currents in the liquid, whereas local inverse segregation was formed when a recess formation was progressed. At this stage, some of the crystals were dissolved, but as

freezing continued crystals began to grow throughout the liquid both under pressure and at atmosphere. It was not clear from the observations whether the growth of crystals in the remaining liquid originated from a fresh nucleation phenomenon or whether the origin crystals were incompletely dissolved and thus acted as growth centres. Anyhow, new crystals generally appeared near the regions where there were some movements in the liquid and thus could be associated with temperature differences in the liquid resulting in convection effects. However, it was clear from the observations that the movement of liquid was more effective under pressure. It was thought to promote convection currents owing to fracturing of dendrites and depression of undercooling during the application of pressure.

At the later stages, equiaxed grains were formed by slow cooling rate in the place of the central region of the mold, but not by convection currents. Some free equiaxed grains from the top surface of the solution came down through the liquid, from the early stages to the later stages. Showering crystals with small size fell out by convection currents in the early stages, and big free equiaxed grains came down as a result of density differences at the later stages.

Finally, it can be concluded that formation of fine equiaxed grains would be achieved in the early stages of crystallisation, and that the application of pressure promotes this formation owing to depression of undercooling and dendrite fragmentation.

4. Summary

The following points were observed when pressure was applied on ammonium chloride solution during crystallisation:

(i) Cooling rate of columnar and/or equiaxed grains was increased, stimulating the depression of undercooling and dendrite fragmentation.

(ii) A recess of columnar or equiaxed zone was formed toward the central region in both the lower and higher pouring temperature resulting in new fragmented crystals in the liquid.

(iii) Columnar and/or equiaxed zones were consolidated, increasing convection currents.

Crystallisation phenomena under pressure greatly differed from the ones at atmosphere; they were as follows:

(i) Cooling rate was much faster under pressure than that at atmosphere.

(ii) A recess of columnar or equiaxed zone by applying pressure stimulated the formation of new crystals, but this effect was not in atmosphere.

(iii) A sweeping effect ahead of the advancing interfaces was much more effective under pressure.

On the other hand, crystallisation phenomena under pressure had similarities with the ones at atmosphere; they were as follows:

(i) Some equiaxed new crystals were observed to drop from the top surface of the punch in both.

(ii) Free equiaxed crystals were attached to columnar or equiaxed zone and started to grow up together in both.

(iii) Equiaxed zones were formed mainly by simultaneous nucleation at the lower pouring temperature, and at the higher ones mainly by convection currents. These effects were more effective under pressure.

Care must be taken with the interpretation of the above results, although the use of ammonium chloride solution to simulate ingot solution can be used to considerable effect[101]: in the first case, ammonium chloride solution becomes less rich as dendrites are precipitated, whereas in metallic solidification, the remaining liquid becomes enriched in the solute elements; secondly, even after all the possible crystallisation has occurred, water still remains between the dendrites, whereas metals became completely solid; thirdly the method used for pouring and precipitating the dendrites does not properly simulate the metallic counterpart; finally, physical and chemical properties are different, especially in density, thermal conductivity and shrinkage. However, if similarities in the solidification structures are observed, it is postulated that they can be accounted for by the same mechanism. Ammonium chloride solution shows very similar solidification structures to those observed in metal castings. Ammonium chloride solution grows dendritically with f.c.c. lattice and the dendrite directions are <100>. Al-Cu alloys grows dendritically with f.c.c. lattice and <100> direction. It is, therefore, possible that the observations on equiaxed zone formation found in the present work can be used to explain the structures in Al-Cu alloys casting under pressure, if care is taken in interpreting the differences mentioned above.

VI. INFLUENCE OF HYDROSTATIC PRESSURE ON MACRO- AND MICRO-STRUCTURES OF ALUMINIUM-COPPER ALLOYS

1. Procedure (II)
2. Results (II)
   - 2.1 Macroscopic point of view
   - 2.2 Microscopic point of view
3. Some considerations on equiaxed grain formation

VI. INFLUENCES OF HYDROSTATIC PRESSURE ON MACRO- AND MICRO-STRUCTURES OF ALUMINIUM-COPPER ALLOYS

Several proposed mechanisms for equiaxed grain formation in cast structures differ substantially: constitutional supercooling, crystal multiplication, showering from surface and so on. Neither has the origin of the fine equiaxed grains yet provided sufficient evidence to show how or when the equiaxed grains begin to form. Generally it is known that final ingot structure markedly depends on the degree of convection in the melt during solidification,[20] and that mechanisms which promote convections such as vibration, electromagnetic stirring, etc. refine the cast structure.

When pressure is applied during solidification, a fine equiaxed zone can also be obtained. However, it is not known whether the application of pressure during solidification promotes convections and whether convection is the sole mechanism originating the equiaxed zone in the castings solidified under pressure. This work was conducted in an attempt to ascertain at which stage during solidification under pressure equiaxed grains originate and then help to provide a further understanding of castings solidified under pressure.

1. Experimental procedure (11)

Experimental studies were carried out with commercial LM11 and Al-4%Cu alloys. Commercial LM11 was supplied by B.K.L. Alloys Ltd. amd Al-4%Cu alloy made for this experiment. Pure aluminium was supplied by The British Aluminium Co. Ltd., and pure copper by British Copper Refiners Ltd.

The pure aluminium and copper was melted in a pot type resistance heated furnace to make a master alloy containing 50%Cu. It is generally necessary to melt aluminium and copper by avoiding superheating, allowing copper to diffuse into aluminium. Pure Al (440gr) was heated to 700°C and the pure Cu (410 gr) added to the molten aluminium. They were held at 700°C for 40 minutes and at 820°C for 30 minutes. Then they were slowly cooled down to 700°C in the furnace and the molten metal was poured into clay graphite molds. The master alloy was 810gr in weight. 40gr of metal was lost by oxidation during melting. Most of the oxidation was thought to be due to the formation of Al_2O_3, so that the master alloy produced would have an approximate composition of 50/50. For making Al-4%Cu alloy, pure aluminium (2000 gr) was melted in a pot type gas furnace and heated to a temperature of 750°C; the master alloy (335 gr) was added to the molten aluminium and then nitrogen gas passed for 5 minutes, keeping the molten metal temperature about 740°C. Then another 2000 gr aluminium was added to the molten metal and nitrogen gas passed again for 10 minutes, keeping the temperature about 740°C. Molten metal was then poured into preheated metal ingots. The chemical compositions of the Al-4%Cu alloy produced and the commercial LM11 were as follows:

	Cu*	Fe	Si	Mg	Mn	Ni	Pb	Sn	Zn	Cr	Ti	Al
Al-4%Cu	4.1	<0.01	<0.01	<0.005	<0.005	<0.01	<0.01	<0.01	0.02	<0.01	<0.005	bal.
LM.11	4.8	0.13	0.06	0.005	0.005	0.01	0.01	0.01	0.03	0.01	0.18	bal.

* Copper figures are chemical

TABLE VI-1 The Chemical composition of Al-4%Cu alloy and LM11

The mold assembly for casting ingots under pressure is shown in Fig. IV-2. The round mold cavity had a 45m/m bottom diameter, 50m/m top diameter and was 90m/m long. These molds were mounted on a 50 ton vertical press which had a hydraulic cylinder on the lower platen to apply pressure to molten metal. To check the actual pressure delivered by the hydraulic cylinder, four foil type strain gauges were attached to the load cell connecting the punch and the top plate of the press, as shown in Fig. IV-2. Mold temperatures were checked by three thermocouples inserted into the mold and connected to a three-pen recorder. The mold was heated by four pipe heaters inserted into it and graphite lubricant was used in the mold cavity. The metal temperatures were also checked by three thermocouples inserted into the mold cavity. Al-4%Cu alloys and LM11 were melted in an electric resistance furnace having a maximum operating temperature of 1000°C. A clay graphite crucible with a capacity of 1 kg of aluminium was used as a melting pot, and 500gr. aluminium alloy charged in the crucible. They were heated up to a maximum of 740~750°C and cooled down to the required temperature for each experimental condition. Degaser and flux were not used in melting for experimental castings made under atmospheric pressure and under higher pressures. The factors which influence cast structures were controlled as far as possible: the pressures used were 70 MN/m^2 and 110 MN/m^2; the holding time of molten metals in the mold was 10 seconds before applying pressure and 15~20 seconds during the application of pressure; pouring temperatures were varied in the ranges from 630°C to 800°C and die temperatures changed from 160°C to 250°C.

2. Results (II)

Detailed experimental data are included in Appendix C. Photographs of macro- and micro-structures are included in Appendix D.

2.1 Macroscopic point of view

The macrostructures of typical ingots of Al-4%Cu alloys solidified under normal static conditions and 110 MN/m^2 hydrostatic pressure are shown in Photograph 8. Sample No. AC11 was cast at 720°C with die temperature of 200°C at atmospheric pressure. It contained a peripheral zone with half columnar grains and a central zone with coarse equiaxed grains. A surface dendrite of about 2m/m thickness was also present. The ingots solidified under pressure showed quite different cast structures. The equiaxed zone was enlarged to cover a large proportion of the ingot poured below 700°C, but in the ingot poured at 780°C the columnar zone was enlarged, as shown in Photograph 8. Especially the ingots (AC2 and AC5) poured slightly above or below the liquidus temperature produced extremely fine equiaxed grains without producing columnar zone. A copper rich band in the central region appeared in the ingots solidified under pressure.

Fig. VI-1 shows the cooling curves at the centre and near the surface of ingot poured at 730°C with die temperature of 210°C under 110 MN/m^2 pressure. During the application of pressure there was an increase in temperature of about 8°C at the centre, whereas there was little increase in temperature near the surface. There was a tendency of accelerating recalescence due to latent heat of solidification, when pressure was applied during solidification, expecially at the centre of the ingot. Fig. VI-1

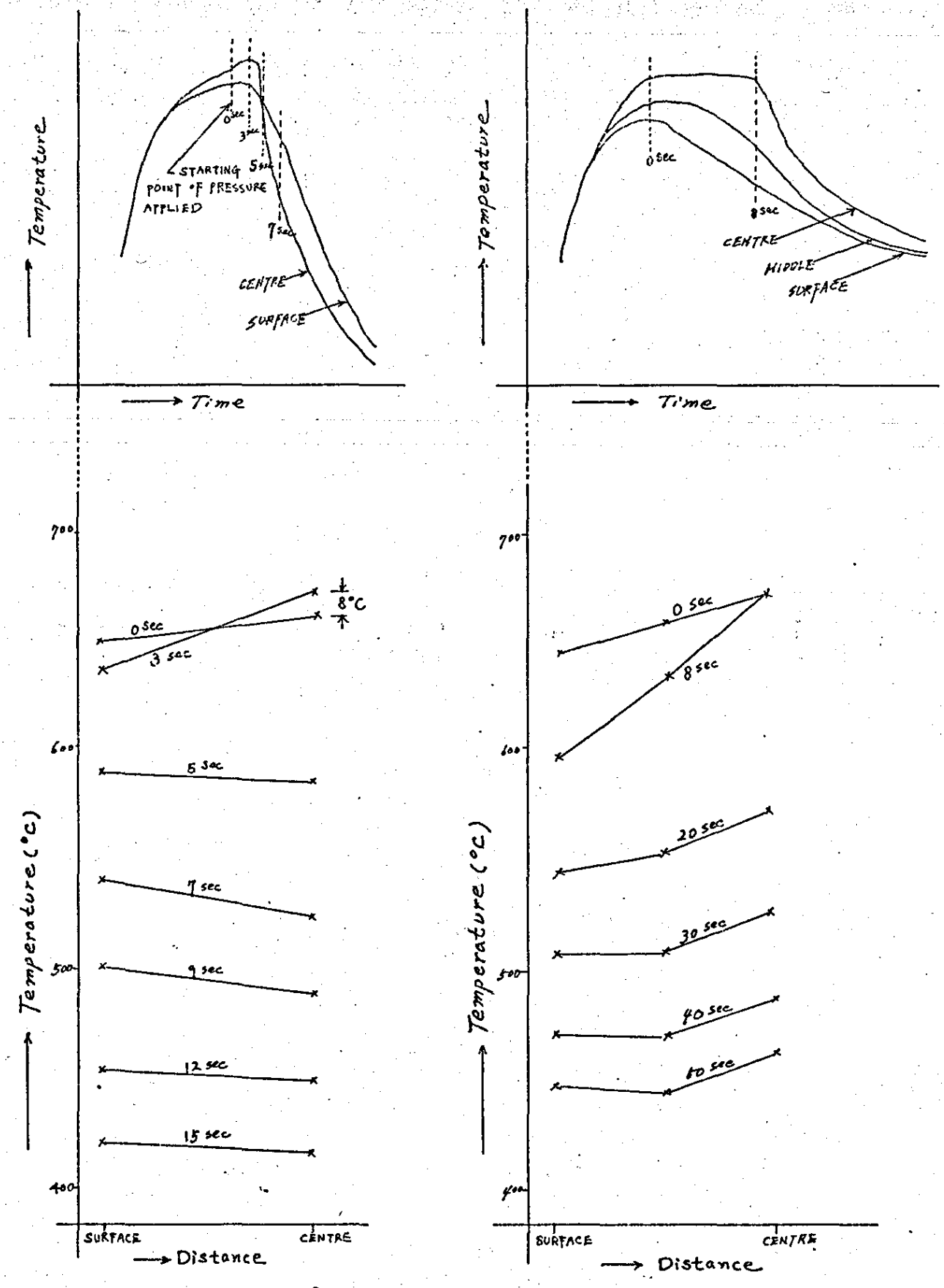

(a) under 110MN/m^2 pressure (b) at atmosphere

Fig.VI-1 Cooling curves and temperature gradients for small ingot (50m/m) poured at 730°C with die temp. of 210°C.

also shows the temperature gradients for different solidification times, at atmosphere and under pressure. There appeared a negative temperature gradient in the ingot solidified under pressure, whereas there was a positive temperature gradient at atmosphere. This was thought to influence the transition of columnar to equiaxed formation.

Photograph 9 shows the influence of die temperatures on the cast structures of ingots poured slightly above the liquidus temperature of Al-4%Cu alloy system under 110 MN/m^2 pressure. The macrostructures showed an equiaxed zone in all samples, but the grains were gradually finer with lowering die temperatures. Copper rich band in the central region which appeared in die temperatures above 180°C, completely disappeared when the ingot (AC 15) was cast at a die temperature of 165°C, and also its macrostructure showed extremely fine equiaxed grains. This indicates that extremely fine equiaxed grains free from a copper rich band in the central region can be obtained when lower pouring and lower die temperatures are employed in ingots solidified under pressure.

To examine whether pressure is a necessary condition to get fine equiaxed structures, the ingots were solidified at atmosphere and under pressure with the same pouring temperature of 660°C and die temperature of 165°C. For the ingot cast under higher pressure the holding time in the mold before applying pressure was 10 seconds and the application of pressure was maintained for 20 seconds. The resulting macrostructures had fine equiaxed structures throughout, under pressure as well as at atmosphere, as shown in Photograph 10. However, some voids appeared in the central region of the ingot

solidified at atmosphere, whereas dense equiaxed grains, without voids, were evident under pressure. The fine equiaxed structure mainly resulted from simultaneous nucleation mechanism in both, and pressure greatly influenced the consolidation of metal by feeding the shrinkage cavities. However, microstructures and hardnesses of the ingots were quite different from those cast at atmosphere. Fig. VI-2 shows the distribution of hardnesses tested in five positions of the surface area which was cut along the vertical centre line. The hardness distribution was checked by Vickers pyramid hardness tester. The hardness distribution was at a higher level under pressure than that at atmosphere for all five zones. Particularly the hardness of sample No.AC16 was much higher than that of sample No. AC18 solidified at atmosphere, Sample No. AC16 was solidified under two step pressures, as shown in Fig. VI-3: after the molten metal had been kept for 2 seconds under a pressure of about 60 MN/m^2, pressure was increased immediately up to 110 MN/m^2. This cast structure had three fine equiaxed layers: the first surface layer extended up to about 4m/m thickness from the ingot surface; the second equiaxed layer was about 10m/m thickness and the third equiaxed layer was formed in the central region with 20m/m thickness.

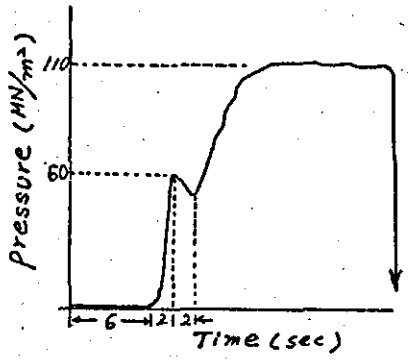

Fig. VI-3 Two-step pressures applied in Sample No. AC16

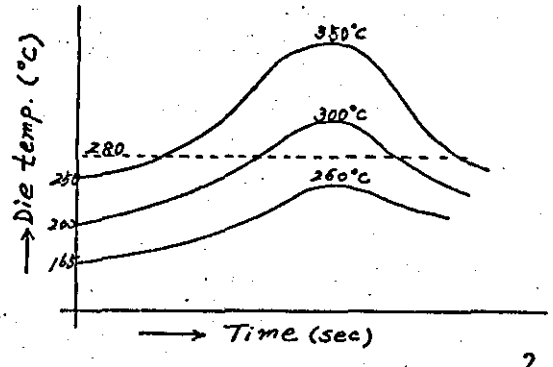

Fig. VI-4 Influence of 110MN/m^2 pressure on die temp

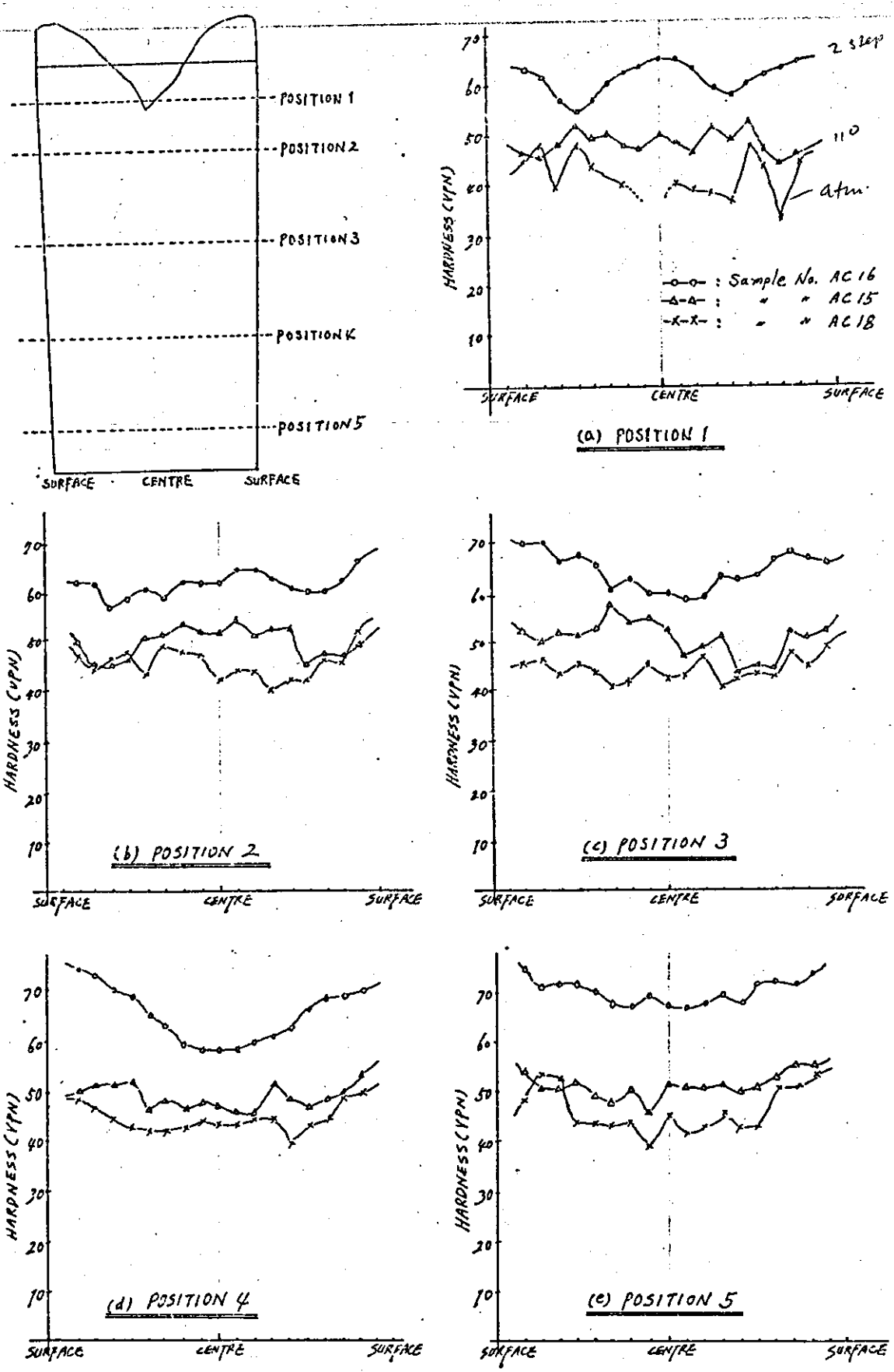

Fig. VI-2 Hardness distribution of sample Nos. AC18, AC15 and AC16

It can be assumed that the first layer was formed before applying pressure, the second layer formed in 60MN/m^2 and the central layer formed in 110MN/m^2. There was quite a difference in solidification rate before and after the application of pressure: i.e., the first layer of 4m/m thickness was solidified for 6 seconds without pressure, whereas the second layer of 10m/m thickness solidified for 4 seconds under pressure building up to 60MN/m^2. There was, therefore, an increase in the solidification rate during the application of pressure up to 60 MN/m^2. This means that solidification rate can be very fast under pressure even for small specific pressures applied. Sample Nos. AC14 and AC15 of Photograph 10 were solidified under single stage pressures of 70MN/m^2 and 110MN/m^2, but there was no clear difference between their macrostructures.

✓ Photograph 11 shows the macrostructure of commercial Al-Cu alloys (LM 11) which includes grain refiners (Ti), and impurities. Fine equiaxed grains appeared even when molten metal was poured at 720°C, but in Al-4%Cu alloy columnar zone appeared when it was poured at 720°C. Nucleation inoculants (grain refiner) and impurities appear to have a much more pronounced effect on the formation of equiaxed grains, without even controlling the casting parameters such as the casting temperature. Photograph 12 shows the macrostructures of a series of commercial Al-Cu alloy ingots poured at various temperatures under the same pressure condition. Columnar zone appeared under the casting conditions of 760°C pouring temperature and 230°C die temperature. When the ingot was poured at 800°C with die temperature of 220°C, columnar zone

and coarse equiaxed grains were formed. This macrostructure was very similar to that of the Al-4%Cu alloy poured at 720^{0}C in the mold heated to 220^{o}C. As shown in Photograph 12, copper rich band in the central zone also appeared in commercial Al-Cu alloy. This band appeared in Sample No. LM 113 which was poured at lower temperature of 660^{o}C with higher die temperature of 220^{o}C, whereas this disappeared in Sample No. LM 114 which was poured at higher temperature of 710^{o}C with lower die temperature of 170^{o}C. The casting condition of lower die temperature seemed to be more effective than that of lower pouring temperature, for eliminating copper rich band in cast ingots of commercial Al-Cu alloys (LM 11) solidified under pressure. Fig. VI-4 shows that the die temperature increased during the application of pressure. When the increase in die temperature resulted in maximum die temperatures below 280^{o}C, there was a tendency to eliminate the copper rich band. It can be inferred that the occurrence of the copper rich band would be greatly influenced by heat extraction through the mold.

2.2 Microscopicpoint of view

Specimens showing macrostructures with extremely fine equiaxed grains, were examined for their microstructures: specimen Nos. AC15, AC16, AC18.

Photograph 13 shows the microstructures of longitudinal and transverse sections for specimens prepared from ingots. The specimens were cut from a location 40m/m in height from the bottom of the ingot and 10m/m from the ingot surface. The specimen (AC18) solidified at atmosphere had many voids along the grain boundaries,

but they did not appear in the specimens (AC15 and AC16) solidified under pressure. It can be inferred that external pressure applied during solidification made an important contribution to eliminate them by feeding molten metal to shrinkage cavities and porosity. Specimens solidified under pressure had smaller substructures than those at atmosphere, as shown in their microstructures in transverse and longitudinal sections. All the specimens had some coarse grains surrounded by small sub-grains. It was thought that coarse grains result from grains growing continuously, and fine grains emerged from constitutional supercooling by increased cooling rate when pressure was applied. It can also be associated with the increasing undercooled temperature with increasing pressure. (See Page 11, Clausius-Clapeyron equation). Specimen No. AC16 which was solidified under a two step pressure caused dendrite fragmentation, as shown in Photograph 13(c), and resulted in uniform sub-grains. It is inferred that a change of pressure during solidification would produce fluctuation in growth rate, resulting in melt-off and/or tear off of dendrites.

Photograph 14 shows the copper rich area formed along the grain boundaries. There was a eutectic growth in the copper rich region in all the specimens. The eutectic growth, however, was observed to be more in specimen numbers AC15 and AC16 than in AC18. There was considerable microporosity along the grain boundaries in specimen No. AC18 solidified at atmosphere. The eutectic morphology (solidified under pressure) appeared to be close to a lamellar eutectic type, whereas that soldified at atmosphere seemed to be a degenerate eutectic growth.

Photograph 15(a) shows that many voids were present in the surface region, when castings were solidified at atmosphere. These voids resulted from the migration of the grain boundaries in a chill surface. Whereas, when castings were solidified under pressure, voids were not present, as shown in Photograph 15(b) and (c). Photographs 15(b) and (c) show dendrite fracture lines filled in with copper rich alloy. It may be inferred that, when copper rich metal was fed into shrinkage cavities by pressure, the liquid metal movement caused dendrite fragmentation, resulting in fine substructures. However, pressure has influenced an inverse segregation, as shown in Fig. VI-5. Fig. VI-5 shows the distribution of copper concentration of specimen No. AC15 solidified under 110MN/m^2 pressure (microprobe analysis-line scan). There was an inverse segregation zone of about 1m/m in depth from the surface of the ingot.

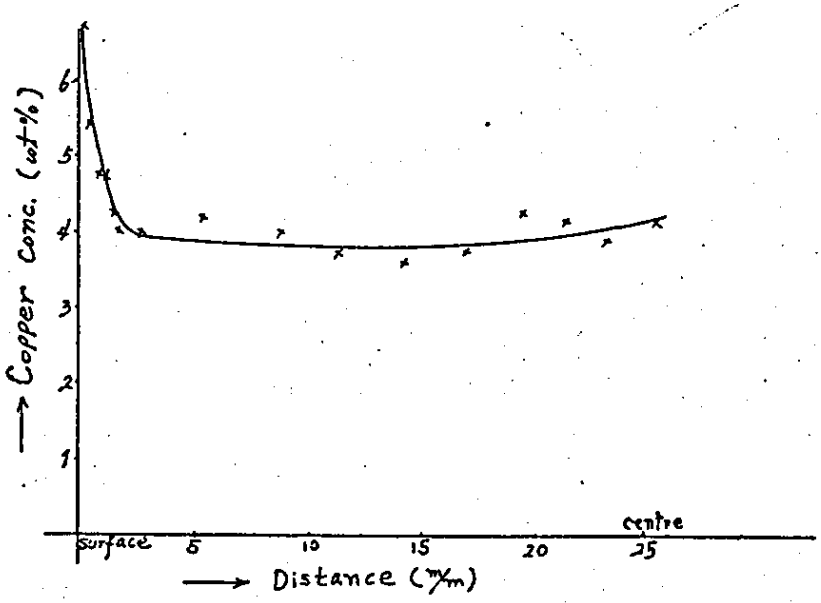

Fig. VI-5 Influence of pressure on segregation (pressure 110MN/m^2, pouring temp.660°C Die Temp.165°C)

3. Some considerations on equiaxed grain formation

The details of how equiaxed grains form in a casting may be determined in two steps. The first part is simply a question of the origin of equiaxed grains, i.e., are there fresh nuclei formed by heterogeneous nucleation, or dendrite bits broken off or melted from the columnar zone or elsewhere, or other solid bits surviving from the outset of freezing? The second is more complex, i.e., the question of the columnar to equiaxed transition (CET): does columnar growth slow down and allow the dominance of equiaxed grains, however they are formed, or do equiaxed grains take over and force columnar growth to stop? Both the CET theory proposed by Winegard and Chalmers[88], which requires constitutional supercooling, and the CET theory suggested by Chamlers,[90] which requires nucleation to occur only on pouring, pertain to the natural equiaxed zone which occurs if solidification proceeds in the absence of disturbance or extraneous forces. The former theory is supported by special versions of undirectional growth whereas the latter theory has been supported effectively for the solidification of small ingots. However, when ingots are solidified under pressure, there is no evidence as to which theory can be supported for this case.

Firstly, the columnar to equiaxed transition under pressure will be discussed within the limitations of the two theories mentioned above. When pressure is applied during solidification, there is an increase in growth rate restricting diffusion in front of the advancing solid-liquid interface and an increase of undercooling by increasing the equilibrium solidification temperature (see

page 11). However, due to rapid heat extraction under pressure (no air gap between ingot and mold) the effect by a change in the equilibrium solidification temperature will have very little significance, since the metal will solidify quite quickly in any case. Recalescence may be pronounced as a result particularly in the central regions (as mentioned in the result section).

The diffusion restricted in front of the solid liquid interface (because of rapid growth and limited time) will change the liquidus temperature ahead of the advancing interface. The temperature gradient in the ingot will also change repidly as shown in Fig.VI-6.

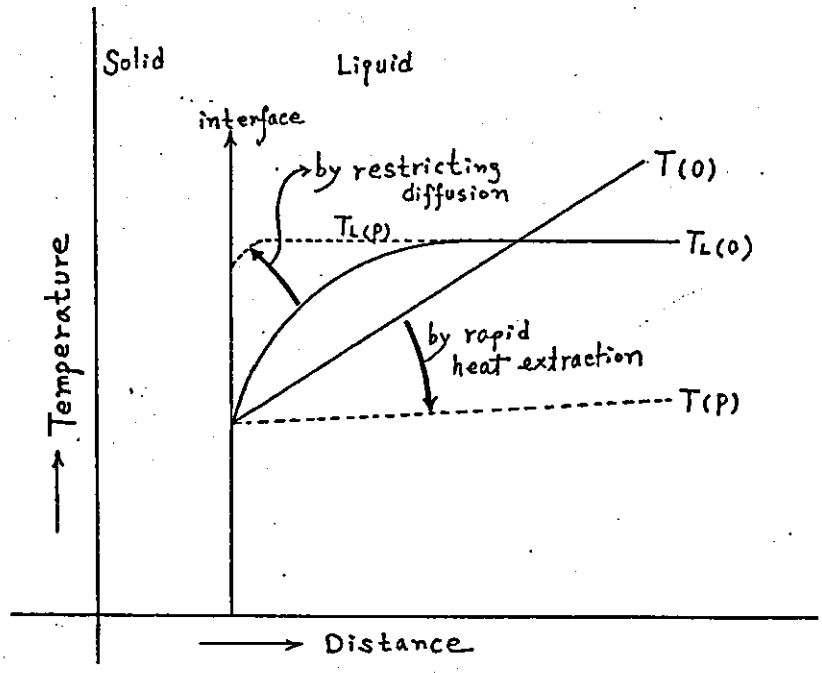

Fig. VI-6 A change of constitutional supercooled region under pressure
$T_L(0)$: equil. liquidus temperature at atm.
$T_L(P)$: " " under pressure
$T(0)$: actual temperature at atm.
$T(P)$: " " under pressure

The application of pressure during solidification, therefore, increases the amount of undercooling ($\triangle T$) so that a lot of nuclei could be produced. The higher the pressure applied, the more pronounced the constitutional undercooling becomes, and the result can produce undercooling in the entire ingot and not restricted to a zone or band ahead of the solid-liquid interface. It can be considered more reasonable to use the concept of overall undercooling rather than restricting it to constitutional undercooling to explain the solidification of alloys under pressure.

Fig. VI-7 shows the schematic drawings of the relationships between the undercooling required for nucleation ($\triangle T_u$) and actual temperature (T) for higher and lower pouring temperature, and die temperature in ingots solidified under pressure. When the pouring temperature is very high, a positive actual temperature gradient ($\frac{\partial T}{\partial x} \gg 0$) will be produced and result in columnar structure in all zones, whereas when the pouring temperature is lower a negative actual temperature gradient ($\frac{\partial T}{\partial x} < 0$) can be formed and result in equiaxed structure in all zones, and columnar and equiaxed grains may be produced in medium pouring temperatures.

A lower die temperature may produce lower actual temperature gradient i.e., near parallel, and a higher pressure may reduce the actual temperature gradient by rapid heat extraction through the mold, resulting in large equiaxed grains covering most of the ingot. This hypothesis agreed well with the experimental results of Al-4%Cu alloy which was examined in this work.

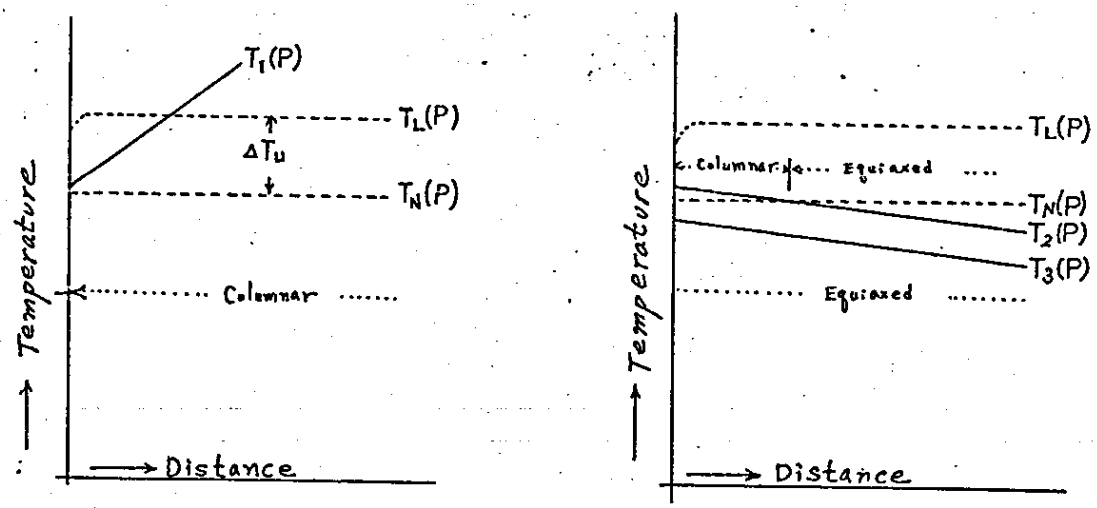

(a) higher pouring temp. (b) lower pouring temp.

Fig. VI-7 Schematic drawing of undercooled temperature under pressure.

$T_L(P)$: liquidus temperature under pressure

$T_N(P)$: heterogeneous nucleation temperature under pressure

ΔT_u : undercooling required for nucleation under pressure

$T_1(P)$: actual temperature gradient at higher pouring temperature

$T_2(P)$: " " at lower pouring temperature with higher die temperature

$T_3(P)$: actual temperature gradient at lower pouring temperature with lower die temperature

The copper rich pool in the central region of ingots solidified under pressure would be produced owing to a steep positive actual temperature gradient ($\frac{\partial T}{\partial x} >> 0$) in the remaining liquid but not in the regions where a solid skeleton had already formed during the application of pressure. It therefore would be better to keep a negative actual temperature gradient ($\frac{\partial T}{\partial x} < 0$) to avoid a solute rich pool in the central region: i.e., by casting with a lower pouring temperature and die temperature. In this case,

simultaneous nucleaton may be produced at the early stages of solidification, similar to that actually observed in the analogue system of ammonium chloride.

Secondly, the possible sources equiaxed grains can be discussed in ingots solidified under pressure, but is difficult to examine its origin in detail. In fact, there is insufficient evidence to support the origin of equiaxed grains even in the case of normal solidification. All methods of grain nucleation such as constitutional supercooling and dendrite remelting and fragmentation can therefore be supported. Under pressure, all these mechanisms are equally feasible. The application of pressure during solidification, however, in some way accelerates the formation of equiaxed grains and results in finer substructures than the normal solidification does. It can be considered to result from rapid cooling rate and breakdown of dendrites under pressure. Growth rate also increases under pressure, as observed in the analogue material of ammonium chloride. Rapid cooling rate will produce micro-dendritic substructures, and rapid growth rate may produce big dendrite substructures. The relationship between growth rate and cooling rate is complex and will depend on the number of growth centres, size of casting and thermal conductivities and parameters of the mold and metal. Fig. VI-8 shows the dendritic tip temperature for three gradients (G) of Al-2wt % according to growth velocity examined by Burden and Hunt.[93]

Burden and Hunt suggested that the undercooling ahead of a dendritic interface increases as the growth velocity increases, - an

opposite effect to that found by Sharp et al[94] and Kramer et al[95] - but they suggested that for high enough velocities the temperature decreases with increasing growth velocity without affecting the gradient, as shown in Fig. VI-8.

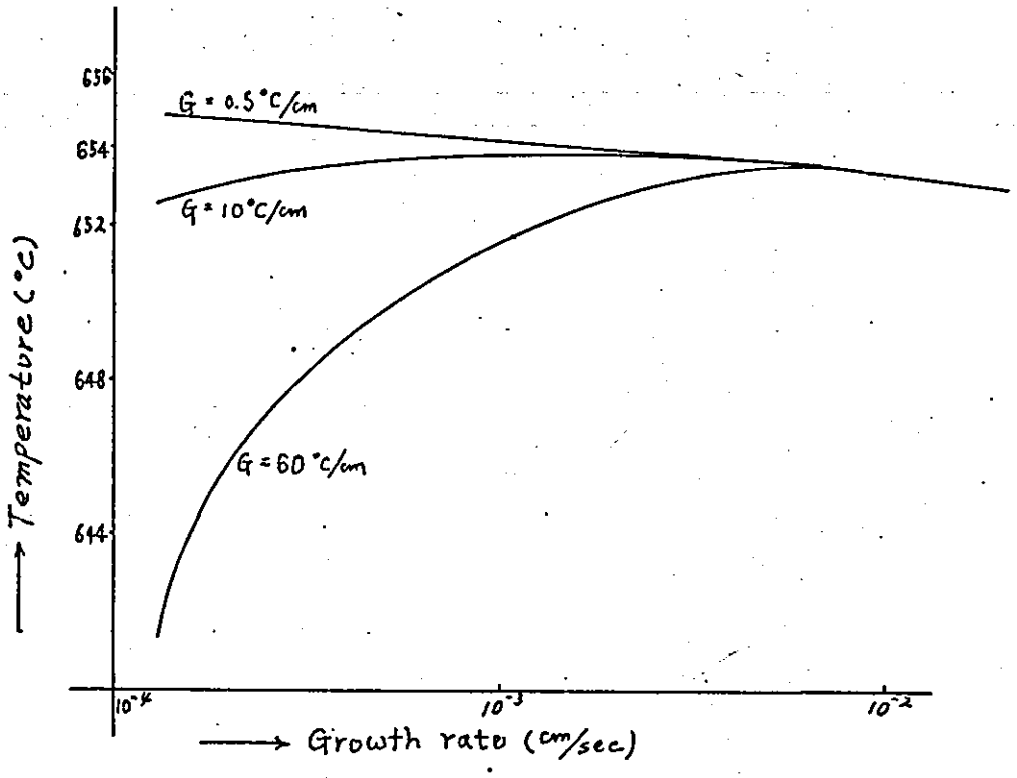

Fig. VI-8 Dendrite tip temperatures for Al-2wt %Cu grown with G_L 0.5, 10 and 60°C/cm.(93)

Thus, considering G^m/R^n values which represent the critical growth conditions for the transition of interface structure, it can be assumed that dendritic growth under pressure directly depends on cooling rate (R), not on gradient (G). It can be considered that rapid cooling rate greatly influences the appearance of micro-dendritic substructures and rapid growth rate influence growth of dendritic substructures which had been

already formed. This relationship would produce irregular substructures in the ingot solidified under 70MN/m^2. However, there was a tendency to reduce the irregular substructures under 110 MN/m^2. The application of two step pressure during solidification may have greatly influenced dendrite fragmentation, resulting in uniform dendritic substructures, as shown in Photograph 13(c). Two-step pressure is thought to accelerate the dendrite breakdown by cracking the dendrite skeleton already formed during the first step and by perturbing the growing liquid-solid interfaces, regulating the relationship between growth rate and cooling rate. This is similar to the occurrence of dendrite cracks actually observed in the analogue system of ammonium chloride when pressure was removed.

VII CONCLUSIONS AND SUGGESTIONS FOR FURTHER STUDY

VII CONCLUSIONS AND SUGGESTIONS FOR FURTHER STUDY

The conclusions reached in small ingots (50m/m dia) solidified under pressure in Al-4%Cu alloys are as follows:

1. Casting defects such as blowholes, porosity and shrinkage cavities, were eliminated when pressure was applied during solidification.

2. Castings with low (as far as practicable) pouring and die temperatures resulted in fine equiaxed cast structures: e.g., pouring temperature 660°C and die temperature 165°C under 110 MN/m^2.

3. The application of pressure during solidification favoured the formation of equiaxed grains and columnar to equiaxed transition, resulting in finer dendritic substructures.

4. The equiaxed zone in small ingots were most likely to be derived from crystallites formed during the early stages of solidification.

5. The application of two-step pressure during solidification greatly influenced dendrite fragmentation. This resulted in increased hardness and a more uniform distribution of hardness, indicating more uniform substructures.

6. When the increase in the die temperature, after casting, was controlled, i.e., the peak temperature was not allowed to go over 280°C., the copper rich pool in the central region of the ingots was much reduced, and in some cases, completely eliminated.

7. Inverse segregation occurred in all ingots solidified under pressure extending to a depth of 1m/m from ingot surface. Changing in casting conditions and heat extraction did not have any significant effect on this segregation.

The following subjects were suggested for further study:

1. Optimum mold conditions for improving quality of castings and ingots solidified under pressure: e.g., thermal analysis by using an analogue of electrical circuit.

2. Influence of punch and press speed on cast structures: e.g., modification of detachable punch and/or press mechanism to enable two-step pressures to be applied.

3. Influence of pressure on the relationship between growth rate and cooling rate.

4. Influence of pressure on the origin of equiaxed grains and micro-segregation: e.g., predendritic solidification and solute distribution under pressure.

5. Influence of pressure on the structures produced in other Aluminium alloy systems: e.g., eutectic systems such as Al-Si.

*** REFERENCES ***

1. R. G. R. Sellors, A. G. Leathan and B. G. Carver: Metals Tech., Mar. 1976, pp 109-117
2. V. M. Plyatskii: Extrusion casting. 1965, pp 1-7
3. B. D. Wakefield: Iron Age, May 28, 1970, pp 97-99
4. K. M. Kulkarni: Foundry M & T, Aug 1974, pp 76-79
5. J. C. Benedyk: Society of Manufacturing Engineers (Tech. paper CM 71-840), 1971, pp 1-26
6. J. C. Benedyk: 6th SDCE International Diecasting Congress, paper no. 86, 1970, pp 1-10
7. W. F. Shaw & Watmough: Foundry, Oct 1969, pp 166-169
8. R. F. Lynch & P. C. J. Gallagher: Trans. AFS, 1975, pp 561-568
9. M. L. Zaslavskii & Yu F. Ignatenko: Russian Castings Production, pp 362-364
10. "Today in Diecasting", Foundry. Sept 1965, p 129
11. W. D. Huskonen: Foundry. April 1969, pp 175-183
12. G. X. Diamond: Modern Casting, Nov 1968, pp 61-63
13. J. A. Woltering: Foundry. June 1968, pp 178-180
14. I. Miki & T. Kido: Light Metal Age, Dec 1973, pp 9-14
15. G. W. Form & J. F. Wallace: Modern Casting, pp 60-69
16. J. L. Reiss & E. C. Kron: Modern Casting, Mar 1960, pp 89-96
17. S. Z. Uram, M. C. Flemings & H. F. Taylor: Trans. AFS (66), 1958, pp 129-134
18. S. Chatterjee & A. A. Das: The British Foundrymen, Nov 1972 pp 420-429
19. J. Campbell: "The Solidification of Metals" ISI pp 18-26
20. J. A. Spittle, G. W. Dellamore & R. W. Smith: ISI (1968), pp 318-322
21. M. H. Burden & J. D. Hunt: Metal Science, May 1976, pp 156-158

22. V. M. Piyatskii: "Extrusion Casting", 1965, pp 18-33

23. S. Chatterjee: 1970, M.Sc. Thesis in Loughborough, pp 15-21

24. V. M. Piyatskii: "Extrusion Casting", 1965, p 56

25. S. Oya, A. Kamio & Y. Matsuura: The Casting Research Lab., Waseda University No 22, Nov 1971, pp 19-28

26. R. A. Lefever: "Aspect of Crystal Growth" (1971), pp 51-60

27. L. A. Girifalco: Metallurgy Society Conferences in Dallas Texas Feb 1963, p 260

28. H. J. Queisser, K. Hubner & W. Shockley: Phys. Rev., (123), 1961, p 1245

29. P. J. Revcroft, H. K. Kevorkian & M. M. Labes: J. Chem. Phys., (44), 1966, p 4416

30. W. R. Wilcox and T. J. La Chapelle: J. Appl. Phys., (35), 1964, p 240

31. A. L. Ruoff & R. W. Balluffi: J. Appl. Phys. (34), 1963, p 1848

32. W. Schule & E. Lang: Bull. Am. Phys. Soc., (12), 1967, p 325

33. M. A. Krivoglaz: Phys. Met. & Metall., (17), 1964, p 1

34. K. B. McAffee: J. Chem. Phys., (28), 1958, p 218

35. A. L. Ruoff & R. W. Balluffi: J. Appl. Phys., (34), 1963, p 2862

36. G. Arai & J. G. Mullen: Phys. Rev., (143), 1966, p 663

37. S. P. Murarka, et al: J. Appl. Phys. (35), 1964, p 1339

38. C. J. Smithells: Metals Reference Book, 3rd ed., Butterworth, London, 1962

39. H. Reiss et al: Bell. System Tech. J., (35), 1956, p 535

40. W. R. Wilcox et al: J. Electrochem. Soc., (111), 1964, p 1377

41. J. E. Lawrence: J. Appl. Phys. (37), 1966, p 4106

42. B. I. Boltaks: "Diffusion in Semiconductors", Academic Press, 1961

43. M. C. Flemings: "Solidification processing" McGraw-Hill, 1974, p 134, p 170

44. B. Chalmers: J. Metal, May 1954, p 519

45. G. J. Davies: "Solidification and Casting" , Applied Science publisher, 1973, p 63

46. W. W. Mullins & R. F. Sekerka: J. Appl. Phys. (34), 1963, p 323

47. R. F. Sekerka: J. Appl. Phys. (35), 1964, p 444

48. R. F. Sekerka: J. Appl. Phys. (36), 1965, p 264

49. R. F. Kekerka: J. Crystal Growth (3), 1968, p 71

50. K. A. Jackson & J. D. Hunt: Acta Met. (13), 1965, p 1212

51. K. A. Jackson, D. R. Uhlmann & J. D. Hunt: J. Crystal Growth (1), 1967, p 1

52. M. G. Glicksman & C. L. Vold: ISI, 1968, p 37

53. W. Tiller, K. Jackson, J. Rutter & B. Chalmers: Acta Met. (1), 1953, p 428

54. W. G. Pfann: Trans. AIME (194), 1952, p 747

55. J. A. Burton, R. C. Prim & W. P. Slichter: J. Chem. Phys. (21) 1953, p 1908

56. B. Sharp & A. Hellawell: J. Crystal Growth (5), 1969, p 155

57. J. Forsten & H. Miek-Oja: J. Inst. Met. (95), 1967

58. F. Weinberg: Trans. AIME (227), 1963, p 231

59. V. G. Smith, W. A. Tiller & J. W. Rutter: Can. J. Phys. (33) 1955, p 723

60. F. R. Mollard & M. C. Flemings: Trans. AIME (239), 1967, p 1534

61. J. Rutter & B. Chalmers : Can. J. Phys. (31), 1953, p 15

62. P. T. J. Hurle: Solid State Electronics (3), 1961, p 37

63. W. Bardsley et al: Solid State Electronics (3), 1961, p 142

64. R. Sharp & A. Hellawell: J. Crystal Growth (6), 1970, p 334

65. M. H. Burden: Ph.D. Thesis, Oxford, 1973

66. L. R. Morris & W. C. Winegard: J. Crystal Growth (6), 1969, p 61

67. M. C. Flemings: "Solidification Processing" Mc-Graw Hill, 1974, p 63.

68. B. Chalmers: "Solidification" seminar of the ASM, Oct 11 & 12 1969, p 304

69. B. Chalmers: "Principles of Solidification" John Wiley & Sons 1965, p 94

70. F. Weinberg & B. Chalmers: Can. J. Phys. (30), 1952, p 488

71. B. Chalmers: "Principles of Solidification" John Wiley & Sons 1965, p 105

72. P. G. Shewman: "Transformation in Metals" McGraw-Hill, 1969, p 177

73. Kattamis, J. Coughlin & M. C. Flemings: Trans. AIME (239), 1967, p 1504

74. K. A. Jackson, J. D. Hunt, D. R. Uhlmann & T. P. Seward III: Trans. AIME (236), 1966, p 149

75. L. A. Tarshis, J. L. Walker & J. W. Rutter: Met. Trans. (2), 1971, p 2589

76. H. Biloni & B. Chalmers: J. Mat. Sci. (3), 1968, p 139

77. R. Morando, H. Biloni, G. S. Cole & G. F. Bolling: Met. Trans. (1), 1970, p 1407

78. G. S. Cole & W. C. Winegard: J. Inst. Met. (93), 1964-1965, p 153

79. B. Chalmers: "Principles of Solidification" McGraw-Hill, 1964, p 258

80. G. S. Cole & G. F. Bolling: Trans. AIME (235), 1965, p 1568

81. D. Uhlmann, T. Seward & B. Chalmers: Trans. AIME (236), 1966, p 527

82. G. S. Cole & G. F. Bolling: Trans. AIME (236), 1966, p 1366

83. S. O'Hara & W. A. Tiller: Trans. AIME (239), 1967, p 497

84. G. S. Cole & G. F. Bolling: Trans. AIME (239), 1967, p 1860

85. G. S. Cole: "Solidification" by ASM, p 248

86. R. Southin: Trans. AIME (239), 1967, p 220

87. F. A. Crossley, R. D. Fisher & A. G. Metcalfe: Trans. AIME (227) 1961, p 419

88. W. Winegard & B. Chalmers: Trans. ASM (46), 1954, p 1214

89. T. Plaskett & W. Winegard: Trans. ASM (51), 1959, p 222

90. B. Chalmers: J. Aust. Inst. Met. (8), 1962, p 225

91. J. D. Hunt & K. A. Jackson: J. Appl. Phys. (37), 1966, p 254

92. G. S. Cole & G. F. Bolling: Trans. AIME (245), 1969, p 725

93. M. H. Burden & J. D. Hunt: J. Crystal. Growth (22), 1974, p 99-108

94. R. M. Sharp & A. Hellawell: J. Crystal. Growth (6), 1970, p 253

95. J. J. Kramer, G. F. Bolling & W. A. Tiller: Trans. AIME (227) 1963, p 374

96. V. M. Plyatskii: Extrusion Casting, 1965, p 46

97. M. C. Flemings et al: J. Iron Steel Inst., (208), 1970 p 371

98. P. K. Rohatgi & C. M. Adams, Jr. : Trans. AIME, (239), 1967, p 1729

99. G. S. Cole: "Solidification" by ASM (Seminar of the ASM - October 11 & 12, 1969), p 259

100. Seidell: "Solubilities of inorganic and metal organic compounds", vol. 1, p 654

101. W. M. J. Salter & P. E. Wandby: "The solidification of metals", ISI, 1968, p 412

APPENDIX A: DIFFUSION COEFFICIENTS AS A FUNCTION OF PRESSURE

APPENDIX B: ASSEMBLY AND DETAIL DRAWING FOR PRESSURE CRYSTALLISATION CASTING EQUIPMENT

APPENDIX C: EXPERIMENTAL DATA OF SAMPLES

APPENDIX D: PHOTOGRAPHS OF APPARATUS, MACROSCOPIC AND MICROSCOPIC STRUCTURES

APPENDIX A

THE DIFFUSION COEFFICIENTS IN SOLID AS A FUNCTION OF PRESSURE

1. Writing the diffusion coefficient as a function of temperature,

$$D = D_o \exp(-Q/kT) \quad \ldots\ 1$$

2. Taking logarithms of 1 eq. and differentiating with respect to pressure gives:

$$\left(\frac{\partial \ln D}{\partial P}\right)_T = \left(\frac{\partial \ln Do}{\partial P}\right)_T - \frac{1}{kT}\left(\frac{\partial Q}{\partial P}\right)_T \quad \ldots\ 2$$

3. Expanding ln D in a Taylor series in the pressure and neglecting the term of $\left(\frac{\partial \ln Do}{\partial P}\right)_T$:

$$D_{(P)} = D_{(0)} \exp\left[-\frac{P}{kT}\left(\frac{\partial Q}{\partial P}\right)_T\right] \quad \ldots\ 3$$

4. Considering the thermodynamic relations $V = \left(\frac{\partial Q}{\partial P}\right)_T$. comp.

$$V_Q \equiv \left(\frac{\partial Q}{\partial P}\right)_T \quad \ldots\ 4$$

5. Restricted to simple diffusion mechanism, such as interstitial diffusion or substitutional diffusion,

$$D_{(P)} = D_{(o)} \exp\left[-PV^{**}/kT\right] \text{ in interstitial mechanism.}$$

$$D_{(P)} = D_{(o)} \exp\left[\frac{-P\,V_v + V^{**}}{kT}\right] \text{ in vacancy mechanism} \quad \ldots\ 5$$

where V_v is the volume increase on forming a vacancy, and V^{**} is the volume of activation for atomic migration.

6. Assuming that V^{**} can be neglected relative to V_v,

$$D_{(p)} = D_{(o)} \text{ in interstitial diffusion}$$

$$D_{(P)} = D_{(o)} \exp\left[-PV_v/kT\right] \text{ in substitutional diffusion} \quad \ldots\ 6$$

Note: Diffusion coefficient by applying pressure is more influenced in substitutional diffusion than in interstitial diffusion.

7. Considering the variation of the vacancy formation volume with pressure,

$$V_{v(P)} = V_{v(o)} - \tfrac{1}{2} P\beta \left(V_{v(o)} + Kpu \right) \qquad \cdots\cdot 7$$

where $\beta\ \beta'$: compressibilities of the perfect crystal and a crystal containing a single vacancy

K_P : proportionality constant $\frac{\beta - \beta'}{\beta} = K_p \frac{1}{N}$

The relative change in compressibility on introducing a vacancy is inversely proportional to the number of atoms in the crystal.

8. Combining with 6 and 7 eq.,

$$D_{(P)} = D_{(o)} \exp \left[-P \left\{ V_{v(o)} - \tfrac{1}{2} P\beta \left(V_{v(o)} + Kpu \right) \right\} / kT \right]$$

where, $D_{(o)}$, $V_{v(o)}$, β , Kp, v are constant in a given solid and the term of $\left\{ V_{v(o)} - \tfrac{1}{2} P\beta \left(V_{v(o)} + Kpu \right) \right\}$ is always positive.

$$\boxed{D_{(P)} = D_{(o)} \exp \left[-P \left(V_{v(o)} - \tfrac{1}{2} \alpha P \right) / kT \right]}$$

9. Conclusion

(i) Diffusion coefficients decrease with increasing pressure, but it is not exponentially dependent upon the increasing pressure. On the other hand, diffusion coefficients increase with increasin temperature and it is exponentially dependent upon the increasing temperature.

(ii) Diffusion coefficients as a function of pressure are more

influenced in substitutional diffusion than in interstitial diffusion.

Note:

1. Diffusion coefficient in liquid as a function of pressure

1. $F = 6\pi r \eta v_\infty$
   $B \equiv v_\infty / F$
   $D = Bk T$

$$D = \frac{kT}{6\pi r \eta} \quad \text{(Stokes-Einstein eq.)}$$

2 $P = F/A$

$\therefore F = 6\pi r \eta v_\infty$

$$\boxed{D = \frac{kT v_\infty}{AP}}$$

3 Adopted a slightly different form of the drag force,

$$D = \frac{kT}{4\pi r \eta} \quad \text{(modified by Sutherland)}$$

4 Conclusion:

(i) Diffusion coefficients in liquid decrease with the increasing pressure and it is inversely proportional to the pressure.

(ii) Diffusion coefficients in liquid increase with the increasing velocity of flow and temperature and it is proportional to them.

2. Diffusion coefficients in gaseous

$$\boxed{D_{AA} = \frac{2}{3}\left(\frac{k^3}{\pi^3 m_A}\right)^{1/2} \frac{T^{3/2}}{P d^2}}$$

$$\boxed{D_{AB} = \frac{2}{3}\left(\frac{k}{\pi}\right)^{3/2}\left(\frac{1}{2m_A} - \frac{1}{2m_B}\right)^{1/2} \frac{T^{3/2}}{P\left(\frac{d_A + d_B}{2}\right)^2}}$$

(i) Diffusion coefficients in gaseous decrease with the increasing pressure and it is inversely proportional to the pressure.

(ii) Diffusion coefficients in gaseous is more influenced in temperature than in pressure.

JAN. 7. 75
FEB. 19. 76

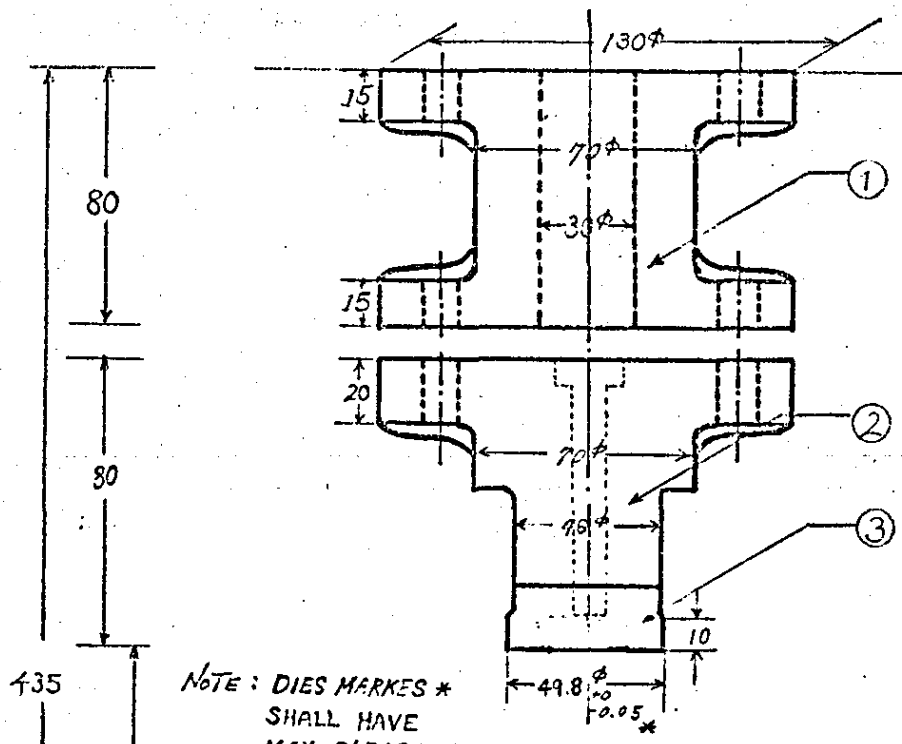

	NAME	Q'TY	MATERIAL	REMARK
①	LOAD CELL	1	AISI No D2	Annealing
②	PUNCH	1	D2	Air Cooling Tempering
③	PUNCH TIP	2	〃	〃 〃
④	RING	1	〃	〃 〃
⑤	CONTAINER	1	〃	〃 〃
⑥	BOTTOM DIE	3	〃	〃 〃
⑦	BASE PLATE	1	〃	〃 〃

ASSEMBLY DRAWING FOR PRESSURE CRYSTALLIZATION CASTING EQUIPMENT

APPENDIX B

FEB. 19 '76

① LOAD CELL (▽▽)

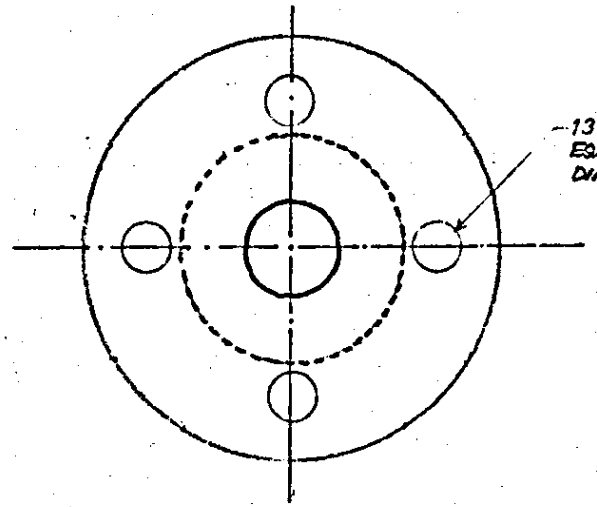

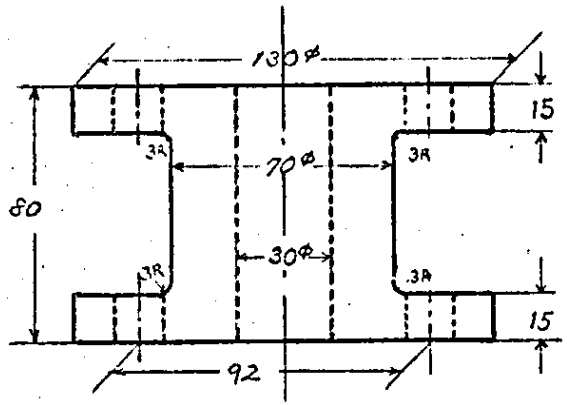

④ RING (▽)

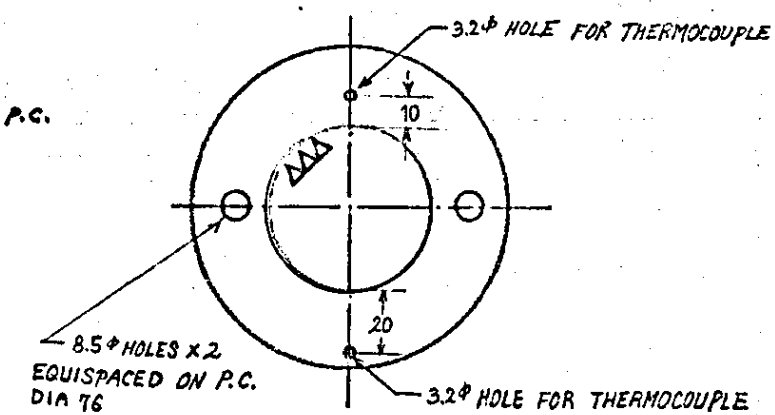

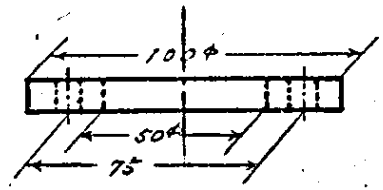

SCALE : m/m

2/3

② PUNCH (▽)

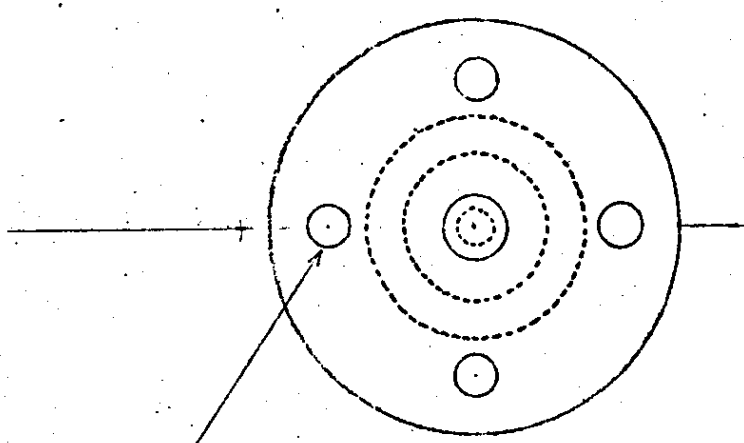

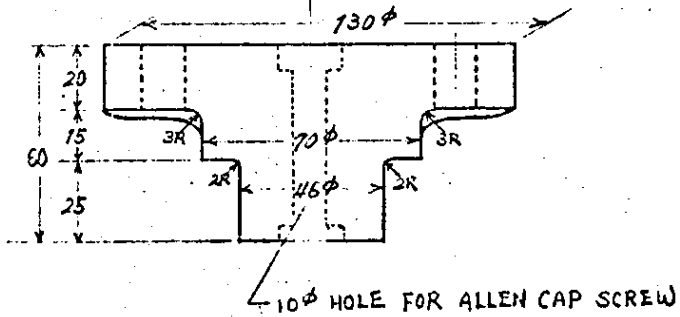

③ PUNCH TIPS (▽▽)

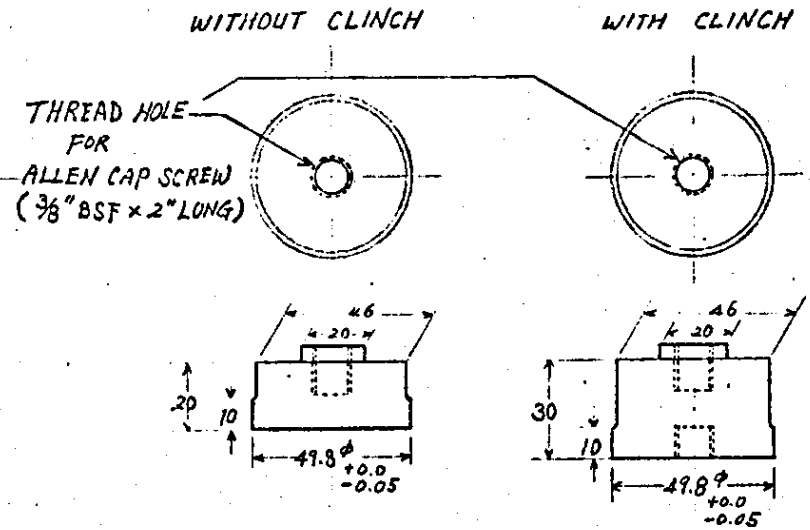

SCALE : m/m

FEB 21.

⑤ CONTAINER (▽)

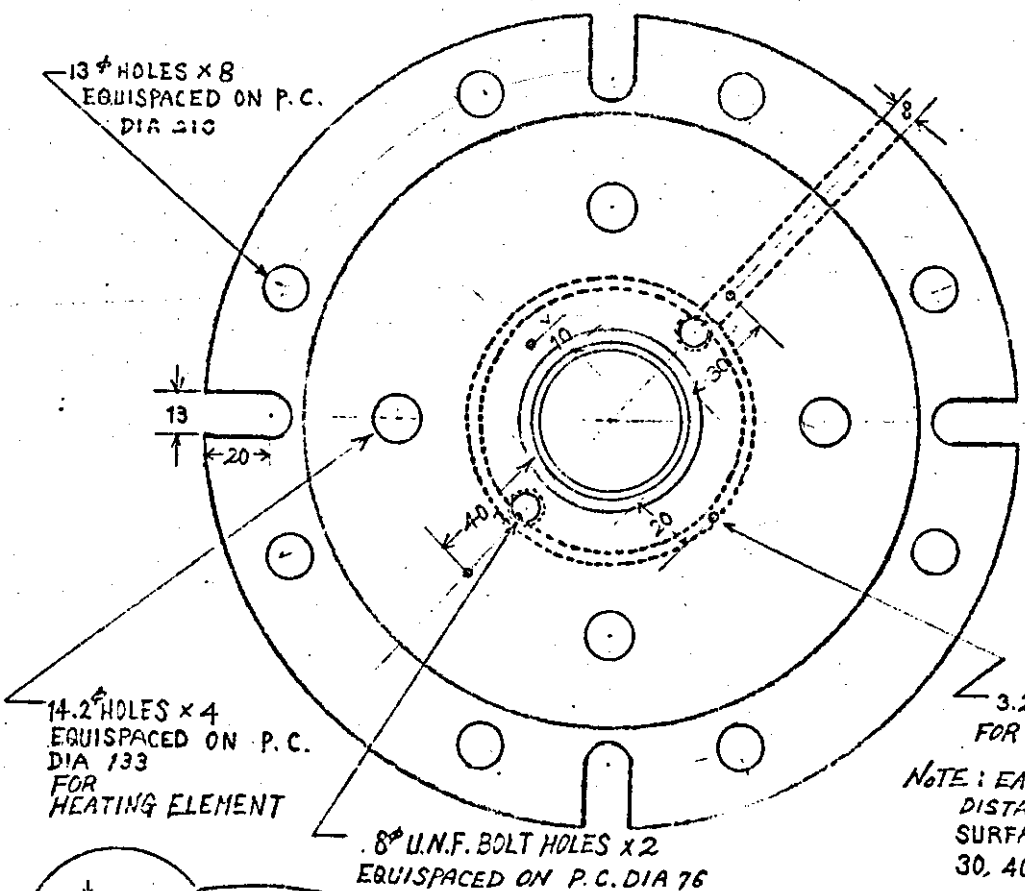

NOTE : EACH HOLE'S DISTANCE FROM DIE SURFACE IS 10, 20, 30, 40 m/m

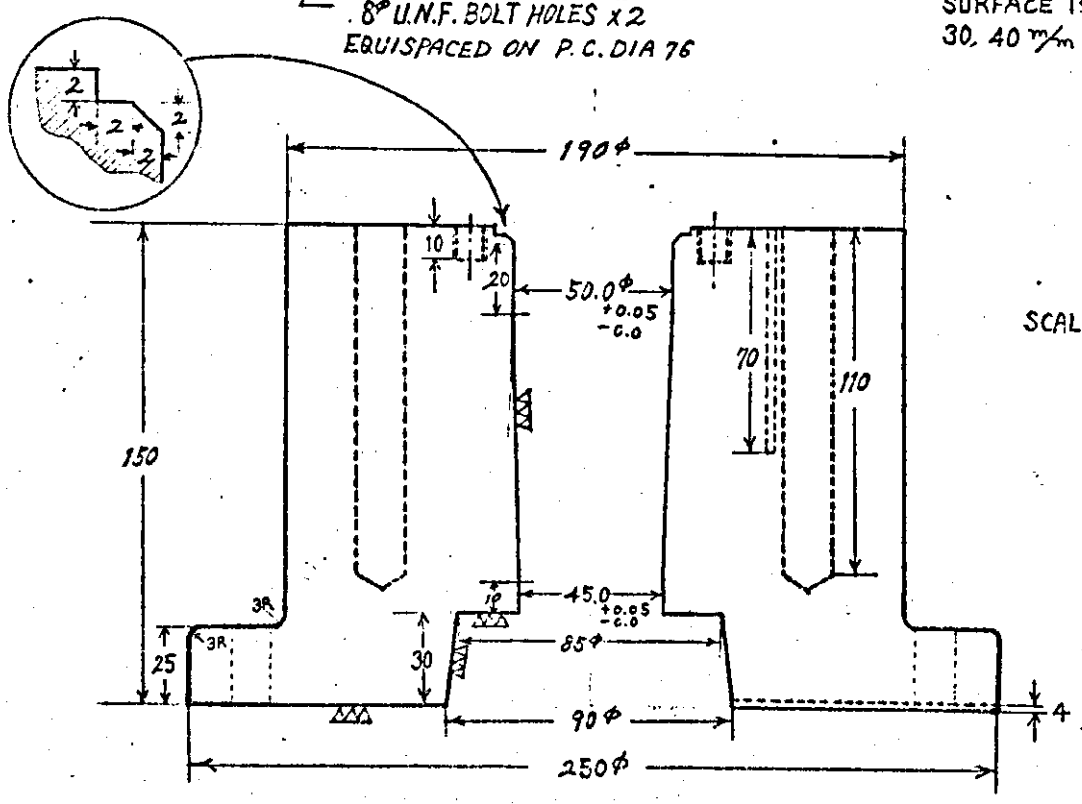

SCALE : m/m

FEB. 21 76
MAR 12 76

⑥ BOTTOM DIES

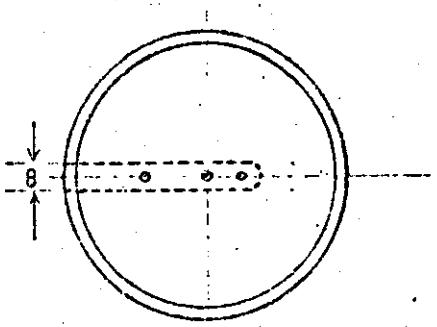

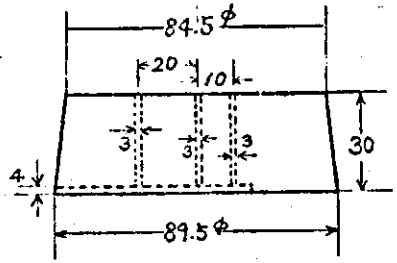

WITHOUT USING THERMOCOUPLE

WITH USING 1 WIRE

WITH USING 3 WIRES

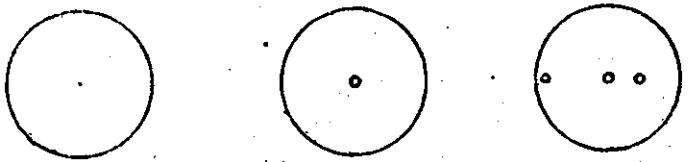

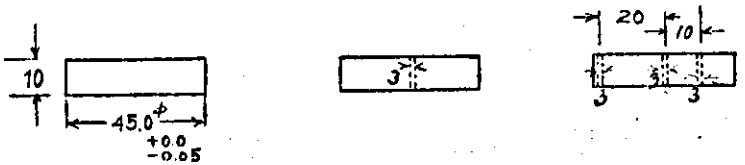

NOTE : TWIN BORE ALUMINA INSULATORS 2.8 ϕ MAX. O.D. OF MAJOR AXIS ARE USED AS THERMOCOUPLE INSULATORS

SCALE : 1/1

FEB 21.

① BASE PLATE

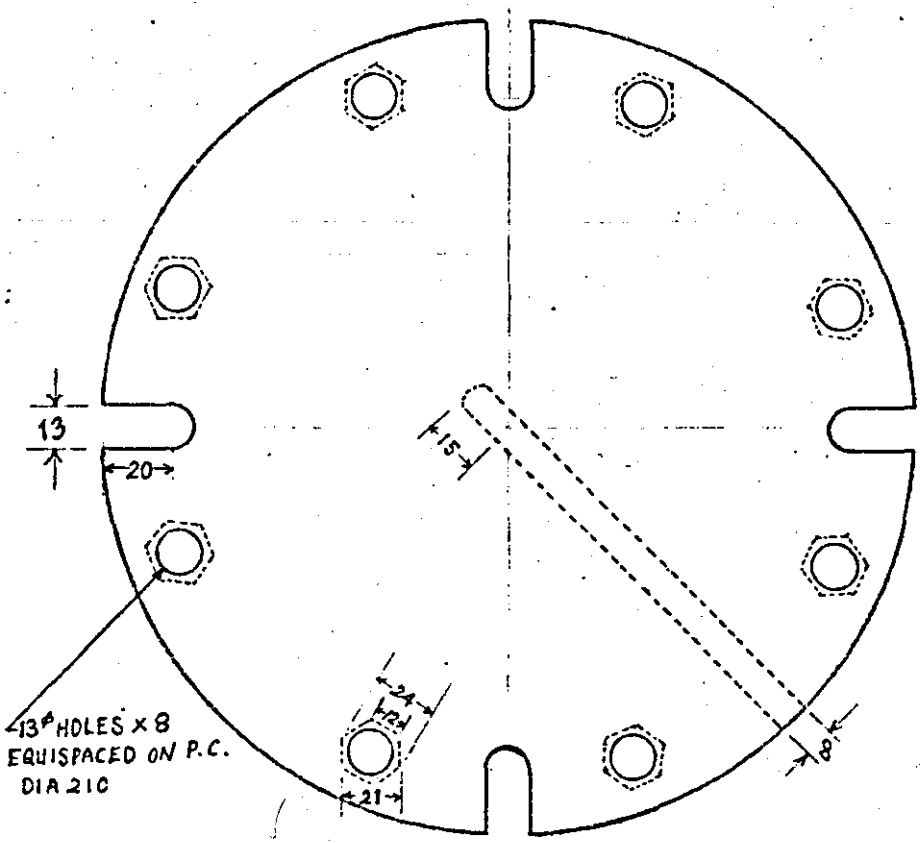

SCALE : m/m

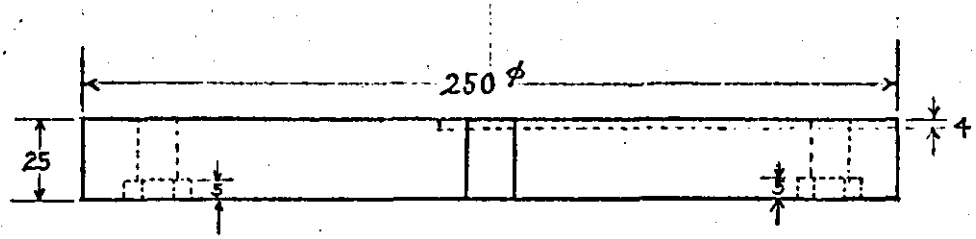

APPENDIX C

EXPERIMENTAL DATA OF SAMPLES

1. Experimental Data in Al-4% Cu alloys

Sample no.	Pressure (MN/m^2)	Pouring Temp (^oC)	Die Temp. (^oC)		macro-structure	copper rich band
			before*	after*		
1	110	680	220	327	Col + Equiaxed	presence
2	110	660	210	315	Equiaxed	presence
3	110	680	250	355	Col + Equiaxed	presence
4	110	680	220	325	Col + Equiaxed	presence
5	110	630	200	285	Fine Equiaxed	presence
6	110	780	190	288	Columnar	presence
7	110	780	210	330	Columnar	presence
11	No pressure	720	200	300	Col + Equiaxed	No
12	70	720	210	310	Col + Equiaxed	presence
13	70	660	175	275	Col + Equiaxed	presence
14	70	650	165	260	Fine Equiaxed	No
15	110	650	165	260	Fine Equiaxed	No
16	1st 60 2nd 110	650	165	250	Fine Equiaxed	No
17	110 with asbestos	650	165	250	Fine Equiaxed	presence
18	No pressure	650	175	260	Fine Equiaxed	No
20	//0	680	180	270	Col + Equiaxed	presence
21	70	680	190	275	Col + Equiaxed	presence

Note: * "before" means "before applying pressure", and "after" means "maximum die temperature increased during applying pressure"

2. Experimental Data in Commercial Al-Cu alloys (LM11)

Sample No.	Pressure (MN/m^2)	Pouring Temp (^oC)	Die Temp (^oC)		Macro structure	Copper rich band
			before*	after*		
LM11 0	no pressure	720	180	275	Fine Equiaxed	No
1	no pressure	790	180		Fine Equiaxed	No
2	70	720	180	280	Fine Equiaxed	presence
3	70	660	190	305	Fine Equiaxed	presence
4	70	710	170	275	Fine Equiaxed	No
5	70	660	165	260	Fine Equiaxed	No
6	110	770	180		Fine Equiaxed	presence
7	70	780	180	280	Fine Equiaxed	No
8	110	800	215	320	Col. + Equiaxed	presence
9	110	760	240	360	Col. + Fine Equiaxed	presence

Note: * - "before" means "before applying pressure", and "after" means "maximum die temperature increased during applying pressure".

APPENDIX D

Photo 1 The particular apparatus for observing the freezing phenomena

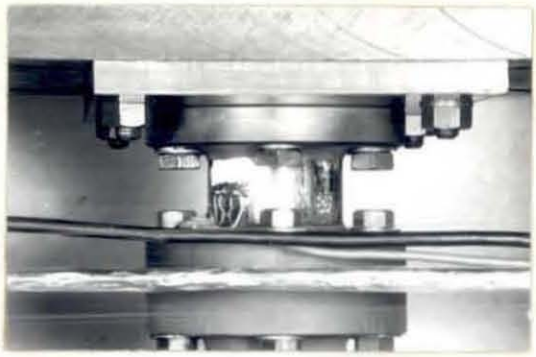

Photo 2 Load cell with strain gauges

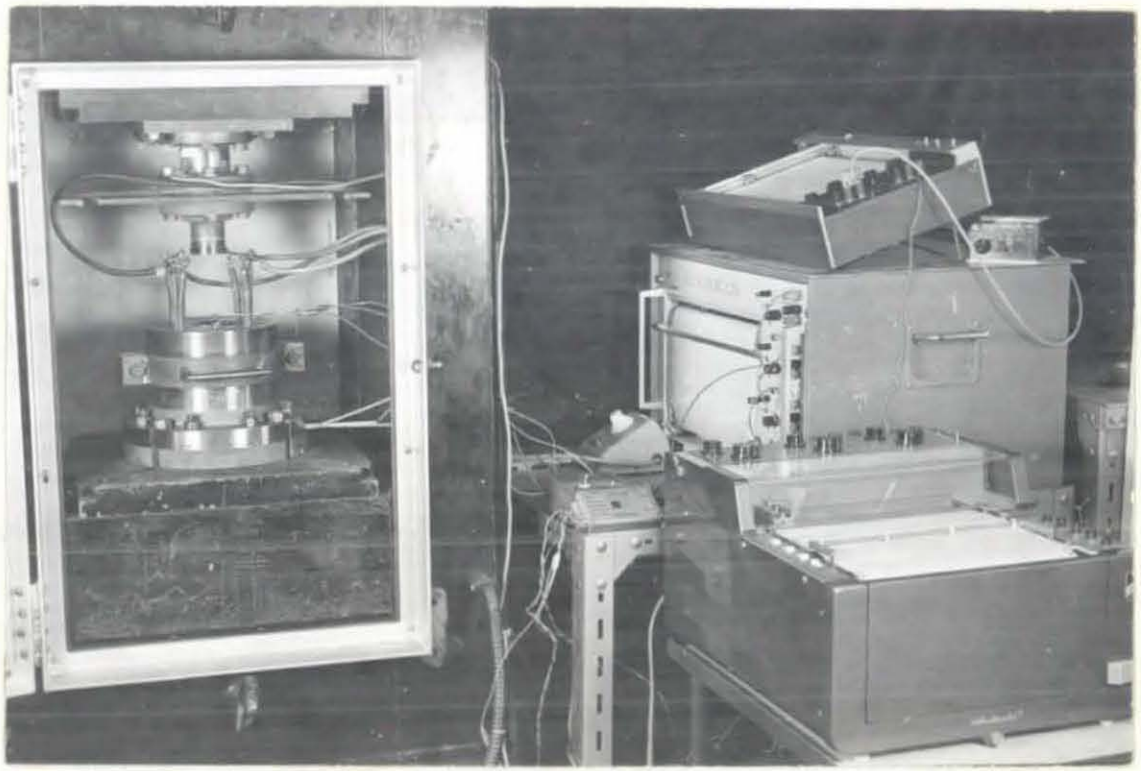

Photo 3 The instruments of the main apparatus

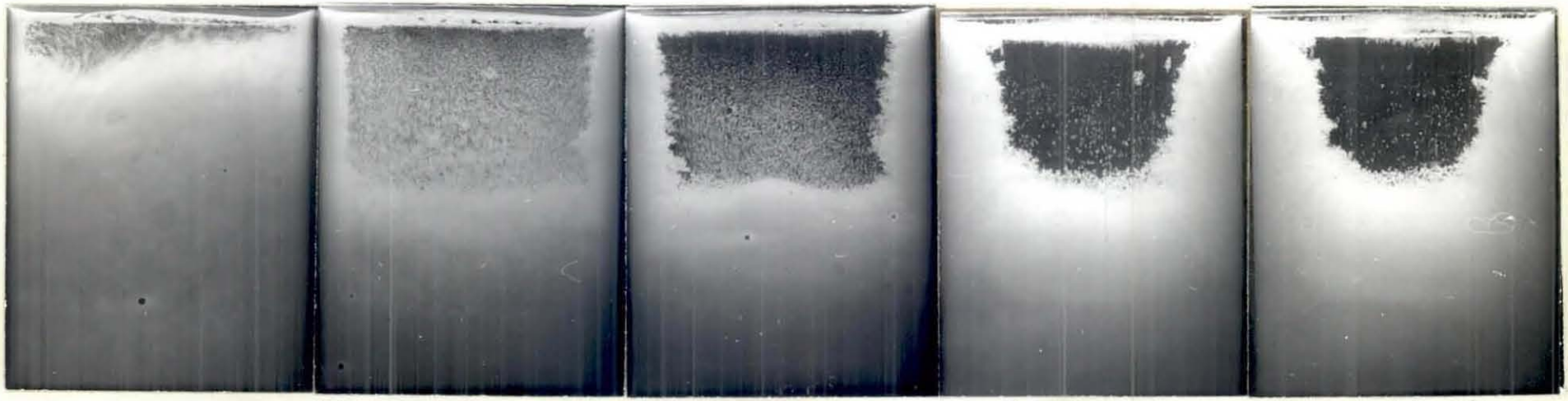

(a) 10 sec (b) 30 sec (c) 60 sec (d) 150 sec (e) 180 sec

Photo 4 Crystallisation of NH_4Cl/ water system solution (saturated at 65°C) poured at 70°C at atmosphere

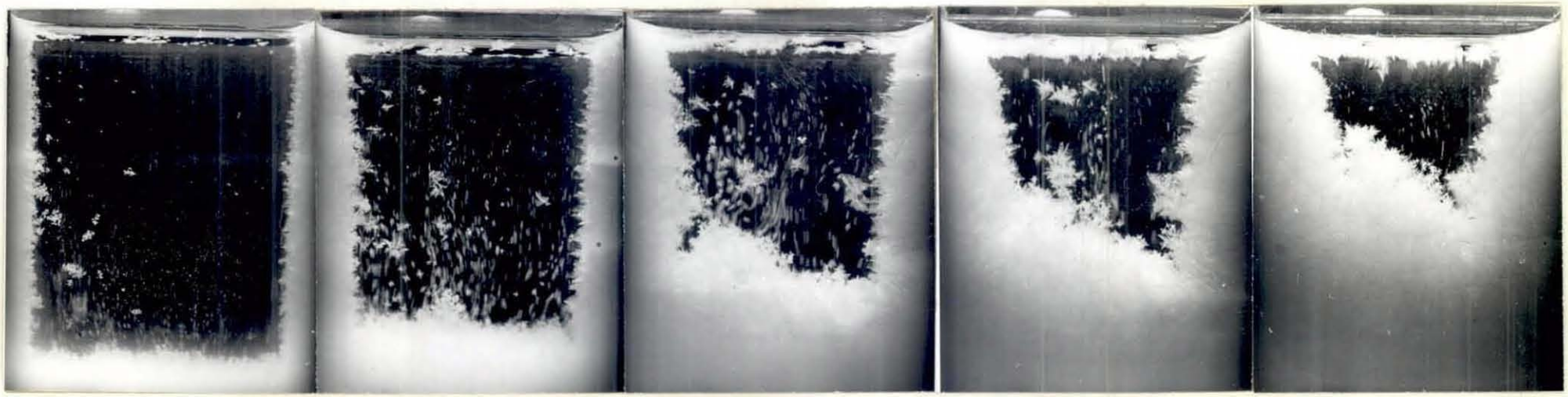

(a) 30 sec (b) 60 sec (c) 90 sec (d) 120 sec (e) 180 sec

Photo 5 Crystallisation of NH_4Cl/water system solution (saturated at 65°C) poured at 80°C at atmosphere

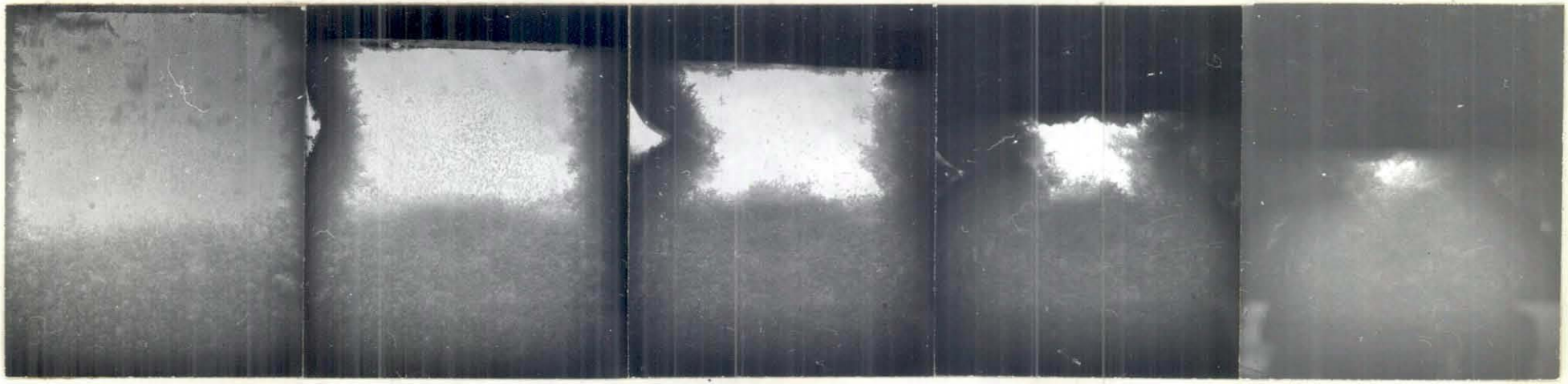

(a) 20 sec (b) 50 sec (c) 80 sec (d) 120 sec (e) 150 sec

Photo 6 Crystallisation of NH_4Cl/water system solution (saturated at 75°C) poured at 80°C under pressure

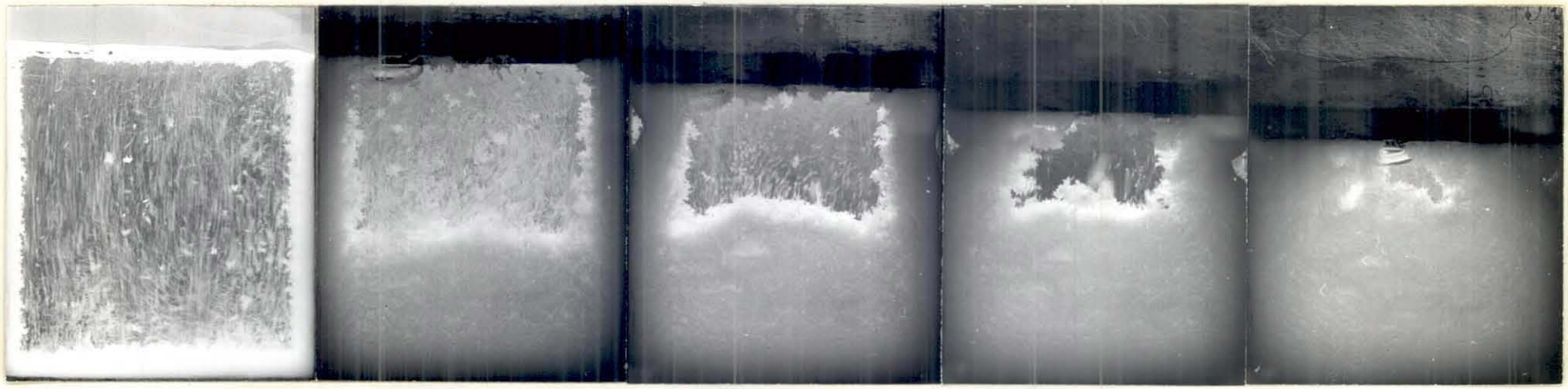

(a) 10 sec (b) 40 sec (c) 60 sec (d) 90 sec (e) 150 sec

Photo 7 Crystallisation of NH_4Cl/water system solution (saturated at 75°C) poured at 90°C under pressure

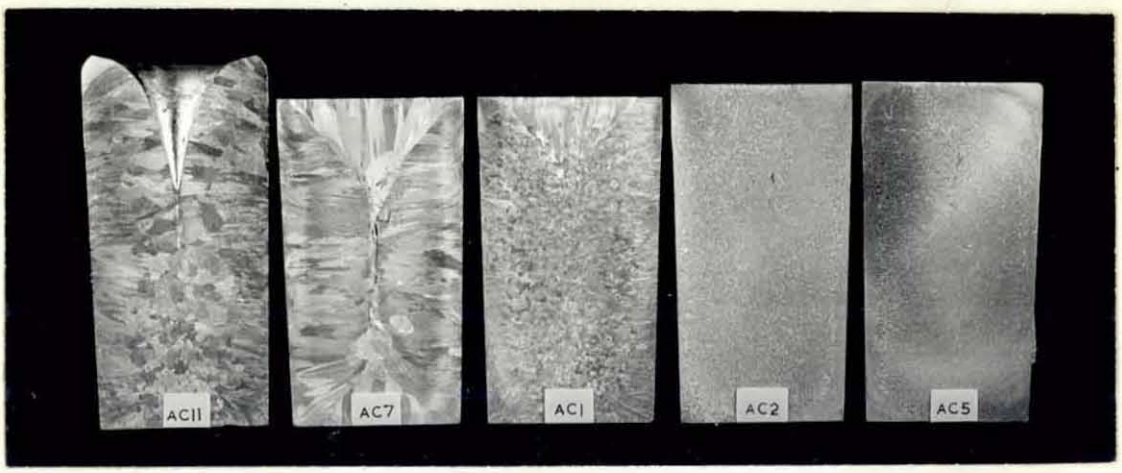

Photo 8 Macrostructures of Al-4% Cu alloy solidified at various pouring temperatures with die temp. of 210°C under 110 MN/m^2 pressure

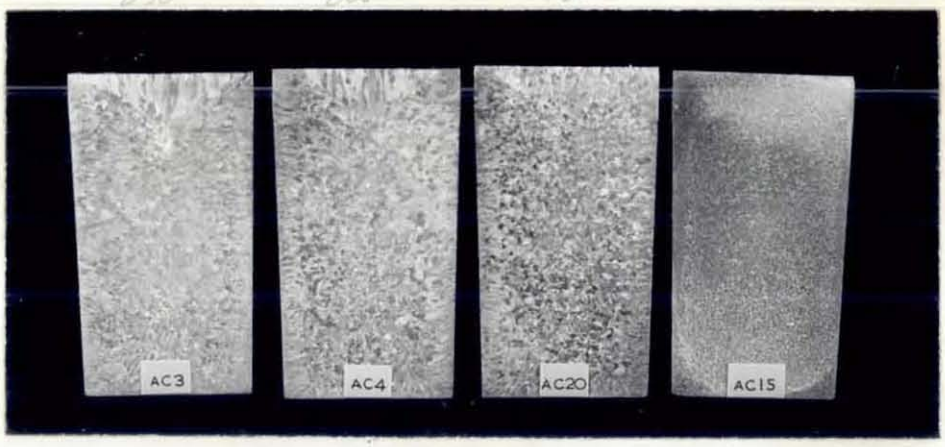

Photo 9 Macrostructures of Al-4% Cu alloy solidified at various die temperatures with pouring temp. of 680°C under 110 MN/m^2

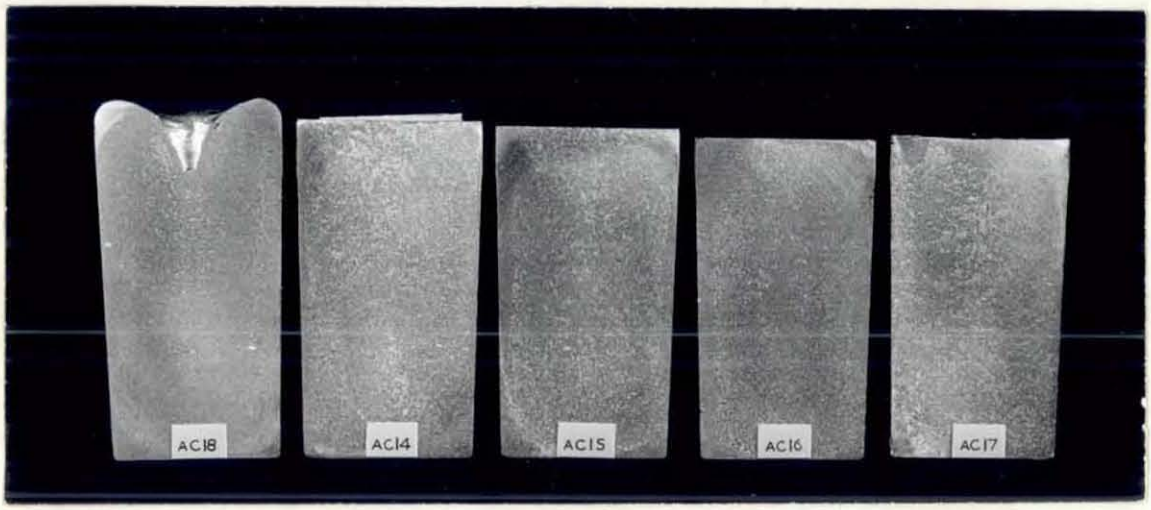

Photo 10 Macrostructures of Al-4% Cu alloy solidified at various pressures with pouring temp. of 660°C and die temp. of 165°C

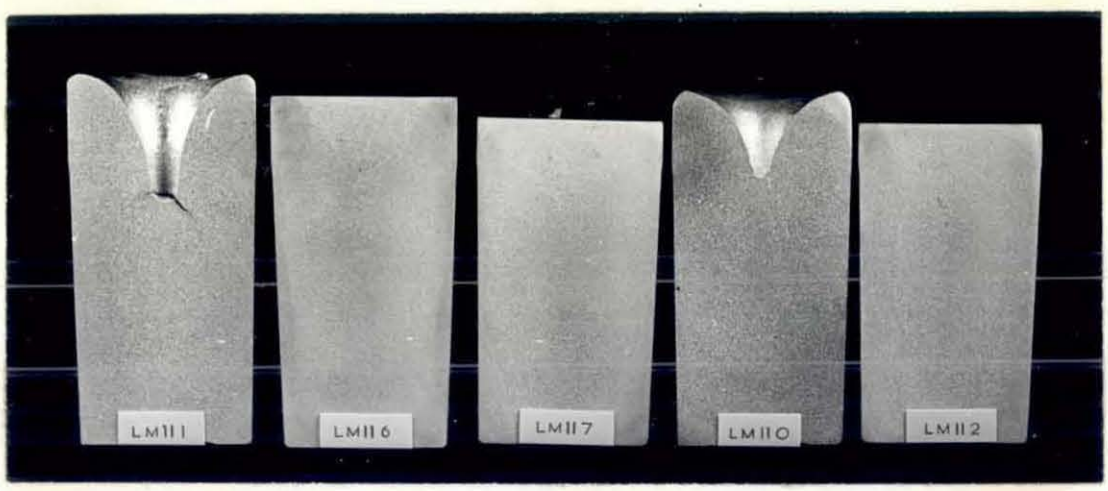

Photo 11 Macrostructures of LM11 alloy solid solidified at the following casting conditions:

LM11 1	pouring temp.	790°C,	die temp.	180°C, at atm.
LM11 7	"	780°C,	"	180°C, under 70 MN/m^2
LM11 6	"	770°C,	"	180°C, under 110 MN/m^2
LM11 0	"	720°C,	"	180°C, at atm.
LM11 2	"	720°C,	"	180°C, under 70 MN/m^2

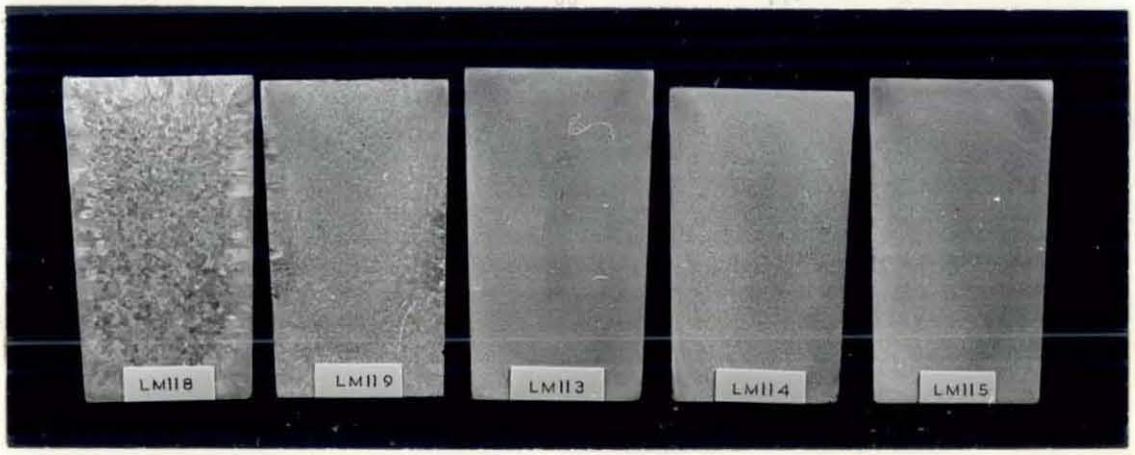

Photo 12 Macrostructures of LM11 alloy solidified at the following casting conditions:

LM11 8	pouring temp.	800°C,	die temp.	215°C under 110 MN/m^2
LM11 9	"	760°C,	"	240°C under 110 MN/m^2
LM11 3	"	650°C,	"	190°C under 70 MN/m^2
LM11 4	"	710°C,	"	170°C under 70 MN/m^2
LM11 5	"	660°C,	"	165°C under 70 MN/m^2

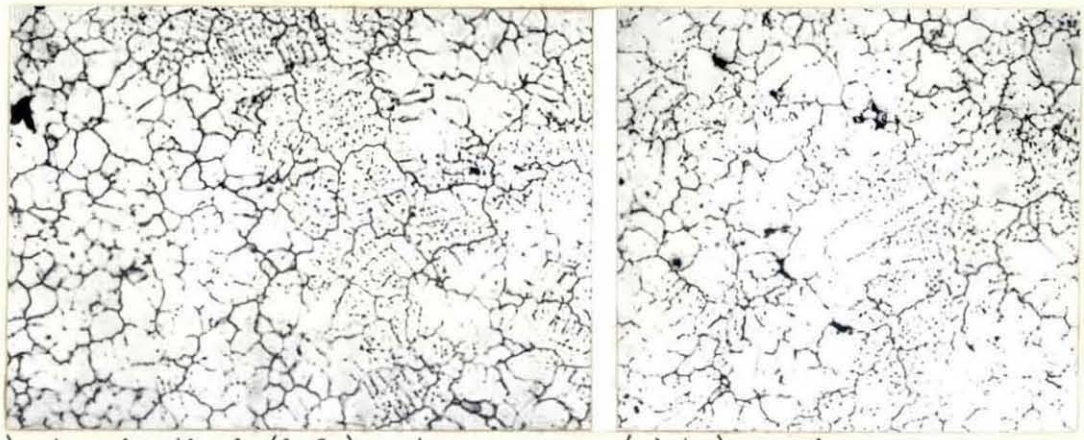

(a) Longitudinal (left) and transverse (right) sections at atm.

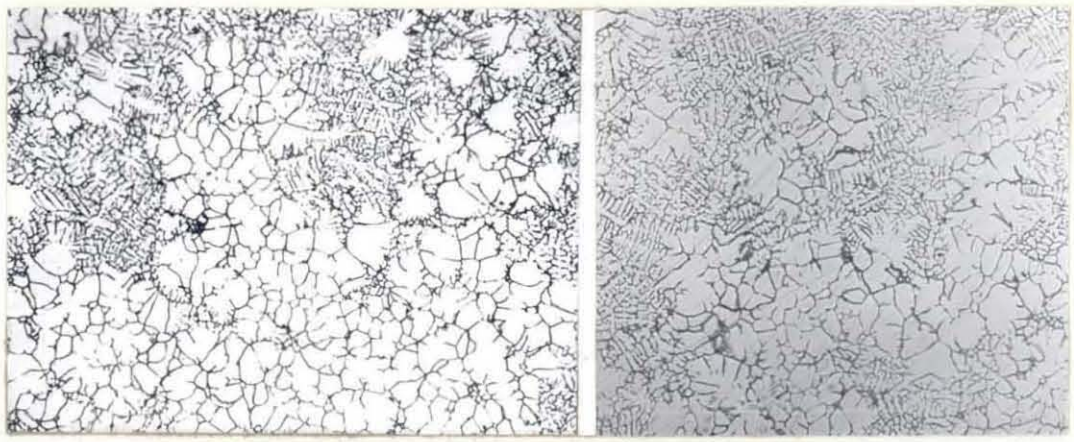

(b) Longitudinal (left) and transverse (right) sections under 110 MN/m^2

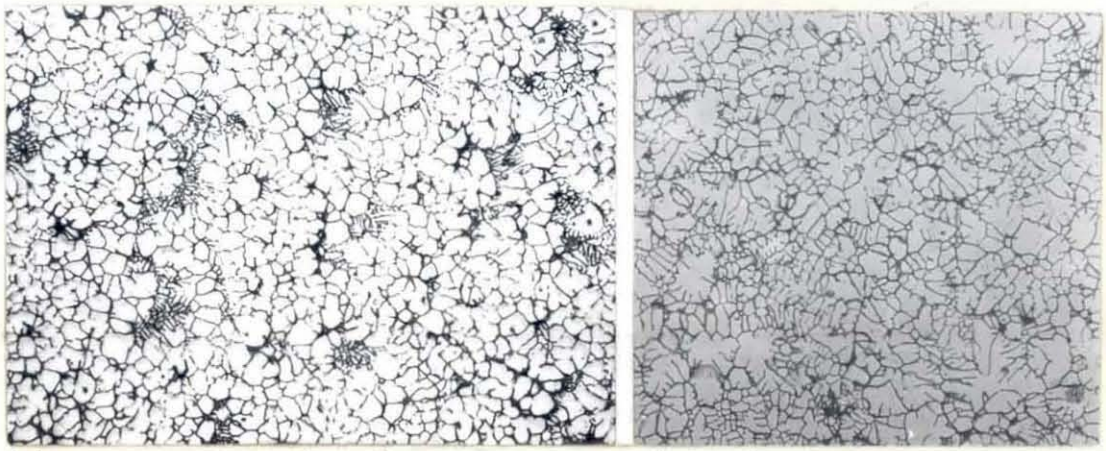

(c) Longitudinal (left) and transverse (right) sections under two-step pressures.

Photo 13 Photomicrographs of equiaxed grains, showing the change of substructure due to pressurisation (x40). Etched by a 0.5% HF.

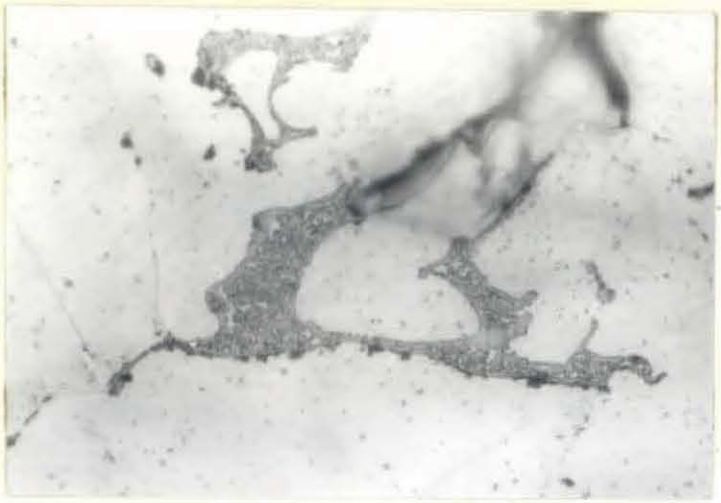

(a) at atmosphere

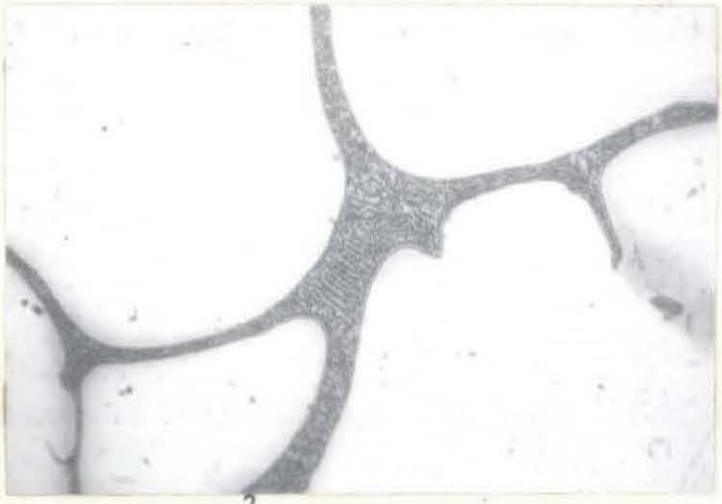

(b) under 110 MN/m^2

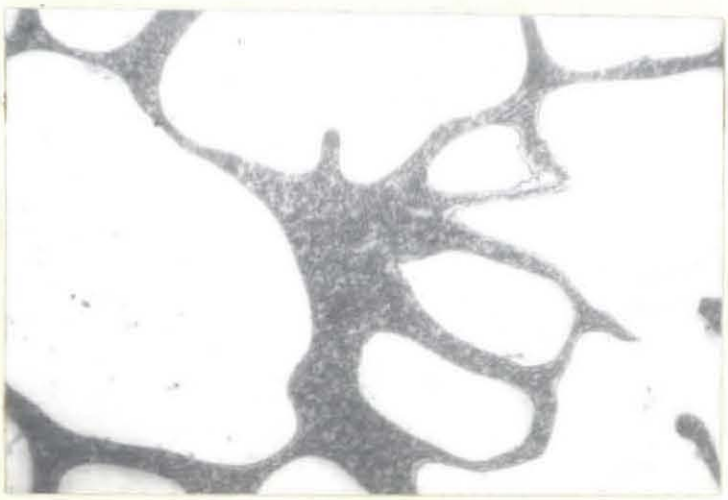

(c) under a two-step pressure

Photo 14 Eutectic structures at atm. and under pressures (x1000). Etched by 0.5% HF.

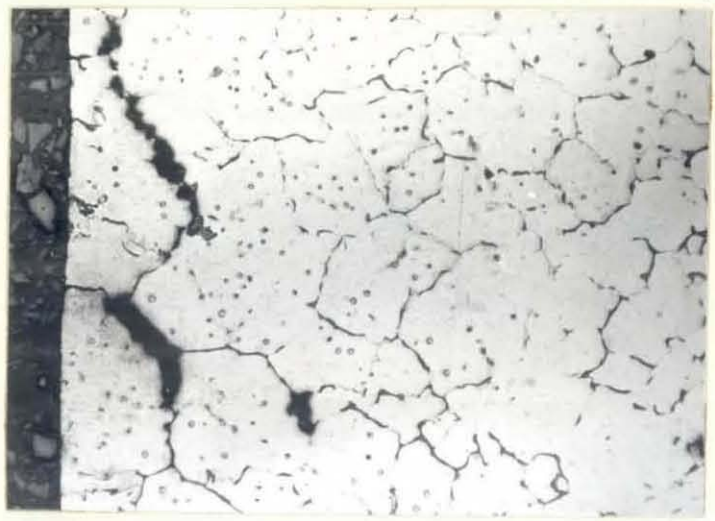

(a) chill surface solidified at atm. (specimen No. AC18)

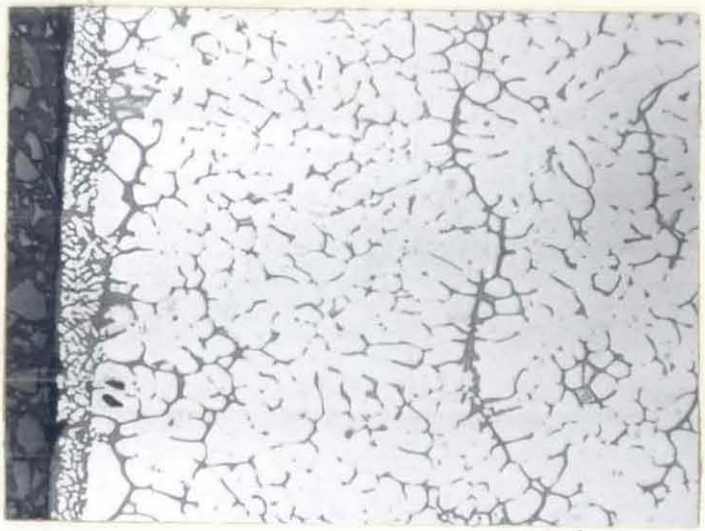

(b) chill surface solidified under 110 MN/m^2 (specimen No. AC15)

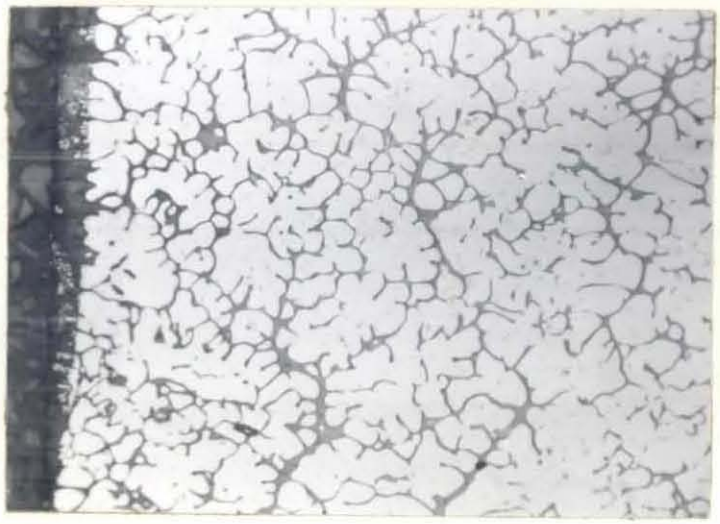

(c) chill surface solidified under a two-step pressure (specimen No. AC16)

Photo 15 Grain boundary migration in a chill surface and dendrite fractures (x100)
Etched by 0.5% HF